12-2012

Differential Activity of the KRAS Oncogene by Method of Activation: Implications for Signaling and Therapeutic Intervention

Nathan Ihle

Differential Activity of the KRAS Oncogene by Method of Activation: Implications for Signaling and Therapeutic Intervention

By: Nathan Ihle B.S.

Approved:

Garth Powis

Supervisory Professor

E. Scott Kopetz

Michael Davies

John E. Ladbury

John S. McMurray

Approved:

Dean, The University of Texas

Graduate School of Biomedical Sciences

Differential Activity of the *KRAS* Oncogene by Method of Activation: Implications for Signaling and Therapeutic Intervention

A

DISSERTATION

Presented to the Faculty of

The University of Texas

Health Science Center at Houston

and

The University of Texas

M. D. Anderson Cancer Center

Graduate School of Biomedical Sciences

in Partial Fulfillment

of the Requirements

for the Degree of

DOCTOR OF PHILOSOPHY

By

Nathan Ihle, B.S.

Houston, Texas

December, 2012

Dedication

To my darling wife and children who have loved and supported me in and despite all the decisions I have made. Mena Abdelmelek, a great help in the preparation of this work and Garth Powis, a great mentor in science and life.

Acknowledgements

All the present and past members of the Powis Lab who have taught me so much through the years. My committee for great insights and input into this work and the hardworking scientists and physicians of MD Anderson. I perhaps owe the greatest acknowledgement to those patients who sacrificed time or comfort to provide samples to perform these studies and made this sacrifice so that future sufferers of cancer may have long healthy lives.

Differential Activity of the *KRAS* Oncogene by Method of Activation: Implications for Signaling and Therapeutic Intervention

By Nathan Ihle B.S.

Despite having been identified over thirty years ago and definitively established as having a critical role in driving tumor growth and predicting for resistance to therapy, the *KRAS* oncogene remains a target in cancer for which there is no effective treatment. KRas is activated by mutations at a few sites, primarily amino acid substitutions at codon 12 which promote a constitutively active state. I have found that different amino acid substitutions at codon 12 can activate different KRas downstream signaling pathways, determine clonogenic growth potential and determine patient response to molecularly targeted therapies. Computer modeling of the KRas structure shows that different amino acids substituted at the codon 12 position influences how KRas interacts with its effecters.

In the absence of a direct inhibitor of mutant KRas several agents have recently entered clinical trials alone and in combination directly targeting two of the common downstream effecter pathways of KRas, namely the Mapk pathway and the Akt pathway. These inhibitors were evaluated for efficacy against different *KRAS* activating mutations. An isogenic panel of colorectal cells with wild type KRas replaced with KRas G12C, G12D, or G12V at the endogenous loci differed in sensitivity to Mek and Akt inhibition. In contrast, screening was performed in a broad panel of lung cell lines alone and no correlation was seen between types of activating *KRAS* mutation due to concurrent oncogenic lesions.

To find a new method to inhibit *KRAS* driven tumors, siRNA screens were performed in isogenic lines with and without active KRas. The knockdown of *CNKSR1* (CNK1) showed selective growth inhibition in cells with an oncogenic *KRAS*. The deletion of CNK1 reduces expression of mitotic cell cycle proteins and arrests cells with active KRas in the G1 phase of the cell cycle similar to the deletion of an activated KRas regardless of activating substitution.

CNK1 has a PH domain responsible for localizing it to membrane lipids making KRas potentially amenable to inhibition with small molecules. The work has identified a series of small molecules capable of binding to this PH domain and inhibiting CNK1 facilitated KRas signaling.

Table of contents

List of Illustrations

Chapter 1

Chapter 2 (no illustrations)

Chapter 3

Chapter 4

Chapter 5

Chapter 6 (no illustrations)

List of Tables

List of Abbreviations

°C degrees celsius

µL microliter

µM micromolar

µg microgram

4E-BP1 eukaryotic initiation factor 4E binding protein

ADP adenosine diphosphate

AKT thymoma in AKR mouse

APC adenomatous polyposis coli

ARF ADP ribosylation factor

ATCC American type culture collection

ATP adenosine triphosphate

BATTLE biomarker-integrated approaches of targeted therapy for lung cancer elimination

C cysteine

CDC2 cell division control protein 2

CDC25 cell division control protein 25

Cdk1 cyclin dependent kinase1

Chk1 checkpoint kinase-1

CNKSR1 connector enhancer of kinase suppressor of ras 1

D aspartic acid

DAG diacylglycerol

DMSO dimethylsulfoxide

DNA deoxyribonucleic acid

ECOG eastern cooperative oncology group

EGFR epithelial growth factor receptor

ER endoplasmic reticulum

ERK extracellular signal-regulated kinase

FAK1 focal adhesion kinase 1

FBS fetal bovine serum

FDA food and drug administration

FGFR fibroblast growth factor receptor

FRS FGFR substrate

G glycine

G protein guanine nucleotide binding protein

GAP GTPase activating protein

GDP guanosine diphosphate

GFP green fluorescent protein

GRB2 growth Factor bound protein 2

GSK glycogen synthase kinase

GTP guanosine triphosphate

HBEC human bronchial epithelial cells

HEK 293 human embryonic kidney 293 cells

HRAS Harvey rat sarcoma

IGFR Insulin-like growth factor receptor

INK4 inhibitor of cyclin-dependent kinase 4

IRS IGFR substrate

KRAS Kirsten rat sarcoma

KSR kinase Suppressor of Ras

LKB1 liver kinase B1

M molar

MAPK mitogen activated protein kinase

MEK Mapk Erk kinase

MEF mouse embryonic fibroblasts

mM millimolar

Mut mutant

MST1 macrophage stimulating 1

mTOR mammalian target of rapamycin

NB no binding

NF2 neurofibromatosis type II

ND not determined

NP-40 tergitol-type NP-40 detergent (nonyl phenoxypolyethoxylethanol)

NRAS neuronal rat sarcoma

NSCLC non-small cell lung cancer

PBS phosphate buffered saline

PH domain pleckstrin homology

PI3K phosphoinositide 3-kinase

PIP_2 phosphatidylinositol 4,5-bisphosphate

PIP_3 phosphatidylinositol 3,4,5-bisphosphate

PKC protein kinase c

PLC_ϵ phospholipase c epsilon

PLK1 polo-like kinase1

PTEN phosphatase and tensin homolog

RA RAS assocation

RAF rat-1 fibroblast kinase

RALA RAS related protein A

RALB RAS related protein B

RALBP ral binding protein

RALGDS Ral guanine nucleotide dissociation stimulator

RAN RAS-related nuclear protein

RAS rat sarcoma

RASSF1 RAS association domain 1

RB1 Retinoblastoma protein

RNA ribonucleic acid

RPPA reverese phase protein array

S6K ribosomal S6-kinase

SDS-PAGE sodium dodecyl sulfate-polyacrylamide gel electrophoresis

Ser serine

shRNA short-hairpin ribonucleic acid

siRNA short-interfering ribonucleic acid

S1P sphingosine-1-phosphate

SH2 src Homology 2

SHP2 SH2 domain tyrosine phosphatases

SOS1 son of sevenless 1

SPR surface plasmon resonance

STK11 serine threonine kinase 11

STK33 serine threonine kinase 33

Thr threonine

TIAM1 T-cell lymphoma invasion and metastasis-inducing protein 1

TSC2 Tuberous sclerosis complex 2/tuberin

V valine

VEGFR3 vascular endothelial growth factor receptor-3

WT wild-type

Y tyrosine

YB-1 Y-box binding protein1

Introduction

1.1 Ras background and function

The Ras superfamily of enzymes consists of over 100 GTP hydrolysis switch proteins (small GTPases) responsible for signal propagation and includes the Ras, Rho, Arf, Ran, and Rab proteins[1]. The name Ras is derived from Rat Sarcoma, the model system in which this class of enzymes was first described in 1962[2]. Twenty years later the human homologues were identified by Scolnick and colleagues as genes important in human cancer [3]. These small GTPases are similar in structure to the G_{α} subunit of the heterotrimeric G proteins (large GTPases) but lack the presence of the G_{β} and G_{γ} subunits as additional regulators [4]. The Ras enzymes exist in dynamic equilibrium, either bound to GDP and considered inactive or bound to GTP in which state they are capable of engaging multiple effecter proteins. Ras enzymes directly bind effecters changing their conformation creating an active state in which downstream signaling is engaged. This signaling can have immediate effects on cellular processes such as metabolism and survival and can influence DNA transcription leading to global cellular outcomes such as altered motility, growth and differentiation. The four identified human Ras proteins (K-Ras4A, K-Ras4B, N-Ras, and H-Ras) within the Ras superfamily share approximately 85% sequence homology. These subtypes differ mainly at a C-terminus in a string of residues termed the "hypervariable region" responsible for the appropriate localization of these enzymes [5]. The two KRas proteins arise from the same gene and are a product of alternative gene splicing and differ in this hypervariable region. Activation of these proteins comes from the gamma phosphate of GTP interacting at the two switch regions (usually at residues threonine 35 of switch 1 and glycine 60 of switch 2) within the Ras proteins pulling them together into what is termed the "loaded spring" confirmation [6]. In this "loaded spring" confirmation the switch regions are contorted in such a fashion that effecter binding becomes favorable. The Ras proteins are capable of acting on their own nucleotide, and thus can self-hydrolyze their own GTP molecule to GDP resulting in de-activation, but

require additional regulator proteins that amplify this process for appropriate physiological control of activity.

1.1.1 The Ras activation Cycle

The Ras proteins are activated in response to the engagement of growth factor receptors. Upon a growth factor binding to the extracellular domain of the receptor, an intracellular region of the receptor undergoes a conformational change and is phosphorylated on tyrosine residues [7]. These phosphorylations promote binding of proteins containing SH2 domains to the tyrosine sites. SH2 domain-containing proteins, known as adaptor proteins, bind to an activated receptor can activate Guanine Exchange factors (GEFs). GEF's interact with the Ras proteins and elicit the release of the currently bound nucleotide[8] The result of this is the exchange of the previously utilized GDP nucleotide for a new GTP, as GTP occurs at a ten-fold higher concentration in the cytosol. The Ras enzyme becomes active and transduces intracellular signals through other GTPases and kinases, thus linking the presence of extracellular growth factors to intracellular signaling cascades. The most extensively characterized GEF is *SOS1*, first identified as an essential regulator of *Drosophila melanogaster* eye development[9] and later characterized in human cells as essential for neurodevelopmental pathway acting as a intracellular messenger for the epithelial growth factor receptor (EGFR) [10]. Later Grb2 was found to facilitate the activation of Sos1 by growth factor receptors either by direct binding [11] or through binding to other adaptor proteins which are directly bound to these receptors such as FRS for FGFR signaling[12] and IRS to elicit insulin receptor induced Sos1 activation and the Ras signaling cascade [13]. Additionally the RasGEF Cdc25 was found through studies in the yeast *S. cerevisiae* as a link between the adenylate cyclase pathway and Ras activation [14] and later the mammalian homolog was established [15]. In murine embryonic cells, the Cdc25 mediated activation of Ras signaling was found to be an important regulator of early development [16].

The Ras enzymes have an intrinsic rate of hydrolysis thus deactivating the enzyme; however this rate is insufficient for appropriate biological control. In 1987, Trahey and McCormick isolated an enzyme, which came to be known as p120 RasGAP, that binds the Ras enzymes and accelerated the rate of hydrolysis of GTP by 300 fold [17,18]. Later NF2 was also discovered to act as a RasGAP during the search to characterize the tumor suppressor responsible for Neurofibromatosis type II, an inheritable condition causing benign brain tumors that result in loss of hearing [19]. These RasGAPs increase the hydrolysis of GTP bound Ras by binding to the catalytic site on this Ras and reorienting a water molecule using an arginine residue dubbed the "arginine finger." Upon RasGAP binding to Ras this water molecule becomes oriented in a position favoring a nucleophilic attack on the GTP nucleotide [20] . This Ras cycle of activation and inactivation is depicted in **Figure 1.**

Figure 1

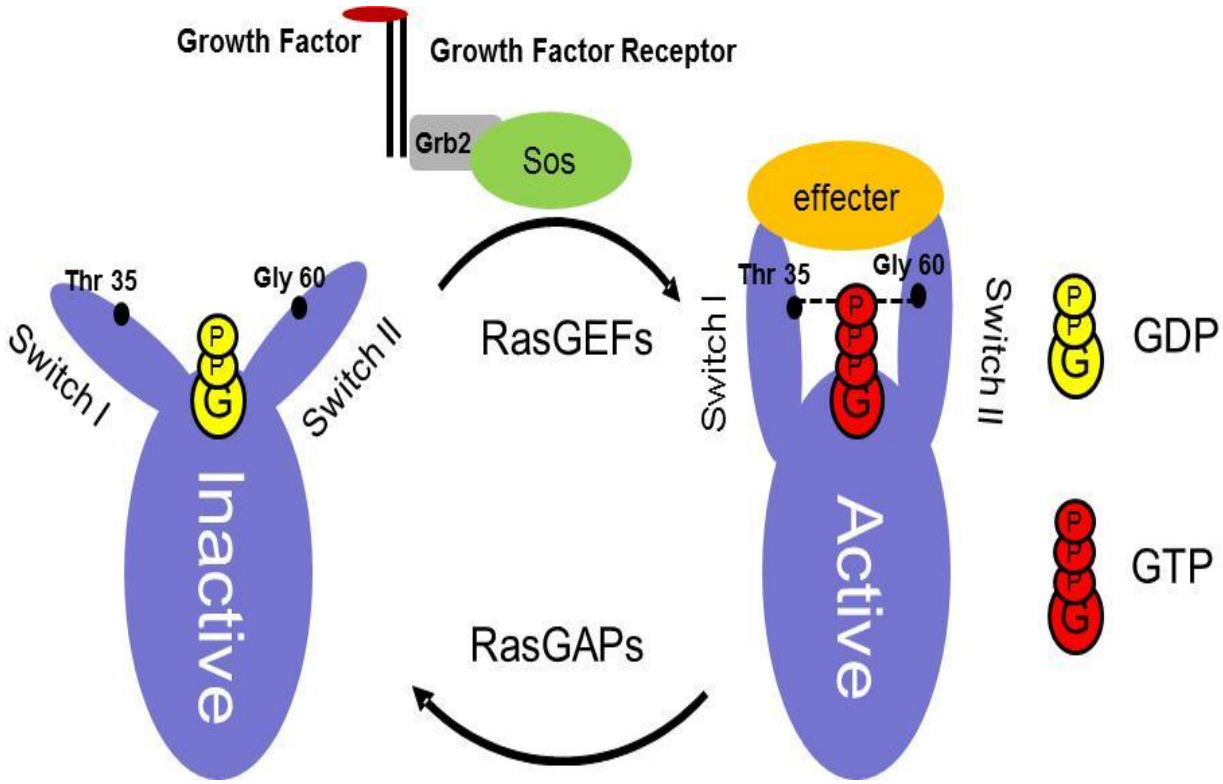

Figure 1: Mechanism of Ras activation. After a growth factor binds a growth factor receptor, Grb2 binds to the receptor allowing the activation of the Sos RasGEF proteins. These Sos proteins promote the dissociation of GDP allowing for the binding of GTP. The gamma phosphate of GTP interacts with the switch I and II regions of Ras resulting in dramatic structural changes allowing effecter binding and activation. Ras has intrinsic GTPase activity and thus removes the gamma phosphate the bound GTP to yield GDP. This conversion is aided by the binding of RasGAPs.

1.1.2 Ras localization

In addition to the nucleotide exchange to GTP, localization of the protein to membranes is necessary for activation of Ras. This localization is accomplished by recognition of post-translational modifications in the C-terminus "hypervariable region" where anchoring moieties are attached [5]. Within this region, a CaaX box of Ras gets farnesylated at the Cys residue in resulting in the insertion for Ras into cellular membranes. This is followed by the tripeptide (aaX) being cleaved from the C-terminus by a prenyl-protein specific endoprotease. The modified C-terminus is then methylated by a methyltransferase in a fashion unique to different Ras isoforms. HRas undergos palmitoylation on two cysteine residues adjacent to the CaaX box and NRas has a single cysteine site that undergoes palmitoylation. These palmintoylations result in the anchoring of these proteins to the membrane. The KRas4A splice variant undergoes a single palymitoylation step similar to NRas but KRas 4B differs in this hypervariable region by having this site replaced by a stretch of positively charged lysines in this region which associate with negatively charged membrane lipids [21]. This result of these modifications is the movement of HRas, NRas, and KRas4A from assembly in the endoplasmic reticulum to the golgi appratus and then to caveloae, a cholesterol binding protein in the membrane[22]. These Ras isoforms then undergo a dynamic cycle of palmitoylation and de-palmitoylation allowing shuttling between the plasma membrane and the golgi apparatus. In contrast, KRas is transported directly from the ER to the membrane by unknown mechanisms and is found independent of caveloae in membranes [23]. The localization of the different Ras isoforms is represented in **Figure 2**.

Figure 2

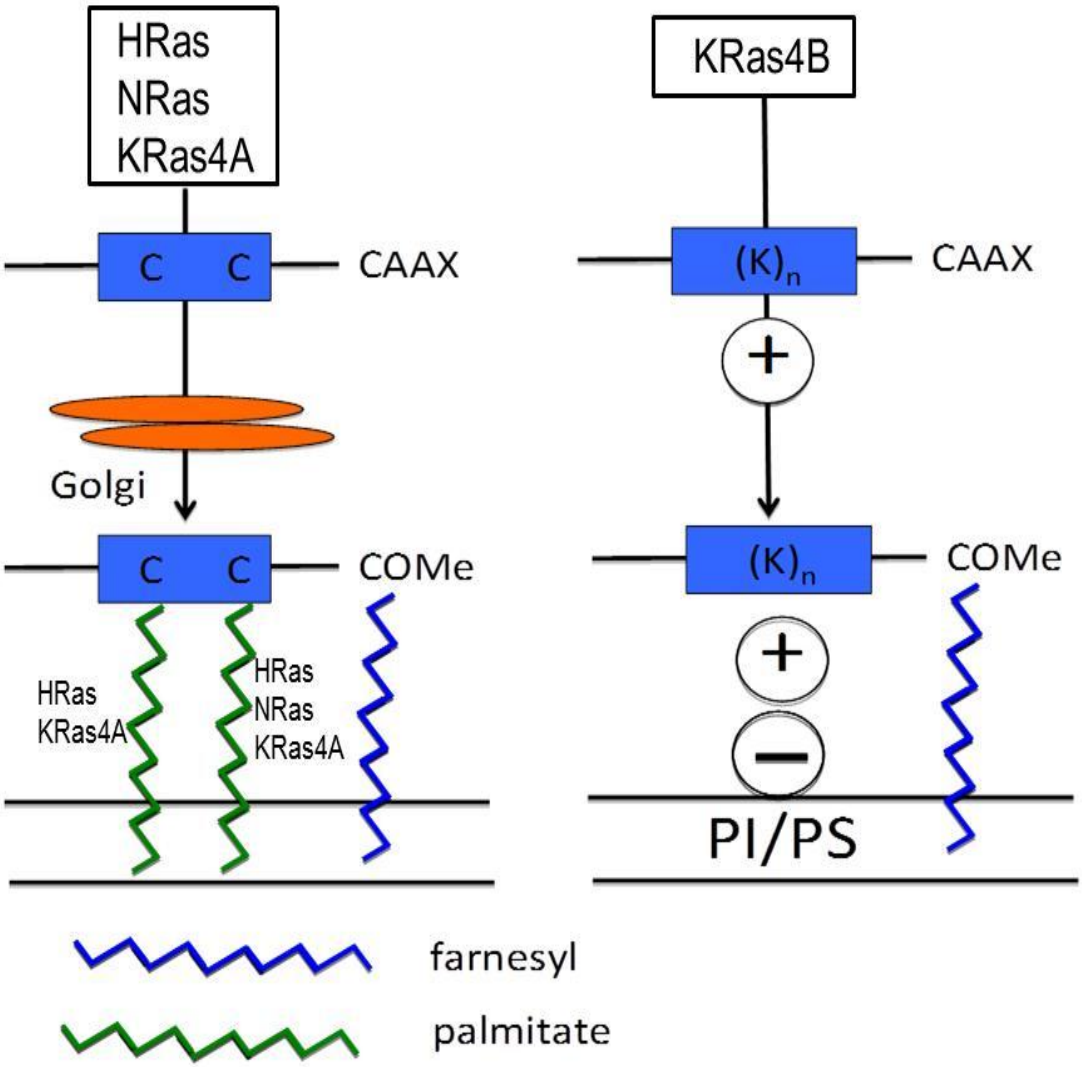

Figure 2: Localization of Ras isoforms to the membrane. The Ras isoforms are anchored to membranes through the addition of a farnesyl group, NRas is additionally anchored to the membrane through the addition of a single farnesyl while HRas and KRas4A have a second farnesyl group. Alternatively KRas interacts with the membrane through a stretch of lysines which create a positive charge attracting the enzyme to negatively charged membrane lipids.

1.1.3 *KRAS* in development

Despite their high homology the function of the Ras proteins differs significantly in normal physiological signaling. Both *HRAS* and *NRAS* have been found to be dispensable for normal development in mice[24,25] as has the *KRAS4A* splice variant of *KRAS*[26]. Additionally, the concurrent deletion of *HRAS* and *NRAS* shows no discernible phenotype [27].In contrast, *KRAS4B* knockout is embryonic lethal although the introduction of alternative *RAS* isoforms at the *KRAS* locus will rescue this phenotype[28]. *KRAS4B* deficient embryos fail in gestation between day 12 and day 14 post fertilization and this lethality is thought to be due to hematopoietic defects caused by a dysfunctional microenvironment in the fetal liver. Despite this, many tissues in the developing mouse undergo normal growth and differentiation despite no compensatory increases in levels of HRas or NRas protein expression being observed [25]. Like *KRAS* deletion microinjection of a dominant negative Ras N-17, which abrogates all Ras signaling was embryonic lethal and suggested that Ras activity is required for mouse embryos to develop beyond the two cell stage presumed to be due to the necessity of this pathway for autocrine factor growth stimulation [29].

In humans a series of inheritable and spontaneous genetic modifications give rise to growth deformities known collectively as “RASopathies.” These are a collection on syndromes all arising from mutations that result in the improper activation of the Ras pathway, and thus may serve as a model for the role of Ras in normal development [30]. The most common RASopathy is the inheritable disorder Noonan syndrome, occuring in 1/1000 to 1/2500 individuals in the United States. This disorder can be caused by activating mutations in *SOS1*, *KRAS*, or inactivating mutations in *SHP2*, a phosphatase that acts on growth factor regulated pathways, including *RAS*. The sites of these activating mutations in *KRAS* are different than those seem in human tumors [31]. This deregulated Ras signaling leads to an extensive set of developmental problems including facial dysmorphism, skeletal defects, blood defects, heart problems, neurological disorders and dwarfism [32].

1.2 KRas signal transduction

There are seven confirmed downstream signaling proteins activated by KRas[33] . The first of these identified was *RAF1*, revealed through detailed screening in *Drosophila melanogaster* where Ras and Raf were shown to phenocopy each other in the regulation of eye[34] and phenocopy vulval fate in *C. elegans* development[35]. This enzyme has been thoroughly characterized as an activator of Mek- Erk signal transduction, important for growth and development[36]. Mammals process three Raf isoforms, *ARAF*, *BRAF*, and *RAF1*. *BRAF* is the isoform with the greatest similarity to Raf in *Drosophila* harboring acidic resides in sites phosphorylated through growth factor stimulation in C-Raf (*RAF1*) and the ramifications of this difference remains unclear [37]. Ras is known to primarily utilize B-Raf to elicit the Mek-Erk response, while C-Raf and A-Raf may have evolved to serve both alternative functions including the inhibition of differentiation and promotion of endocytosis respectively [38,39]. The next Ras effecter elucidated was the p110 catalytic subunit of PI3K[40]. When discovered, PI3K had already been characterized as an enzyme responsible for converting the membrane lipid PIP_2 to PIP_3. PIP_3 results in the recruitment of a specific subset of signaling kinases containing a pleckstrin homology (PH) domain to the membrane for activation. The best characterized of the PH domain containing proteins in this group is Akt which plays an important role in growth and metabolism. Four isoforms of PI3K exist: alpha, beta, delta and gamma of which *a*lpha and gamma are confirmed Ras effecters [41]. Mice created with a PI3Kα isoform which was genetically modified to be deficient in Ras binding showed embryonic lethality due to deficient lymphogenesis, displaying a phenotype similar to mice with vascular endothelial growth factor receptor-3 (*VEGFR3*) deficency [42]. These proteins allowed the elucidation of the common structural features of Ras effecters, the Ras binding domain or the Ras association domain (RA), and more effecters began to emerge as a result of massive screening efforts. The first of these was *RALGDS*, an activator the *RALA* and *RALB* GTPases, which contains an RA domain[43]. The Ral GTPases have been demonstrated to play an important role in endocytosis,

the exocyst complex, and nutrient sensing. Ras also binds PLCε [44], a phospholipase C isoform with an RA domain responsible for Ras mediated production of the membrane lipid DAG which results in calcium release and activation of the PKC signaling cascade[45]. Finally, Ras binds Tiam1, an enzyme which is utilized in integrin signaling[46] and plays an extensive role in T cell trafficking through its control of the chemokine and S1P response making it necessary for the mounting of an appropriate immune response[47].

While these effecters are associated with growth and survival another set of Ras effecter RA domain containing proteins associated with apoptosis have been identified; namely the RASSF family of enzymes[48]. While the entire set of RASSF proteins have a RA domain, only a subset is confirmed as Ras binders. While it is known that the Ras-RASSF complex engages the pro-apoptotic complex Mst1 many details of this pathway remain to be discovered[49]. The Ras effecters are shown in **Figure 3**.

Figure 3

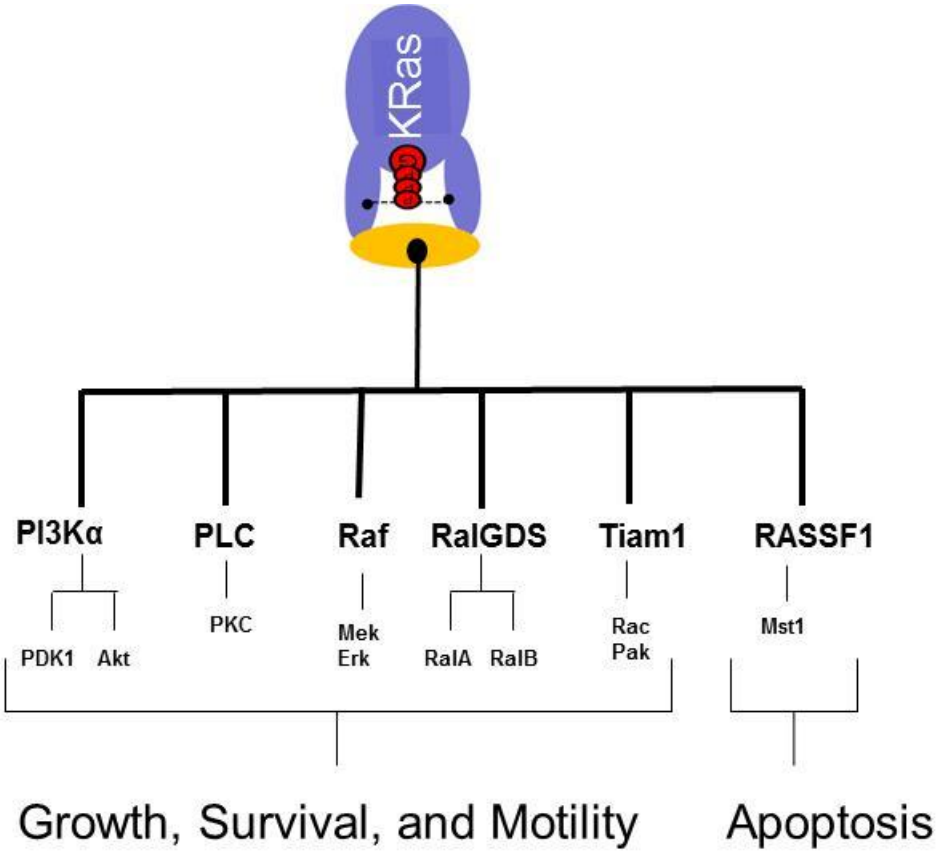

Figure 3: Ras effecter pathways. Validated effecters of Ras signaling and the pathways activated by each. A majority of Ras effecter pathways promote cellular functions such as growth, survival, and motility. Unique among these effecters is RASSF1 which is known to induce apoptosis.

1.3 K*RAS* in Cancer

The Ras proteins have been intertwined with the study of cancer biology cancer since the initial discovery as the oncogenic Harvey sarcoma activating virus in 1964 and the Kirsten murine sarcoma virus in 1967[2,50]. In 1981, the insertion product from these viruses was identified in DNA isolated from a human cancer cell line and by 1982 it was discovered that mutations were present in *RAS* which promoted transformation [3]. Over thirty years later, we know an estimated 320,000 individuals diagnosed with cancer in the US will carry mutant *KRAS* (mut-*KRAS*), yet there is still no effective therapy directed against activated KRas [51].

Of the *RAS* isoforms, *KRAS4B* is the most frequently activated through mutation in human cancer. Mutations in *KRAS* are particularly prevalent in cancers that arise from the ectoderm, such as colorectal cancer [52], lung cancer [53] and pancreatic cancer [54] for reasons not currently delineated. *KRAS4A* is not activated in cancer and instead is thought to induce apoptosis upon activation, even being hypothesized to be a tumor suppressor [55]. *HRAS* and *NRAS* are both known to be activated in specific disease types with *HRAS* commonly activated in bladder cancer and *NRAS* being activated in melanoma. The reason for the disease specific prevalence of activating mutations in these isoforms remains a matter of debate [56].

1.3.1 Activating *KRAS* mutations

Amino acid substitution mutations occurring in codon 12 are the most frequent in human tumors but substitutions in codons 13 and 61 also occur and result in KRas activation. These mutations result in the enzyme being “locked” or spending increased time in the GTP bound state due to an insensitivity to RasGAPs [17]. Glycine, an amino acid lacking a side chain, is the amino acid found at both the 12 and 13 codons in the wild type KRas protein. The introduction of any side chain containing amino acid at the codon 12 or 13 positions with the exception of proline serves to hyperactivate the KRas enzyme [57]. These amino acids at codon 12 inhibit the formation of Van der Waals bonds between RasGAP and Ras by disrupting the proper orientation of the catalytic glutamine for the γ-phosphate of GTP found at

codon 61[58]. Alternatively, codon 61 substitutions that occur less frequently, activating KRas through a similar mechanism indicating the essential nature of codon 61 in KRas deactivation. Intriguingly, despite the observation that a majority of amino acids at codons 12,13 and 61 are activating for KRas particular amino acid substitutions are associated with both cancer and particular codon and amino acids are associated with particular types of cancer[56].

1.3.2 *KRAS* as a driver of tumorigenesis

Early studies to establish *KRAS* as a driver of tumorigenesis were hindered by the finding that overexpressed activated KRas in mouse embryonic fibroblasts resulted in growth arrest unless cell cycle inhibitory checkpoint proteins are deleted [59]. It was later discovered that endogenous levels of active KRas in these cells leads to overexpression of key components of the cell cycle and enhanced proliferation without the deletion of these checkpoints [60]. *KRAS* mutations are among the highest prevalence in solid tumor malignancies as approximately 30% of cancer patients are likely to have *KRAS* mutated tumors [61]. *KRAS* has also been established in multiple systems to be integral in driving other hallmarks of cancer development and progression, such as the evasion of apoptosis and angiogenesis under hypoxic conditions[62], cancer invasion into proximal tissues and the establishment of cancer metastases at distant sites[63]. In human tumors activating *KRAS* mutations occur frequently in lung adenocarcinomas, particularly non-small cell lung cancer (NSCLC) where around 30% of patients have *KRAS* mutations [64] and in colorectal cancer where approximately 35–40% of patients have *KRAS* mutations, which are classically described as being associated with progression of a benign adenoma to a dysplastic adenocarcinoma[52]. In pancreatic cancer, a majority of ductal endocarcinomas have *KRAS* mutations [54]. Much of the evidence that *KRAS* is driver of tumorigenesis has come from mouse models where a mutant KRas (usually G12D) is specifically activated in a tissue after full development of the mouse to induce tumorgenesis. To fully recapitulate advanced human disease it is necessary to have alteration of a second gene with *INK4A/ARF* deficiency

cooperating with *KRAS* in the induction of mouse pancreatic tumors [65] and the loss of *APC* cooperating with *KRAS* in the induction of colon tumors [66]. In contrast to these finding is the observation that mutant *KRAS* is sufficient by itself to induce cancer in the lungs [67]. However, the combination of *KRAS* with other genetic alterations commonly found in lung tumors, such as *STK11* (LKB1) or p53 loss, increase the severity of the disease resulting in decreased differentiation and increased metastasis [68], providing increased resistance to multiple therapies [69].

1.3.3 *KRAS* in cancer therapy

In the last ten years the focus of cancer therapy has shifted from the inhibition of global cellular processes, particularly chemotherapy that aims to inhibit cell division, to targeted therapies to inhibit the specific deregulated enzymes found uniquely in tumors. Arguably the first attempt at a "targeted therapy" was against active Ras. While some of these efforts focused on the development of a small molecule mimetic to RasGAP[70], the most promising approach was thought to be the inhibition of Ras farnesylation which would block the post translational modification responsible for the correct membrane localization of active Ras with its effecters and thus inhibit its activity [71]. Additional excitement behind this concept was driven by the knowledge that the farnesyl pyrophosphate that attaches this group to proteins is an obligate intermediate component of the mevalonate-cholesterol synthesis pathway already targeted by the drug lovastatin, approved by the FDA in 1987. However, the clinically relevant concentration was found to be much lower than the concentration needed to block Ras farnesylation ruling out this agent as a viable option for cancer therapy[72]. The effort was specifically targeted toward the development of agents inhibiting the enzyme responsible for the addition of the farnesyl group to Ras, namely farnesyltransferase, and resulted in the development of potent inhibitors to this enzyme [73]. These inhibitors showed antitumor activity in HRas driven models [74]. However it was soon found that both KRas and NRas could undergo an alternative prenylation via the geranylgeranyltransferase enzyme when

farnesyltranferase was inhibited still allowing for correct membrane localization[75]. As activated KRas and NRas are far more common in human cancers than HRas the FTIs subsequently failed in clinical trials but are still being evaluated in bladder cancer which has a high proportion of *HRAS* mutations[56].

From this early role as a candidate target for directed therapy, today mutated *KRAS* has emerged as a confirmed predictor of resistance to many targeted cancer therapies[76]. While, the effects of mutated *KRAS* on chemotherapy are still debated. In targeted treatment *KRAS* is widely accepted as a resistance mechanism for growth factor receptor directed therapies such as EGFR inhibitors, where it serves as a clinical marker which excludes such treatment for patients with colorectal cancer [77]. Therapies to individual KRas effecters have proven effective in diseases where KRas effecters are activated independently of KRas including the clinical activity of selective BRaf inhibitors in melanomas with activating BRaf mutations [78], and studies showing increased efficacy of PI3K inhibitors in PI3K mutant tumors [79]. In contrast, mutant *NRAS* or *KRAS* have shown to predict lack of response to both these agents [80]. This is hypothesized to result from redundant growth and survival signals relayed simultaneously through Ras which activates multiple effecters simultaneously. This led to the idea that concurrent inhibition of multiple KRas effecters may lead to patient response in tumors with a mutant KRas [79] currently being tested in clinical trials.

Materials and methods

2.1 BATTLE clinical trial

Data from the BATTLE clinical trial of patients with refractory NSCLC who agreed to a baseline tumor biopsy procedure, receiving either erlotinib, vandetanib, bexarotene and erlotinib, or sorafenib was analyzed for the effects of different mut-KRas amino acid substitutions on patient progression free survival. Radiographic imaging of tumors was reviewed to determine suitability for biopsy. Eligibility included age $\geq$ 18 years and adequate performance status (ECOG grade 0 – 2). Prior treatment with erlotinib was allowed but these patients were excluded from the erlotinib-containing study arms, and stable (for at least 4 weeks) or treated brain metastases were permitted. All participants provided written informed consent.

2.2 Patient microarray data

Frozen tissue for mRNA profiling was obtained from 189 patients. Among 139 patients with available gene expression profiles, 101 were randomized and evaluable for 8 week disease control. The patient breakdown was 27 erlotinib, 8 erlotinib and bexarotene, 47 sorafenib, and 19 vandetanib. All steps leading to generation of gene expression profiles from patient tumor core biopsies were conducted by the University of Texas M.D. Anderson Cancer Center Genomics Core Facility using the human Gene 1.0 ST Array (Affymetrix). RNA was extracted and purified from OCT-embedded tissue using the RNeasy Mini Kit (Qiagen) including on-column DNase (Qiagen) digestion as described by the manufacturer's protocol. An H&E stained section of all the samples was available to check for presence of stratified epithelium. After RNA quantification using a ND-1000 spectrophotometer (Nanodrop Technologies), all RNAs were serially diluted in RNAse-free water to obtain a 250 pg/μL stock solution. RNA quality was measured by analyzing separation trace of RNA using the RNA6000 PicoAssay for the Bioanalyzer 2100 (Agilent). Aliquots were prepared and stored at -80°C. The

same RNA was used for all experiments as starting RNA for amplification. Each aliquot was used once.

RNA amplifications were performed using the WT-Ovation™ Pico RNA Amplification System (NuGEN). For all experiments, the manufacturers' protocols were strictly followed. The Ribo-SPIA™ technique is a three-step process that generates amplified cDNA from as little as 500 picograms of total RNA. First strand cDNA is prepared from total RNA using a unique first strand DNA/RNA chimeric primer mix. The primers have a DNA portion that hybridizes either to the 5' portion of the poly(A) sequence or randomly across the transcript. Reverse transcriptase extends the 3' DNA end of each primer generating first strand cDNA/mRNA hybrid. Second strand cDNA synthesis step generates double stranded products with RNA-DNA heteroduplex at one end. The third step is the DNA amplification using a specific DNA/RNA chimeric primer, DNA polymerase and RNase H in a homogeneous isothermal assay that provides highly efficient amplification of DNA sequences. RNase H is used to degrade RNA in the DNA/RNA heteroduplex at the 5' end of the first cDNA strand. This results in the exposure of a DNA sequence that is available for binding a second SPIA™ DNA/RNA chimeric primer. DNA polymerase then initiates replication at the 3' end of the primer, displacing the existing forward strand. The RNA portion at the 5' end of the newly synthesized strand is again removed by RNase H, exposing part of the unique priming site for initiation of the next round of cDNA synthesis. The process of SPIA™ DNA/RNA primer binding, DNA replication, strand displacement and RNA cleavage is repeated, resulting in rapid accumulation of cDNA with a sequence complementary to the original mRNA. WT-Ovation™ Pico products (NuGEN) are labeled using the FL-Ovation™ cDNA Biotin Module V2 (NuGEN). Each labeled cRNA targets are synthesized according to manufacturer's protocols. The quantity and quality of the amplified cRNA or cDNA were assessed by a ND-1000 spectrophotometer (Nanodrop Technologies), and Agilent Bioanalyzer (Agilent Technologies), respectively.

Hybridization mixtures were prepared according to Affymetrix procedures to accommodate 5 µg of cDNA targets from NuGEN amplification. Human Gene 1.ST platform were hybridized, revealed and washed according to the Affymetrix protocol. Gene chips were scanned using a 7 G scanner (Affymetrix) and images (DAT files) were converted to CEL files using GCOS software (Affymetrix).

2.3 Cells and culture conditions

Cell lines were provided by Dr. John Minna (UT South Western, Dallas, TX) or obtained from the the American Type Culture Collection (ATCC) and grown in RPMI media, unless otherwise specified by the ATCC. The identity of each cell line was confirmed by DNA fingerprinting by the Univeristy of Texas M.D. Anderson Cancer Center Characterized Cell Line Core Service at the same time as total protein lysate preparation. Immortalized human bronchial epithelial cells (HBEC3-KT) containing wild type and mutant KRAS were maintained in K-SFM (Life Technologies Inc) media containing 50 µg/mL of Bovine Pituitary Extract (BPE) (Life Technologies Inc.) and 5 ng/mL of EGF (epidermal growth factor) (Life Technologies Inc.) as described previously[81]. All cell lines were mycoplasma tested by e-Myco kit (Boca Scientific). MiaPa Ca-2 and HCT-116 and the isogenic variants lacking an oncogenic KRAS were kindly provided by Dr. Natasha Ignatenko (University of Arizona, Tucson,AZ).

2.4 Preparation of protein lysates and reverse-phase protein array (RPPA).

For each cell line, protein lysate was collected from sub-confluent cultures after 24 hours (h) in media with 10% fetal bovine serum (FBS) (“full serum’), 0% FBS (“serum starved”), or 24 h of 0% FBS followed by 30 minutes of 10% FBS immediately prior to protein harvest (“serum added”). For total protein lysate preparation, media was removed and cells were washed twice with ice cold phosphate buffered saline (PBS) containing Complete protease inhibitor cocktail tablets and PhosSTOP Phosphatase inhibitor cocktail tablets (2 tablets each per 500mL PBS) (Roche Applied Science) and 1 mM Na_3VO_4. Lysis buffer (1% Triton X-100, 50 mM HEPES [pH 7.4], 150 mM NaCl, 1.5 mM $MgCl_2$, 1 mM EGTA, 100 mM

NaF, 10 mM NaPPi, 10% glycerol, 1 mM phenylmethylsulfonyl fluoride, 1 mM Na_3VO_4, and 10 µg/mL aprotinin) was added to the cells and samples were vortexed frequently on ice for 20 minutes, followed by microcentrifugation at 14,000 rpm for 10 min. Cleared supernatants were collected, followed by protein quantification using the BCA reaction kit (Pierce Biotechnology, Inc.). Proteins and phosphoproteins were then quantified by reverse phase protein array (RPPA), as previously described[82]. After quantification, data was logarithm transformed (base 2) for further processing and analyses. Then median-control normalization was applied on the dataset. The statistical analyses were performed using R (version 2.7.0).

2.5 Immunoblots and immunoprecipitations

Cells were washed twice with ice-cold PBS and lysis buffer containing 50 mmol/L HEPES (pH 7.5), 50 mmol/L NaCl, 0.2 mmol/L NaF, 0.2 mmol/L sodium orthovanadate, 1 mmol/L phenylmethylsulfonyl fluoride, 20 µg/mL aprotinin, 20 µg/mL leupeptin, 1% NP40, and 0.25% sodium deoxycholate. Protein concentration was determined by bicinchoninic acid assay (Pierce Biotechnology) and 50 µg of cell lysate protein were boiled for 5 min with denaturing buffer containing 0.25 mol/L Tris (pH 6.8), 35% glycerol, 8% SDS, and 10% 2-mercaptoethanol, loaded on a 10% acrylamide/bisacrylamide gel, and separated by electrophoresis at 150 V for 40 min. Proteins were electrophoretically transferred to a nitrocellulose membrane; preincubated with a blocking buffer of 137 mmol/L NaCl, 2.7 mmol/L KCl, 897 mmol/L $CaCl_2$, 491 mmol/L $MgCl_2$, 3.4 mmol/L Na_2HPO_4, 593 mmol/L KH_2PO_4, and 5% bovine serum albumin; and incubated overnight with anti–phosphorylated Thr^{308}-Akt,Ser^{473}-Akt, anti-CRaf Ser ^{338} Mapk Thr^{202}/Tyr^{204}, p70 S6K Thr^{389} or anti-Akt. (Cell Signaling 1:1000), anti-CNKSR1 (Signal Transduction labs) anti-lamin A/C and anti–β-actin (Santa Cruz Biotechnology1:2000Donkey anti-rabbit IgG peroxidase-coupled secondary antibody (GE Healthcare) was used for detection). For measurement of active RalA and RalB, Ral and RalB activation kits were used (Biorad). Band density was measured using the Renaissance chemiluminescence system on Kodak X-Omat Blue ML films (Eastman Kodak).

2.6 Viral vector construction

Vectors expressing wild type and mut-KRas-G12C and mut-KRas-G12D were constructed from a previously described vector, pLenti6-KRAS-V12[24], using a site-directed mutagenesis kit (Stratagene) and transected into HBEC cells with stable siP53 as previously described[81]. Correct sequences were confirmed by sequencing for all vectors. Infected cells were selected with blasticidin (2 µg/ml) for 5 days. The cDNA of transformed HBEC3-KT cells were sequenced to confirm presence of KRAS mutations.

2.7 Soft agar growth assays.

Soft agar-growth assays were performed as previously described[81] seeding 1,000 viable cells in 12-well plates in triplicate and counting colonies after four weeks. Each experiment was performed in triplicate.

2.8 Molecular modeling

The HRas proteins in PI3K-HRas complex (1HE8) and RalGDS-HRas heterotetramer complex (1LFD) were employed as templates to build wild-type, G12C and G12D KRas models. The derived models were slightly minimized by NAMD and then molecular dynamics (MD) studies were carried out as reported[83]. Parameters for GTP were generated as the chimeric analog of ATP and guanine using CHARMM27. The system was solvated in a water box in which every protein atom was at least 8Å away from the boundary of the box. Sodium chloride at 100mM was added to neutralize the system charges. After 400ps for equilibrium, we conducted 8ns MD simulations, and the trajectory was recorded every 200fs. Trajectories for the last 6ns were evaluated and they were superimposed with WORDOM[84]. The average structures were obtained and then followed with carbon-tethered energy minimization in MOE to eliminate structural defects. The snapshots in every 100ps were used to calculate the binding of KRas to PI3K and RalGDS using ZRNAK program[85].

2.9 Screening of compounds against isogenic mutant *KRAS* lines.

SW48 and the isogenic KRAS lines harboring G12D, G12C, and G12V were obtained from Horizon Discovery labs on a one year lease. These cells were cultured in McCoys media with 10% FBS to 80% confluency. Cells were then released from flasks via trypsinization and plated into 96-well plates at an initial density range of 2000 cells per well. Cells were allowed 24 hours to attach, and then the following drugs were added to the culture media at a range of concentrations from 0 – 5 μM: GSK60693, GSK1120212, MK2206, AZD6244 (produced at the MDACC translational chemistry facility). Cells were incubated for 72 hours with the drugs, and then viability was assessed using an MTS viability assay. Cells were exposed to MTS reagent (Promega) dissolved in PBS (Hyclone) at a concentration of 200 μL reagent/mL media for 2 hours. Absorbance was then read at 490 nm, and viability was expressed as a percentage normalized between the negative control (no cells plated) and the condition of cells with no drug added (100% viability) normalized as the upper limit of viability.

2.10 Screening of compounds against NSCLC cell line panel.

Our panel of 30 cell lines and an extensive characterization were a generous gift from Dr. John Minna (UTSW) All cell lines were cultured in RPMI 1640 with 10% FBS. Cells were treated with concentrations of MK2206 and AZ6244 at concentrations 0.01 to 50μM and evaluated for as described above. IC50's were determined using Excelfit.

2.11 siRNA screening

MiaPaCa-2 and M27 were confirmed mycoplasma negative by the siRNA screening service at MD Anderson and maintained in DMEM with 10% FBS. Optimization was carried out using in house optimization methods in house. A parallel screen was then carried out with a genome wide siRNA library (Dharmacon)

2.12 Individual siRNA and plasmid transfection.

For transfection in a six well plate, cells were plated at 100,000 cells per well in 2mls media and allowed to attach overnight. Per well 5µl of Dharmafect 2 (Dharmacon) was added to 200µl OptiMEM (Gibco) and 4µl of the siCNKSR1 smartpool Dharmacon (M-012217-01-0020) or individual siCNKSR1 siRNAs (Qiagen SI02665411) was added to 200µL to OptiMEM in parallel and allowed to sot for 5 minutes. These tubes were mixed and incubated at room temperature for 20 minutes. 1.6 of the appropriate media was then added to this mixture. and then media in the wells removed, This mixture was then added to the cells in a dropwise fashion and the cells were incubated for 48-72 hours. For the GFP control and CNK1 PH domain plasmids 175,000 cellsper well plated in a 6 well plate. Per well 2.5µl of lipofectamine 2000 (Gibco) and 125µl of OptiMEM were combined and 2.5µg of the appropriate plasmid and 125µl of OptiMEM were combined in separate tubes and allowed to incubate at room temperatue for 5 minutes. These two tubes were then combined and allowed to incubate for 20 minutes. 200µl of this mixture was then added to 1ml of fresh media already in the appropriate well and allowed to incubate for 5 hours. The transfection efficiency was determined through the expression of GFP after 24 hours and the cells were counted with a hemocytometer after 72 hours to determine viability.

2.13 Spheroid formation

The plates were optimized for the best cell density and found to be 20,000 cells per mL. The lid was removed from a a 96-well Greiner plate and turned upside down. 20 uL of the 20,000 cells per mL suspension was then added directly into the middle of the circles found on the lid of the 96-well plate forming a small drop. 100 uL of media was added into the corresponding wells, used to maintain the temperature of the drops, and the lid was flipped back over carefully placing it back onto the plate without disturbing the drop. The plate was then placed into the incubator for 3 days to allow the cells to migrate to the bottom of the drop due to gravity. After 3 days, 400 uL of media was added to the corresponding wells a SCIVAX 96-well plate. The lid from the Greiner 96-well plate was removed and placed onto the SCIVAX

plate allowing the drop to come in contact with the media and placed back into the incubator. After one hour, 200 uL of media was removed from the corresponding wells carefully without disturbing the spheroid and imaged.

2.14 Anoikis assay

Transfected cells were grown to sub-confluence in 75-cm^2 tissue culture flasks. For cultures in suspension, cells were detached from the tissue culture flasks using 0.25% trypsin-EDTA (Invitrogen). Once detached, cells were cultured in complete medium on a six-well plate (5×10^5 per well) coated with Ultra Low Attachment Surface (Corning,) for defined hours. The growth rate of cells in suspension were measured using the trypan blue exclusion assay and the viability was measured quantitatively using the Cell Death Detection ELISA (Roche), by detecting cytoplasmic histone-associated DNA fragments (mono- and oligo-nucleosomes) after induced cell death. Briefly, anti-histone antibody is fixed in 96-well plate. After cells harvested, the number of cells needed for the assay was retained (1x 10^5 cells) and lysed. Then, lysed samples were loaded onto plates and after 90 min of incubation, conjugated solution (diluted anti-DNA peroxidase antibody) is pipetted into each well. After further incubation of 90 min, wells are washed and substrate solution containing ATBS (2,2'-azino-di-[3-ethylbenzthiazoline sulfonate]) is added. The plate is read in a plate-reader (Fluostar Omega, BMG Labtech) at 405 nm and 490 nm (reference wavelength), and the data is expressed as absorbance 405-490 nm.

2.15 Cell cycle analysis

0.7 mL of ice cold 100% ethanol was added to 1 x 10^6 stained cells contained in 0.3 mL cold PBS then incubated overnight. The sample was then centrifuged and the supernatant removed. 250 µL of 500 units/mL Rnase in PBS with 1.12% sodium citrate was added to the cell pellet. The sample was then vortexed gently and incubated at 37°C for 30 minutes. 250 µL of propidium iodide (Sigma) at 50 mg/mL was then added to the sample and the cells were

incubated at room temperature for at least 1 hour in the dark. Finally the samples were read on the facility flow cytometer

2.16 Confocal imaging

HEK293T cells were co-transfected with CNK and either wild type or G12D mutant KRAS. 24 hours post-transfection, cells were seeded on glass coverslips and allowed to grow a further 24h and then serum deprived overnight. Cells were fixed with 4% (w/v) paraformaldehyde pH 8.0 for 20min at room temperature. Following 6-7 washes with PBS (pH8.0) the coverslip was mounted onto a slide with mounting medium (0.1% *p*-phenylenediamine/75% glycerol in PBS at pH 7.5–8.0). Confocal laser scanning microscopy was performed with a Leica SP5 confocal microscope system with 63X oil-immersion objective (numerical aperture NA=1.4), a line scan speed of 600 Hz, with image size of 1024x1024 pixels. GFP was excited with an argon-visible light laser tuned to 488 nm, mRFP were excited with a krypton laser tuned to 543 nm. GFP and RFP fluorescence emissions were collected using a photomultiplier tube via 514/10 nm and 595/10 nm band selections respectively.

2.17 Fluorescence lifetime imaging microscopy (FLIM)

FLIM experiments were carried out using a Leica TCP SP5 inverted advanced confocal microscope system with internal photomultiplier tube (PMT) detector for TCSPC (time-correlated single-photon counting). The sample was excited with a tunable femtosecond (fs) titanium-sapphire laser with repetition rate of 80MHz and pulse width less then 80fs (Spectral Physics, Mai Tai BB). The wavelength used for two-photon excitation was 930 nm and the fluorescence was detected through a 525±25 nm interference filter. Images were obtained with oil-immersion objective (numerical aperture NA=1.4), a line scan speed of 400 Hz, with image size of 512x512 pixels. For FLIM analysis the pixels were reduced to 256x256. FLIM data was collected using Becker & Hickl SPC830 data and image acquisition card for TCSPC. The fluorescence decays were fitted with a single exponential decay model using Becker and

Hickl's SPCImage software and the GFP fluorescence lifetimes were displayed in a false colour map.

2.18 Surface plasmon resonance spectroscopy binding assays

All interaction analyses were done with a Biacore 3000 Control Software v3.2, and BIAevaluation v4.1 analysis software (Biacore). The PH domain His-fusion proteins (CNK1 and AKT1) were expressed at the Center for Biomolecular Structure and Function at MD Anderson and immobilized on a NTA chip to a level of 10,000 response units or less. Small molecule analytes at concentrations ranging from 50μM to 0.010 μM were injected at a high flow rate (30 μL/min). DMSO concentrations in all samples and running buffer were 1-5% (v/v)

KRas effecter utilization is determined by the type of activating mutation

3.1 Introduction

A number of previous studies have suggested that the method by which *KRAS* is activated may influence the behavior of cancer cells or patient prognosis [64]. The first studies after the identification of mutant Ras in human patients defining the transforming properties of these performed by Levinson *et al* found differences in transformation dependent on the identity of the amino acid substituted at codon 12 and postulated that different amino acids activating Ras may have different biological outcomes[57]. Early work in the determining crystal structures for the transformed Ras proteins additionally found that the flexibility of the switch II region, responsible for interacting with effecters in the protein was determined by the identity of the substituted amino acid [86]. Subsequent to this work, the multi-center international RASCAL trial, aimed at definitely defining *KRAS* mutation as a poor prognostic event in colorectal cancer, found that those patients with *KRAS* activated by a G to T nucleotide substitution (resulting in a glycine to valine or cysteine amino acid substitution) resulted in a worse prognosis for patients [87]. These results were later validated in the RASCAL II trial [88]. Small studies later suggested differences in cellular invasive capacity [89] and tumorgenicity based on both the identity of the amino acid activating the protein[90] and the codon location of the substitution[91]. Murine tumor models characterizing the effects of activated *KRAS* specifically in the lung have largely focused on the KRas G12D [69,79] substitution although this alteration is more predominant in human colon and pancreatic cancer than in human lung cancer[22]. The most common activating mutation in human lung tumors, a KRas G12C amino acid substitution, has been made in a lung specific fashion in a mouse model but displayed a strikingly different phenotype resulting in a longer time to tumor development than the KRas G12D model displaying a decreased frequency of progression [92]. Notably in murine cells activating KRas mutations showed inconsistences in the activation of the expected KRas effecter pathways with the KRas G12D mutant mice having lowered but constitutive Akt

activation[66] while both KRas G12C and KRas G12V lung models having no detectable Akt activation[92,93]. These observations led to our hypothesis that different activating *KRAS* mutations may have different responses to targeted therapies due to different signaling outputs elicited by the different signaling cascades.

In the BATTLE trial conducted at MD Anderson no association was found between *KRAS* mutations and the targeted therapies used in the trial adding to a conflicted body of literature that showed an inconsistent association between *KRAS* and various trials with targeted therapies. However, when we reexamined the data by looking at the amino acid substitution which activated *KRAS* a significant association was found between a C or V substitution at KRas codon 12 and decreased response to targeted therapies measured by progression free survival with the strongest association found seen with sorafenib. We then looked across a large number of lung cancer cell lines and also expressed the different forms of activated *KRAS* in immortalized human bronchial epithelial cells we observed differential activation of KRas effecter pathways. Finally using the crystal structures of HRas to create a homology model of KRas and comparing the effects of KRas interaction with different effecters we were able to show how different substitutions impacted KRas binding to effecters.

3.2 Results

3.2.1 Patients with different forms of oncogenic *KRAS* vary in their response to targeted therapies

The BATTLE-1 trial for patients with refractory NSCLC was conducted at MD Anderson between November 30, 2006 and October 28, 2009. Patients received either erlotinib, vandetanib, bexarotene and erlotinib, or sorafenib and were additionally tested in mandatory tumor biopsies for markers thought to be associated with response to these agents[94]. Using these criteria, the BATTLE-1 data was reanalyzed for the effect of different mut-KRas amino acid substitutions on patient progression free survival. There were 258 evaluable patients and

the primary endpoint was 8-week disease control rate, with patients being treated until disease progression or unacceptable toxicity. There were 46 total KRas mutations with 43 [95] at codon 12, and no codon 13 mutations. We found that mut-KRas G12C/ V was associated with overall decreased patient progression free survival compared to other mut-KRas (mostly G12D), or WT-KRas (P = 0.046). The negative prognosis conferred by the C or V substitution was most pronounced in the sorafenib treatment arm (P = 0.026) **(Figure 4)** This is the first indication in NSCLC of different amino acids substitutions within mut-KRas influencing patient response to targeted therapy in lung cancer.

3.2.2 Gene expression analysis in patients with different *KRAS* activating mutations

We next analyzed patient gene expression profiles using tumor biopsies from mutant *KRAS* patients to determine which gene probes were responsible for the greatest variation. Using these probes we were able to observe the genes which most accurately defined the differences between the two *KRAS* groups by applying a false discovery rate of 0.3. These probes are displayed in the heat map **(Figure 5)**. The genes probes which showed the greatest variation were primarily involved in cell cycle regulation, particularly mitosis. These gene probes included Polo Like Kinase 1 (*PLK1*) which triggers the G2/M transition through the phosphorylation and subsequent activation of the Cdc25c phosphatase which dephosphorylates and activates the Cyclin B/Cdc2 complex, the primary cyclin complex involved in mitosis Additionally both Cyclin B1 and Cyclin B2 expression were upregulated in those patients without a G12C/V mutation which predominantly consisted of G12D substitutions. The observation that these cell cycle proteins are up regulated in KRas G12D tumors is significant in regards to two previous studies. The first is the finding that KRas G12D selectively drives cell cycle progression in a mouse colon model while NRas G12D selectively promoted inhibition of apoptosis [66]. The second is that a KRas G13D driven colon line was found to be selectively sensitive to knockdown of genes coding components of the mitotic machinery including Plk1when compared with an isogenic line with a silenced mut-*KRAS* allele

when a genome wide shRNA screen was performed, [96]. These BATTLE microarray results indicate that these results may not be universal for oncogenic *KRAS* but specific for the aspartate substitution.

Figure 4

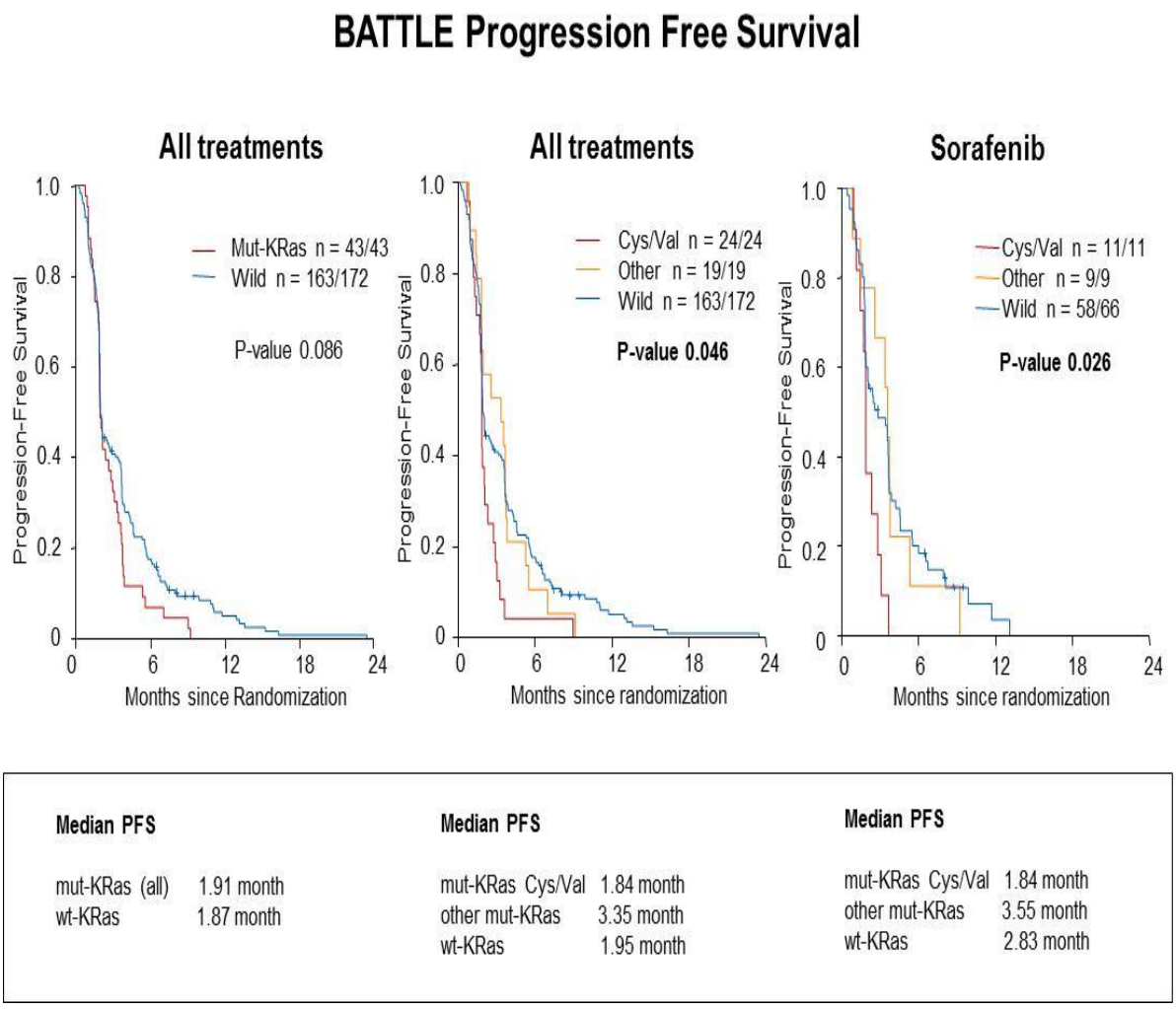

Figure 4: Progression free survival in response to targeted therapies by KRas G12C/V amino acid substitution. Patients were evaluated for progression free survival to targeted therapies by the presence of any activating KRas mutation, and then by the presence of a G12C or G12V mutation or other KRas mutations (mostly G12D). Analysis of patients treated with sorafenib by type of KRas mutation. Patients with a wild type KRas or mutations other than G12C or G12V had significantly longer progression free survival when treated with all targeted therapies and sorafenib. Reprinted with permission from [97]

Figure 5

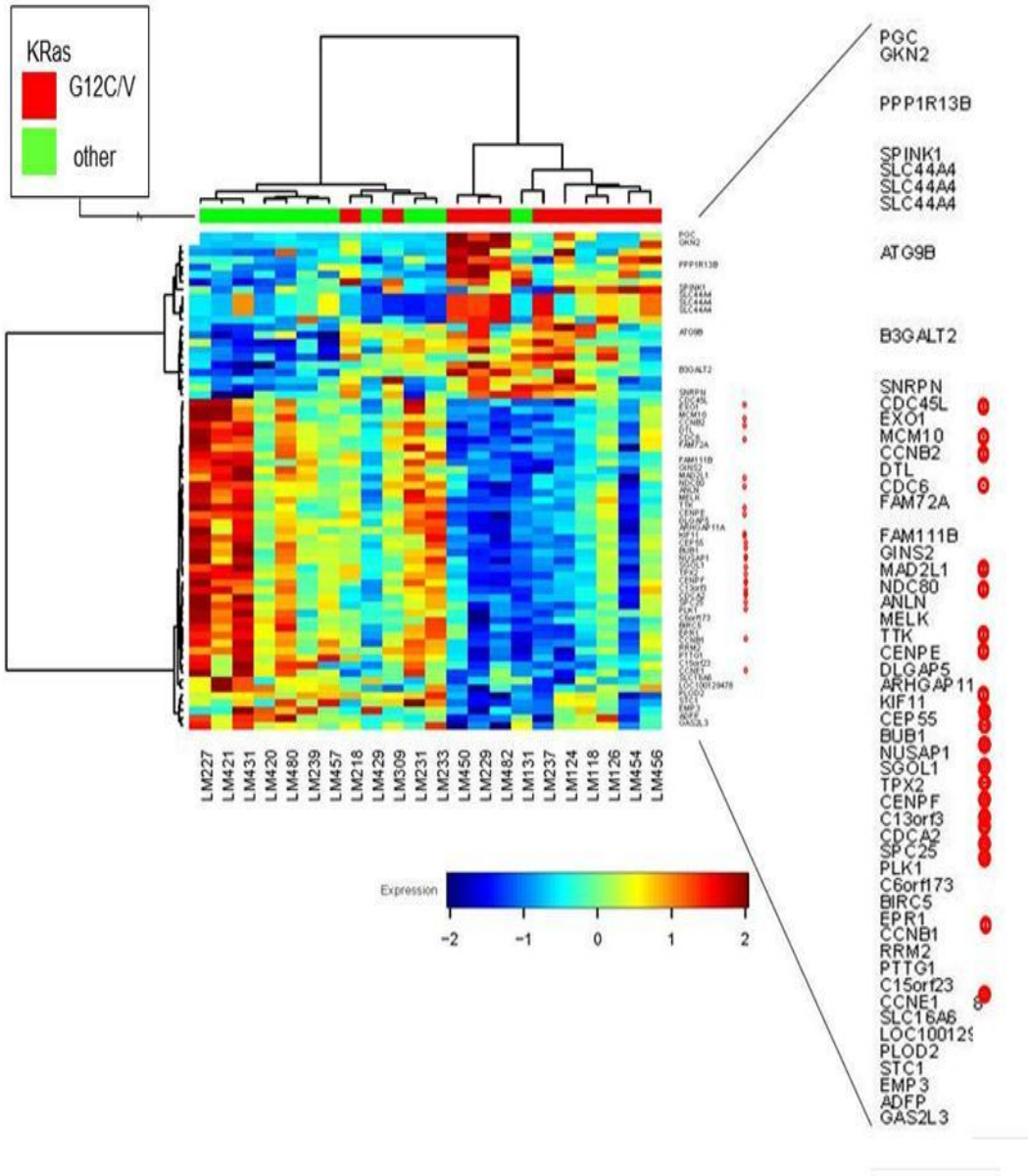

Figure 5: Microarray of BATTLE patients with mutant KRas. Heat map of non-supervised clustering of the expression of the top genes between patients with KRAS G12C or G12V and other activating KRas mutations. Patients with G12C or G12V mutations had lower expression of cell cycle proteins associated with mitotic progression including *PLK1* and *CCNB1* and *CCNB2* (Cyclin B1 and Cyclin B2). Reprinted with permission from [97].

3.2.3 Oncogenic *KRAS* signaling across a panel of lung cancer cells

To explore the differences in signaling activities through a comprehensive analysis of protein signal transduction we conducted reverse phase protein array (RPPA) analysis across a panel of 58 genetically characterized NSCLC cell lines comparing mut-KRas-G12C/ V, other mut-KRas and WT-KRas . The cell lines were grown under three conditions as it is unclear which best recapitulates an in-vivo environment: cells maintained in 10% serum, cells that were starved of serum for 16 hours and cells starved of serum for 16 hr and then serum added back for 30 minutes. The Ras effecters measurable by RPPA were then observed **(Figure 6)**. The KRas effecter Raf activates Mek resulting in cellular proliferation and survival [36]. while p38 is activated by the Ras effecter Tiam1 and has a diverse set of cellular functions [98] Analysis of these proteins showed neither active Mek or p38 showed significant activation differences between the KRas mutant groups or between cell lines with activated KRas and wild type KRas cell lines. In contrast, the target of the Ras effecter PI3K, Akt showed decreased activation measured by phospho-Akt relative to WT-KRas cells in mut-KRas-G12C/ V cells, and elevated in the remaining mut-KRas cells **(Figure 6)**. These findings were confirmed by Western blot analysis in a smaller set of NSCLC cell lines with KRas codon 12 mutations **(Figure7)**. Additionally a subset of genes involved in the Akt signaling pathway were analyzed to determine if signaling was decreased across the entire PI3K-Akt axis or localized to Akt itself. The data from cell lines in our panel of NSCLC lines with mutant KRAS were subjected to hierarchical clustering based on activation of the Akt and mTOR signaling and revealed that while Akt and its effecters were down regulated, mTOR known to be activated by Akt signaling[99] ,was at levels comparable to wild type KRas or other activating KRas mutations **(Figure 8)** Thus in NSCLC cell lines differences in activation of KRas effecter signaling, with mut-KRas G12C/V displaying significantly less Akt activation than other KRas activating mutations, suggesting that mut-KRas G12C/V cells may not activate PI3K as efficiently as other forms of activate KRas.

Figure 6

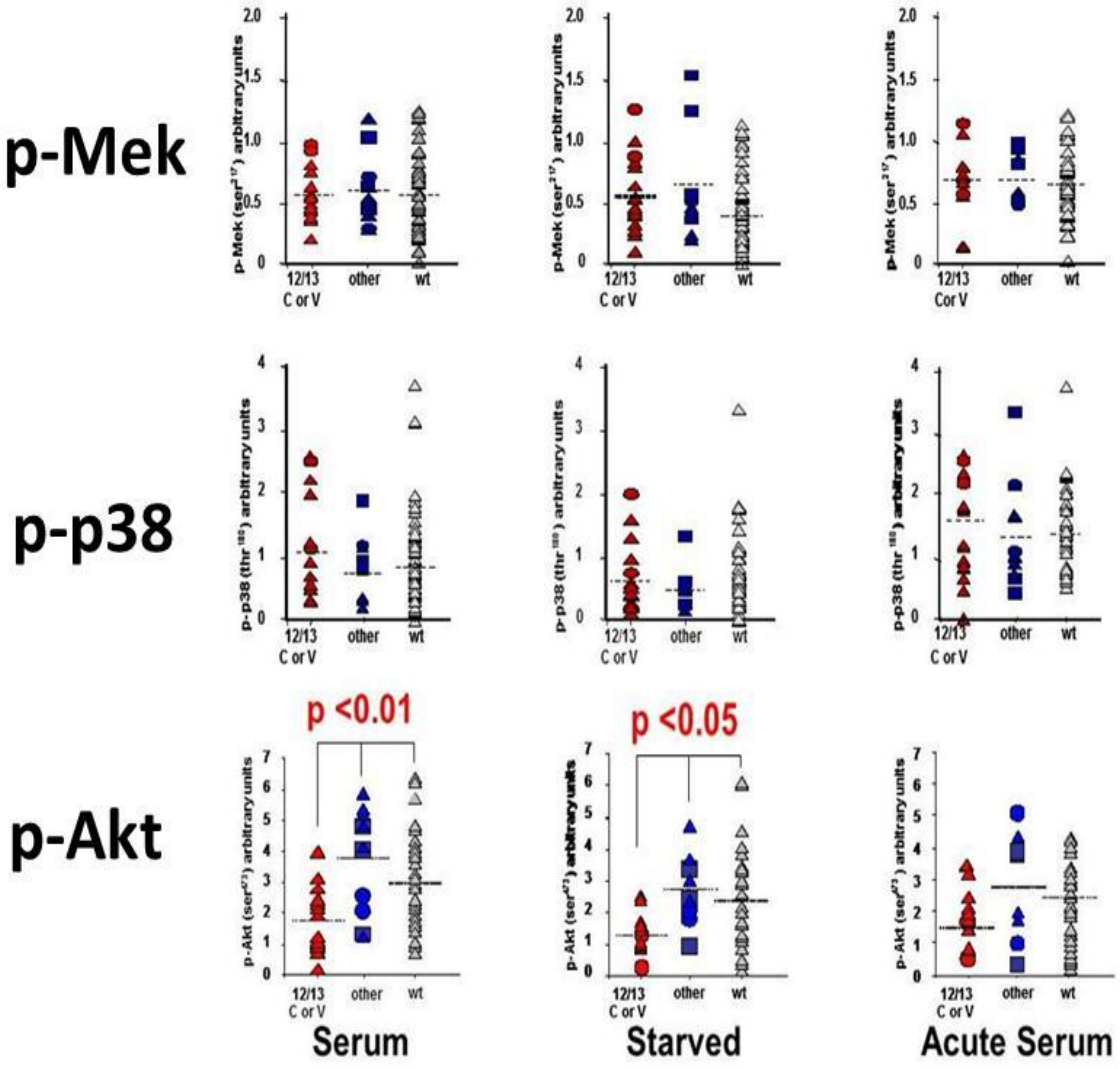

Figure 6: Signaling through KRas effecter pathways in a panel of NSCLC cells. Activation of Ras pathways measured by RPPA of phosphorylated Mek, p38, and Akt in cells grown in serum, in serum free media for 16 hours, or in serum free media followed by an acute 30 minute exposure to 10% serum. Mutant KRas G12C/V, other forms of mutant KRas and Wild type KRas were compared. Activated Akt (phospho-ser473) was significantly reduced in mutant KRas G12C/V when compared to other forms of mutant KRas of wild type KRas in serum or serum free conditions while other forms of mutant KRAS showed higher Akt activation. Reprinted with permission from [97].

Figure 7

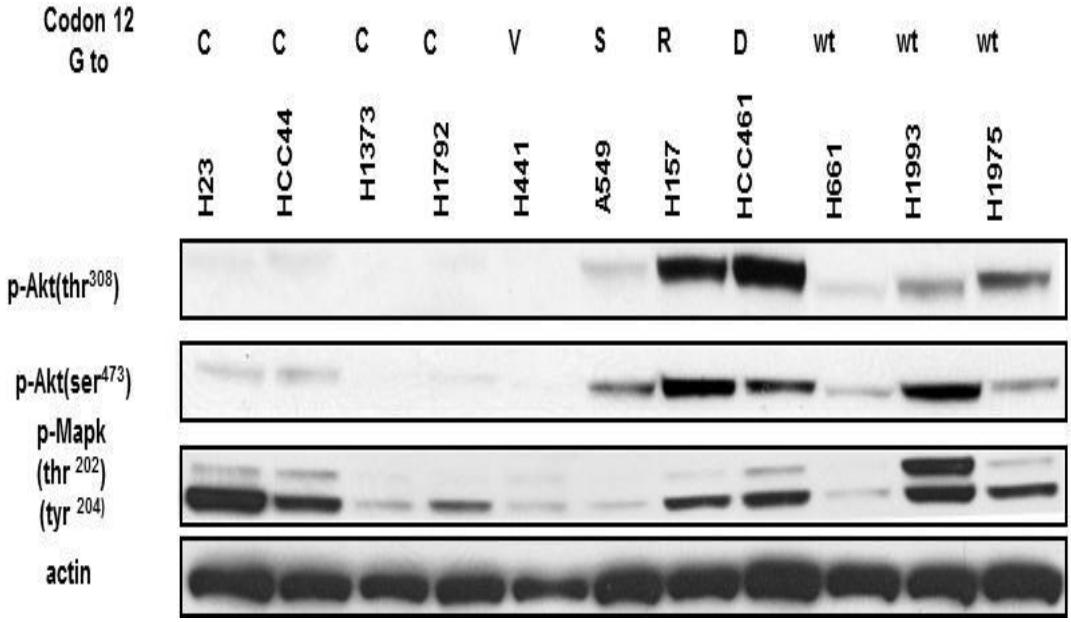

Figure 7: Validation of RPPA findings in a panel of lung cancer cells. Activation of Akt was measured at Akt thr^{308} and Akt ser^{473} across a panel of lung cancer cells stratified by KRas status. Akt was reduced in mutant KRas G12C/V. Mapk activation was additionally measured by phosphorylation of Mapk thr^{202} and Mapk tyr^{204} but showed no pattern of activation with the method of KRas activation. Actin served as a loading control. Reprinted with permission from [97].

Figure 8

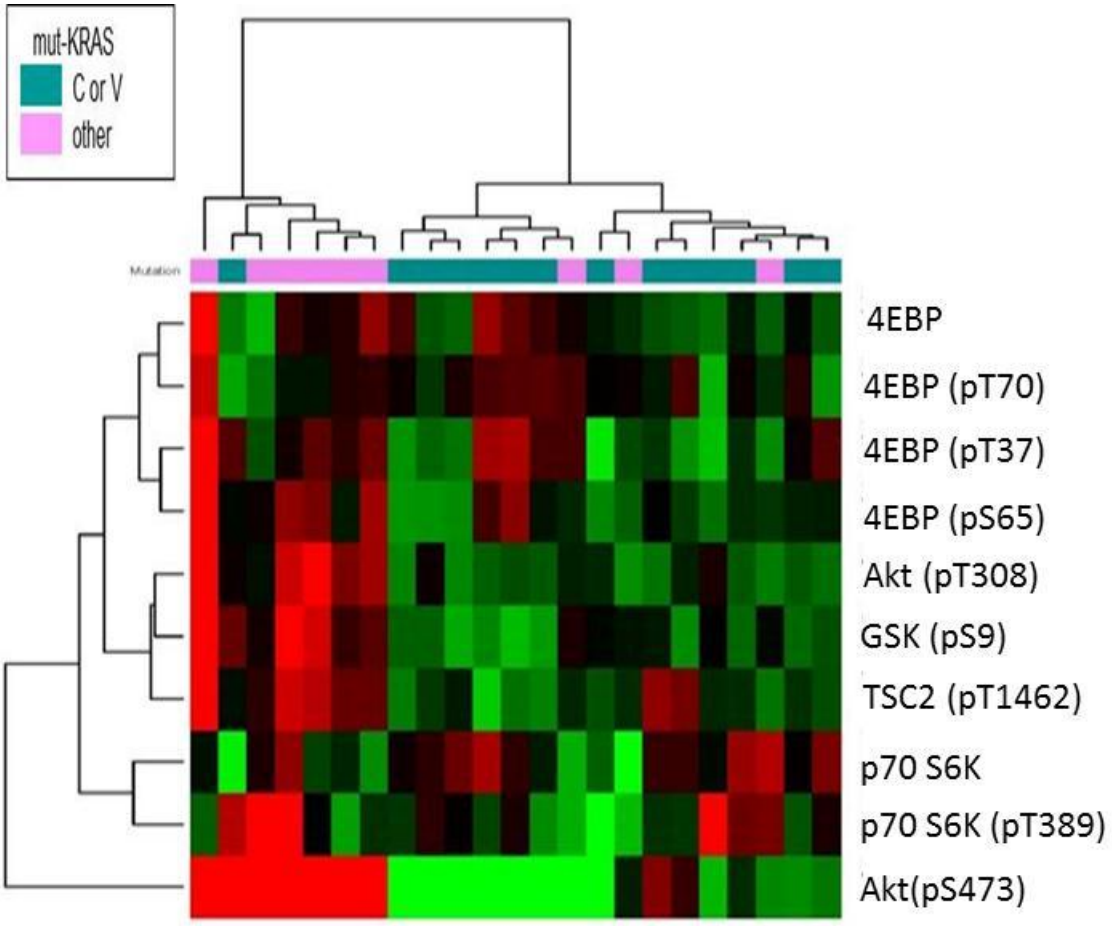

Figure 8: Heatmap of Akt pathway activation. The Akt/mTOR pathway components available on the RPPA organized into a heat map with mutant *KRAS* annotation at the top. As had been observed previously Akt activation was lower in the mutant KRas G12C/V and this was mirrored by activation of the direct Akt effecters GSK and TSC2 as measured by phosphorylation. In contrast, multiple mutant KRas G12C/V lines showed activation of the mTOR effecters p70 S6K and 4EBP1 as measured by phosphorylation. Reprinted with permission from [97].

3.2.4 Oncogenic *KRAS* expressed in HBEC cells

To confirm the findings in a uniform cellular background, the most common mut-KRas in CRC, G12D; the most common mut-KRas in NSCLC, G12C; and WT-KRas were introduced into previously characterized immortalized human bronchial epithelial cells [81] with P53 knockdown (HBECsiP53), as p53 has been shown to induce apoptosis as a result of cellular stress in Ras transformed cells [100]. Plasmid DNA was extracted from the cell lines and KRas was sequenced to ensure that the correct mutt-KRas was present **(Figure 9)**. Additionally elevated levels of KRas protein were seen in the transfected lines. The oncogenic KRas G12D HBECsiP53 cells with the highest Akt activation of the four lines indicating increased activation of the KRas effecter PI3K **(Figure 10)**. In contrast, the KRas G12C mutants had blunted Akt signaling representing the lowest of the four lines. Despite these differences the levels of activated p70 S6K, an indicator of mTOR activity, remained constant between these lines. Additionally, extracts from the four lines were incubated with beads with the Ral binding domain of the shared effecter of RalA and RalB proteins, RalBP **(Figure 11)**. In contrast to what was seen with Akt activation, KRas G12D had the lowest RalA and RalB while KRas G12C and overexpressed KRas WT had the highest. This pattern of signaling is consistent with what was observed previously when these mutations were introduced into the lungs of mice, where mut-KRas G12D induced Raf and Akt activation when expressed both endogenously and ectotoapathally [60] while mut-KRas G12C resulted in only Raf and Ral activation, with minimal Akt activation regardless of expression level[92,101].

Figure 9

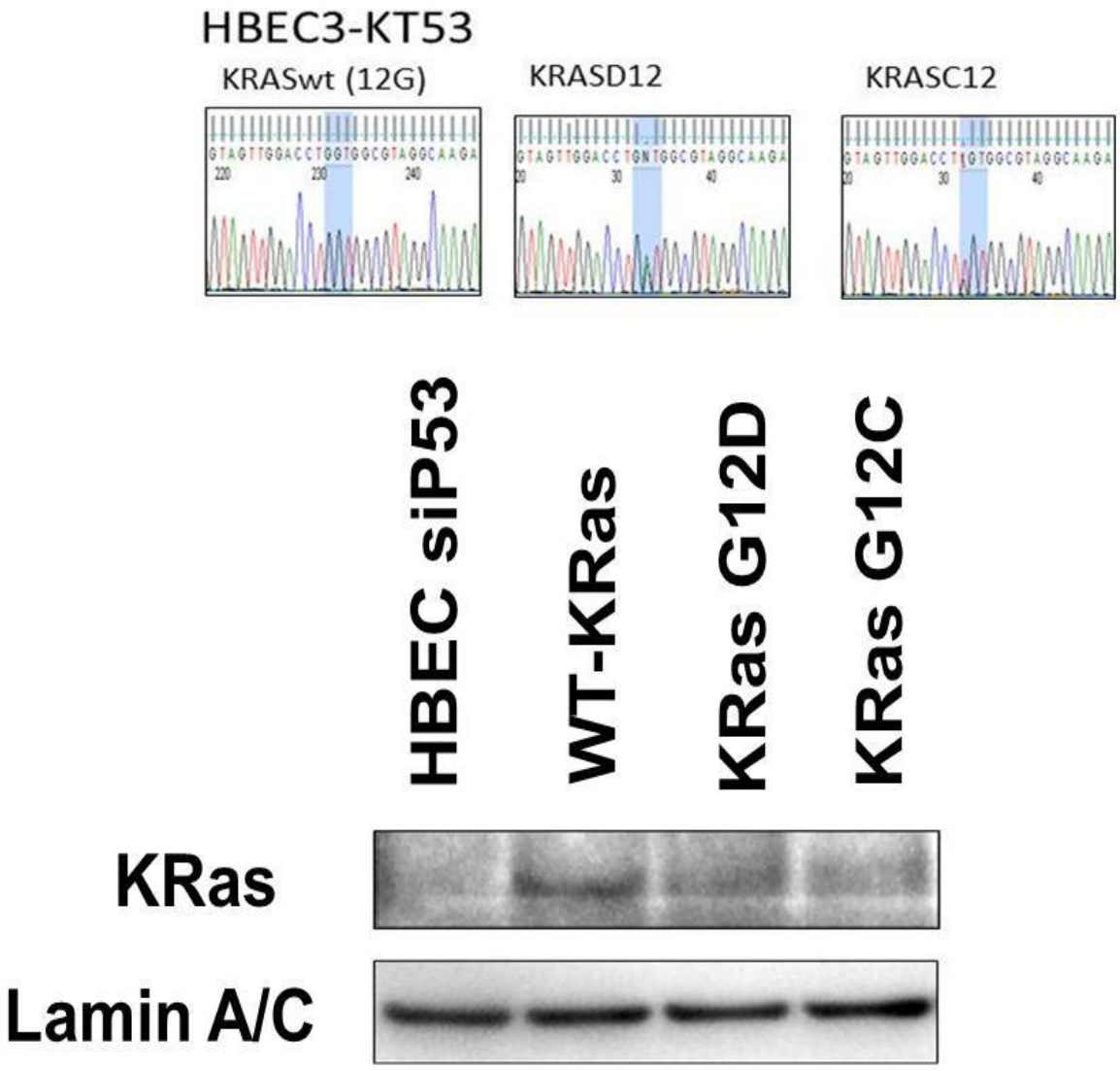

Figure 9: Validation of transfection and expression of wild type and mutant *KRAS* plasmids in immortalized bronchial epithelial cells (HBEC). Sequencing of plasmids extracted from HBEC cells and measured of KRas protein in HBEC cells. Reprinted with permission from [97].

Figure 10

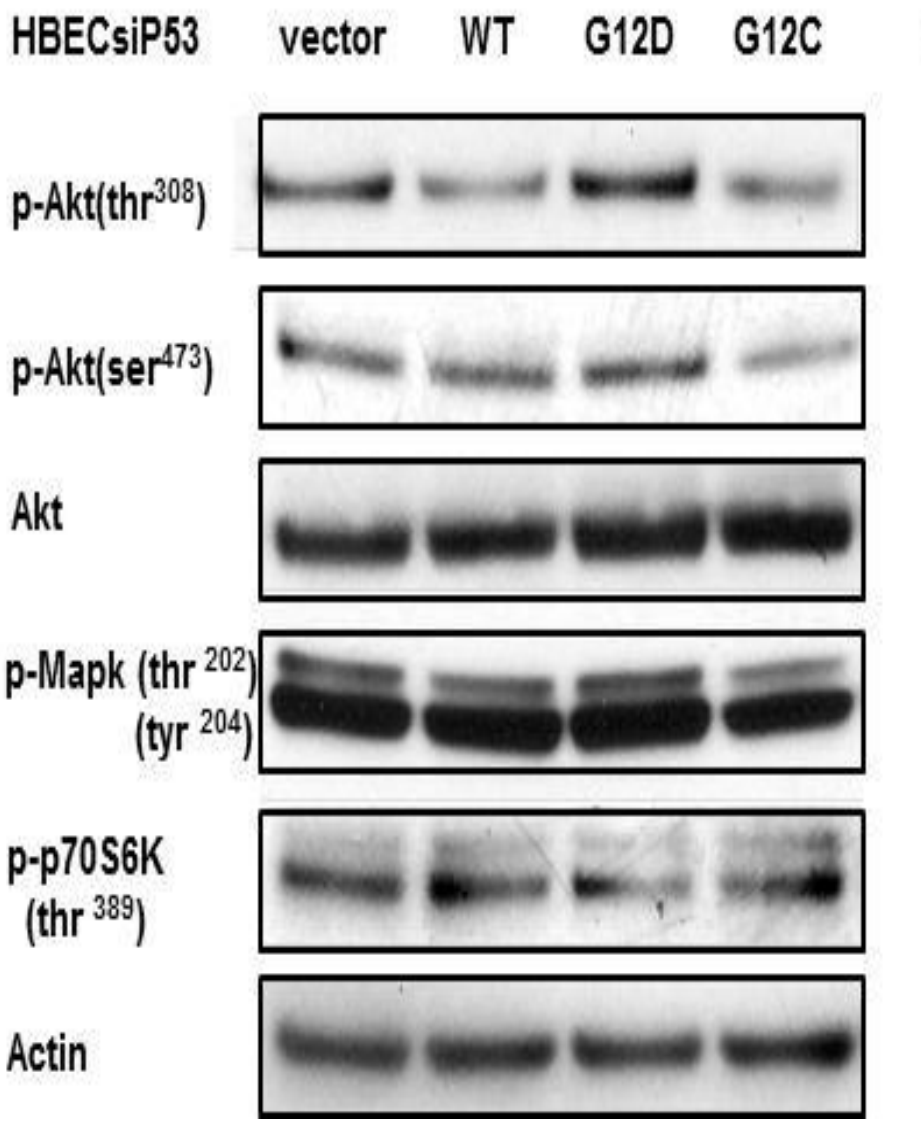

Figure 10: Expression of Akt and Mapk pathway activation in HBEC cells. Activation of the Akt and Mapk pathways were measured in HBEC cells by the expression of phosphorylated proteins. Akt activation was higher in KRas G12D when compared to WT or KRas G12C as had been seen in a panel of cell lines in **Figure 6**. No differences were seen in the activation of Mapk or p70 S6K. Reprinted with permission from [97].

Figure 11

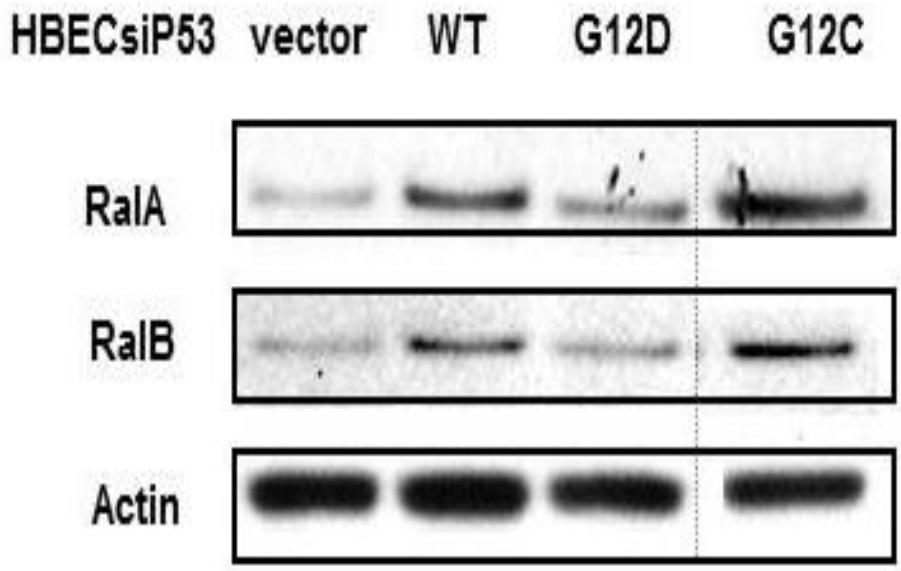

Figure 11: Activation of Ral A/B by KRas. Ral activation was measured in different forms of *KRAS* transfected HBEC cells. Conversely to Akt activation, both RalA and RalB were most active in HBEC cells with either overexpressed WT or mutant KRas G12C transfected. KRas G12D transfection showed a low level of Ral activation with levels comparable to vector control. Figure Reprinted with permission from [97].

3.2.5 Behavior of different activating *KRAS* mutations in growth assays

In addition to studying the effects of these different KRas mutants on downstream signaling, studies were performed to determine to effects of different activating *KRAS* mutations on cell growth. We performed a growth assay on these cells in culture and surprisingly found that despite the differences among effecter signaling cascades we had seen our cells with activating *KRAS* mutations or overexpressed wild-type *KRAS* the cells grew at a similar rate, and initially at a rate similar to our cells transfected with only the vector **(Figure 12)**. The primary difference observed was when these cells approached confluence, those cells with vector control stopped growing, while the addition of overexpressed wild type or mutant KRas abrogated this growth arrest. This is consistent with the reports of elevated KRas signaling abrogating cell-cell contact mediated growth inhibition in early reports of *HRAS* transformed cells [70]. We also looked at the ability of these cells to form colonies in an anchorage independent growth assay. We found that the HBEC*siP53* cells with overexpressed wild type or mutant *KRAS* were able to form colonies more effectively than the vector alone cells **(Figure 13)**. However, our cells with oncogenic *KRAS* mutations were able to form more colonies than the cells expressing wild type KRas and additionally the mutant KRas G12C mutation formed more colonies in the assay than mutant KRas G12D despite displaying sharply reduced PI3K- Akt signaling. As the KRas G12C cells had elevated Ral signaling, this observation may reflect the reported effects of Ral mediating Ras induced anchorage independent growth[102].

Figure 12

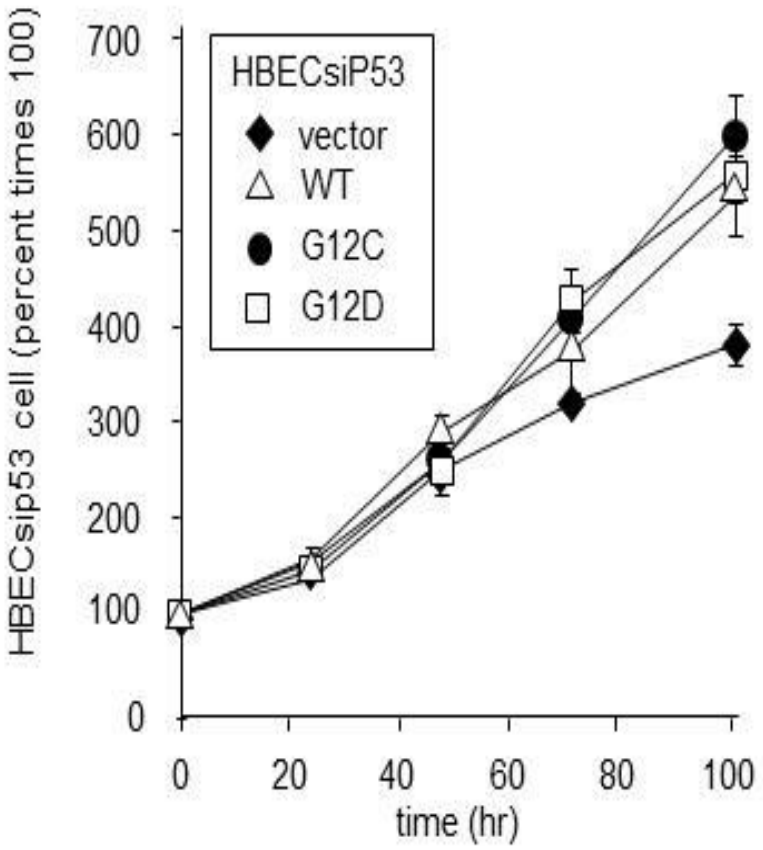

Figure 12: Growth of Cultured HBEC *siP53* cells with vector or *KRAS* transfects. In a standard growth assay (96 well tissue culture dishes, 10% FBS) Both the primary p53 deleted HBEC's and the transfectents grew at a similar rate. At Confluence (~60 hours) the vector control began to decline in growth rate while the wild type and mutant *KRAS* transfects continued to grow. Reprinted with permission from [97].

Figure 13

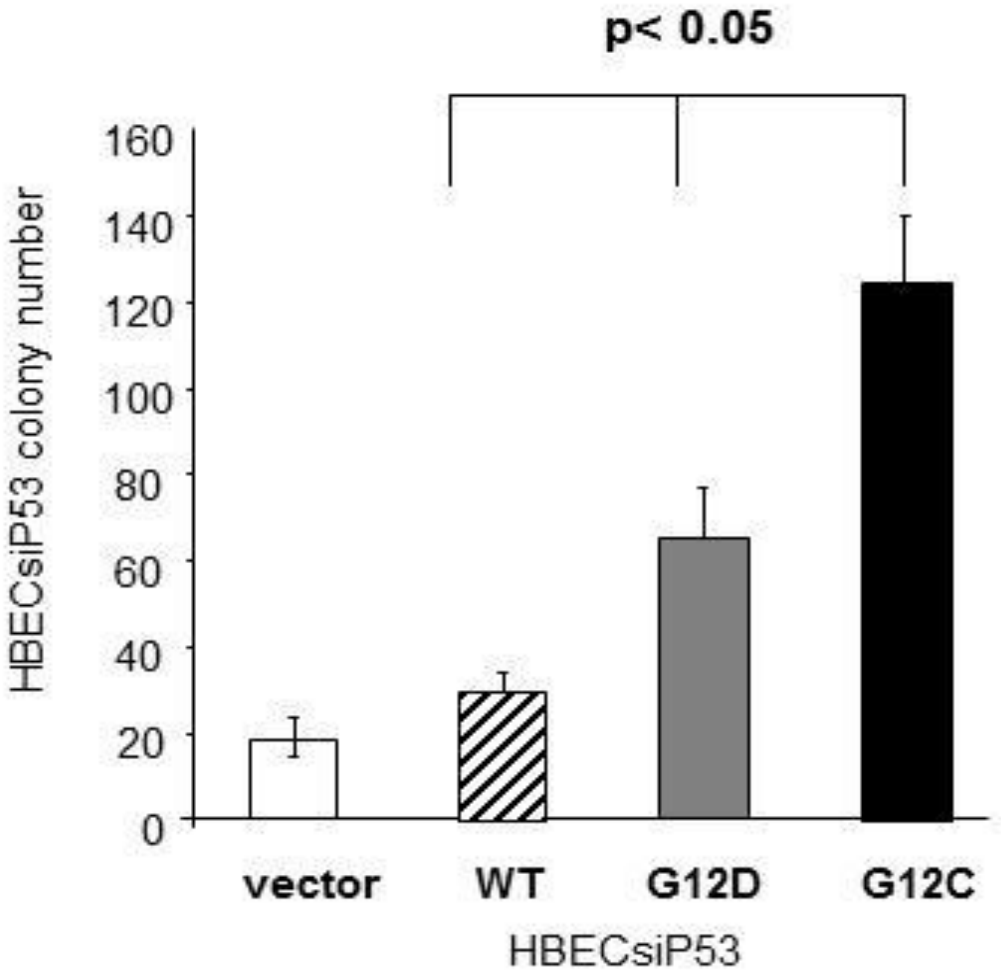

Figure 13: Clonogenic Assay with HBEC *siP53* cells. In clonogenic assays performed with HBECs transfected with different forms of oncogenic *KRAS*, a higher number of clones were seen with the transfection of either a mut-KRas G12D or G12C than a wildtype or vector transfection while the KRas G12C HBEC line formed significantly more colonies than any of the other lines tested. Reprinted with permission from [97].

3.2.6 Effect of different forms of oncogenic *KRAS* on growth factor signaling

Our observations that both KRas G12C NSCLC cell lines in our panel and KRas G12C transfected HBEC cells lacked Akt activation even in the presence of growth factors present in serum was intriguing as growth factors are capable of activating this signaling cascade in a KRas independent fashion. We had previously observed the KRas G12C/V patient tumors showed repressed activity through the proximal Akt pathway, although many lines with minimal Akt activation showed robust activation of mTOR effecter proteins. The p70 S6 kinase, an output of mTOR, has been shown to exert a feedback to restrict growth factor signaling to the Akt pathway and this led us to postulate that this may be a contributing factor to our lack of observed Akt activation [103]. To address this, we first observed the baseline levels of activated p70 S6K in our panel of cell lines. Analysis of phosphorylation the mTOR effecter p70 S6K revealed no significant difference between these groups under serum or serum deprived conditions and surprisingly under conditions of acute serum stimulation cells with KRas G12C or G12V had significantly higher phosphorylated p70 S6K **(Figure 14)**. HBEC KRas G12C or G12D activating mutations were treated with rapamycin an inhibitor of mTOR and, thus, of p70S6K signaling. In the mut-KRas G12C HBEC cells inhibition of p70S6K resulted in a robust increase in p-Akt **(Figure 15)**. This was additionally seen in all the cell lines tested from the NSCLC panel **(Figure 16)**. In contrast in KRas G12D lines which already showed p-Akt, rapamycin resulted in only a slight further increase in Akt signaling both in HBEC G12D transfects and cell lines from the NSCLC panel harboring G12D or G12R. Cells with a mutationally activated EGFR showed no increase in phosphorylated Akt when treated with rapamycin. Thus the results indicate that KRas driven mTOR signaling is inhibiting the Akt activation which would occur through growth factor activation in cells with a KRas G12C mutation.

Figure 14

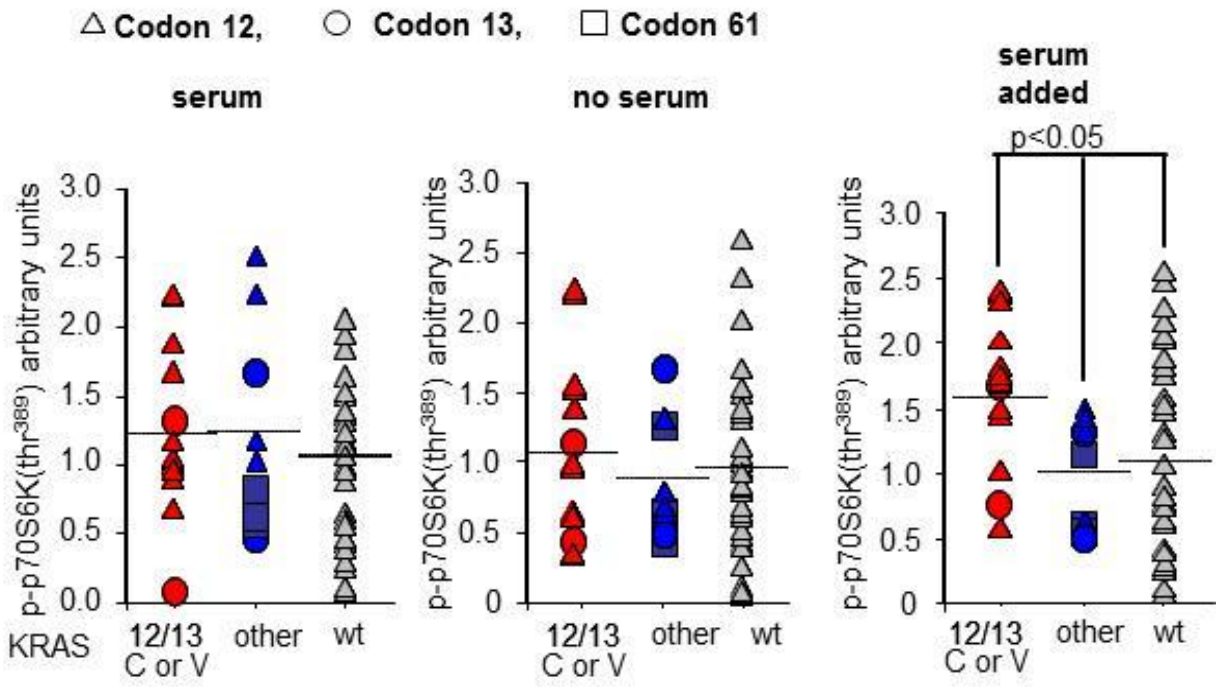

Figure 14: RPPA measurement of the mTOR effecter p70 S6K. p70 S6K was measured in either serum, serum free or acute serum stimulation conditions as described previously. Despite lower levels of activated Akt in the mutant KRas G12C/V group under serum or serum free conditions **(Figure 6)** no significant difference was observed in activation of the mTOR effecter p70 S6K as measured by phosphorylation. In contrast, p70 S6K activation was significantly higher in cells with serum acutely added. Reprinted with permission from [97].

Figure 15

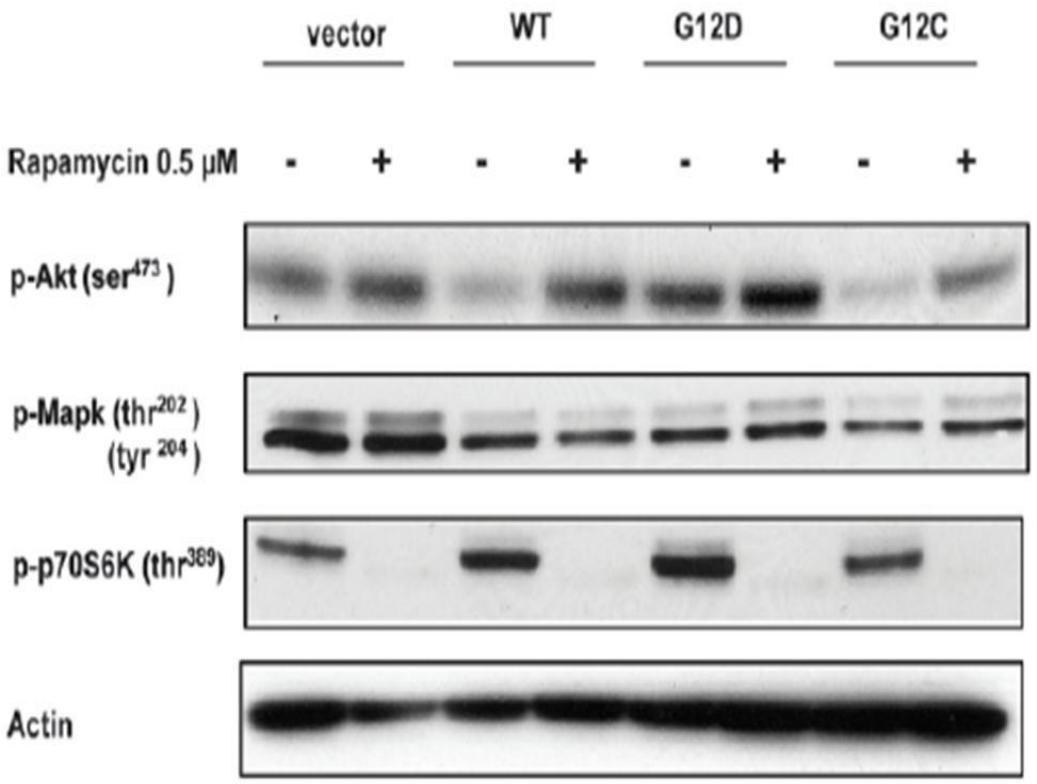

Figure 15: Mutant KRas G12 C/V restrains Akt signaling through mTOR mediated repression of growth factor signaling in HBEC cells. HBEC cells were treated with 0.5 µM of the mTOR inhibitor rapamycin. In cells with overexpressed WT or G12C KRas showing no expression of active Akt at baseline, an activation of Akt signaling was observed. In the vector control or G12D KRas where Akt was observed to be activated at baseline, only a marginal further increase in Akt activation was observed. Reprinted with permission from [97].

Figure 16

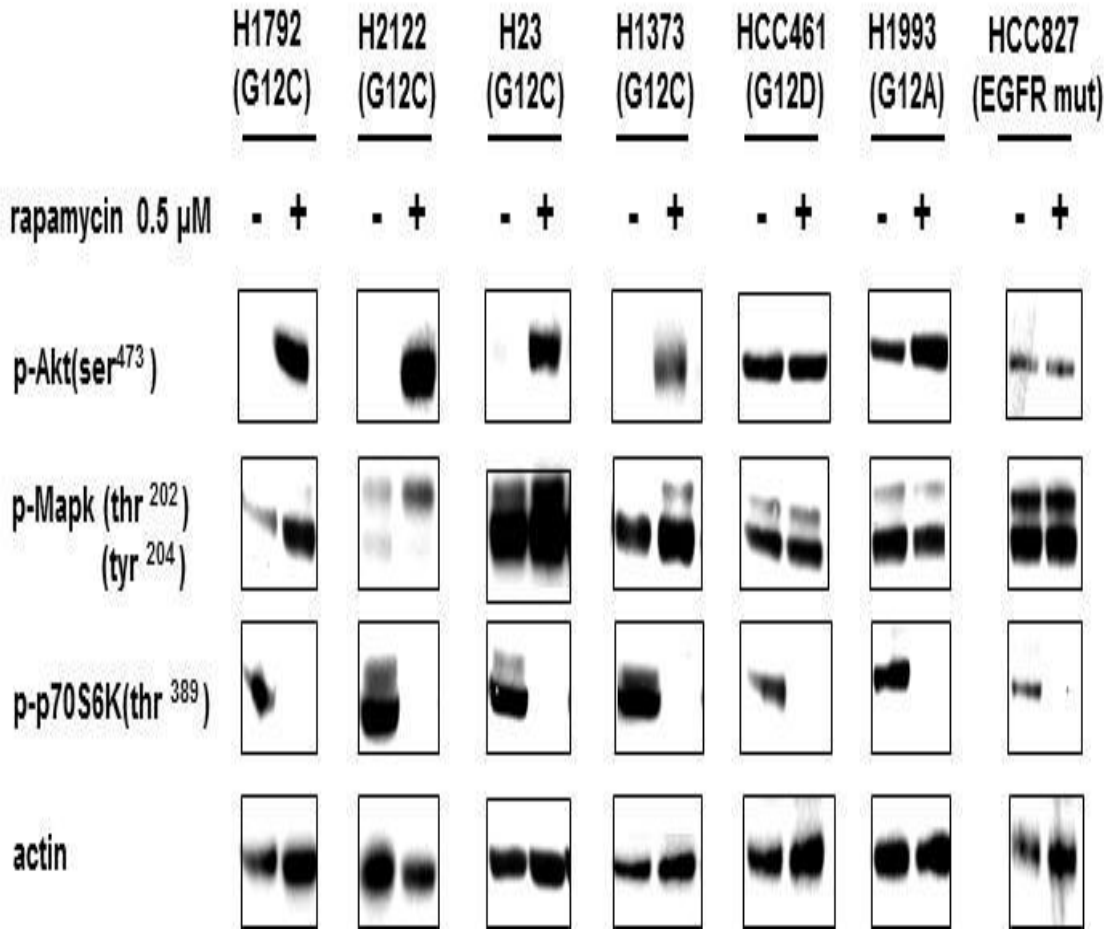

Figure 16: Mutant KRas G12 C/V restrains Akt signaling through mTOR mediated repression of growth factor signaling in NSCLC cell lines. Various NSCLC cell lines were treated with 0.5 μM of the mTOR inhibitor rapamycin. In cells with G12C KRas showing no expression of active Akt at baseline, an activation of Akt signaling was observed. In other mutant KRas lines or an EGFR mutant line, Akt was observed to be activated at baseline, only a marginal further increase in Akt activation was observed. Reprinted with permission from [97].

3.2.7 Computer modeling of different forms of oncogenic KRas

Finally, we performed molecular modeling studies of the KRas protein using the available crystal structures of HRas (~95% sequence identity to KRas) to create homology models of mut-KRas G12D and G12C, followed by molecular dynamics for structural refinement. KRas interacts with its different downstream effecters by undergoing large conformational changes in the switch I and switch II regions of the protein surrounding codon 12 and 13 amino acids. When bound to PI3K the switch II regions of mut-KRas G12C and WT-KRas exist in a similar conformation that exposes the bound GTP for hydrolysis, thus, inhibiting KRas activity. In contrast, the introduction of the aspartate side chain results in electrostatic repulsion which pushes the y-phosphate in the GTP nucleotide towards the Thr35 residue in Switch I, weakening the H-bond between the y-phosphate of Gly60 (in Switch II) in particular. This creates a pocket for Gln61 side chain, and forms H-bonds between OE1 of Gln61 and HN in Gly60, whille Gln61 amine group binds to y-phosphate. PI3K and Ral compete for activation by KRas although the way in which KRas activates Ral is dramatically different to PI3K, with two KRas molecules forming a homodimer to facilitate RalGDS binding. The Y32 of one KRas interacts with GTP in the other KRas and is critical for RalGDS activation[20] **(Figure17).** Our modeling shows that in mut-KRas G12D the bulky D pushed aside the Y32 preventing homodimer formation and Ral activation. In contrast, the smaller C of mut-KRas G12C enhances homodimer formation and Ral activation. Both molecular dynamic and protein-protein docking data show the results of these changes with mut-KRas G12C having a higher affinity for RalGDS and mut-KRas-G12D preferring PI3K (**Figure18**).

Figure 17

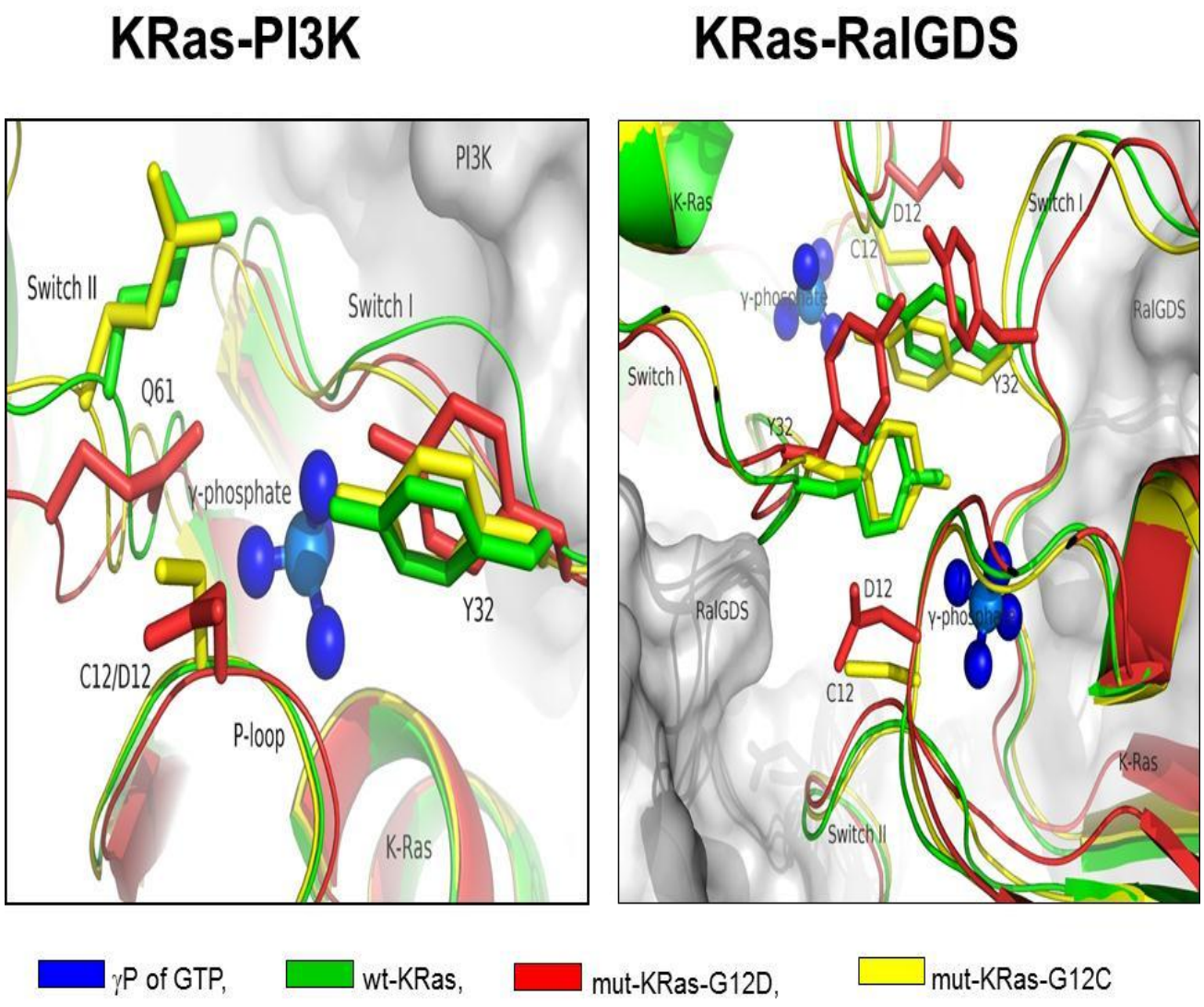

Figure 17: Computer modeling of different substitutions at codon 12 in the KRas protein. A homology model of KRas was created from the publically avaliable crystal structure of HRas. This structure was then applied to docking models with PI3K and RalGDS. These structures revealed that an aspartate at codon 12 contorted the key Q61 and Y32 regions of KRas due to interactions with the gamma phosphate of bound GTP. This new conformation stabilized GTP binding when KRas was bound to PI3K. In contrast, the new conformation of Y32 inhibited the ability of KRas to form the tetramer necessary for RalGDS interaction. Reprinted with permission from [97].

Figure 18

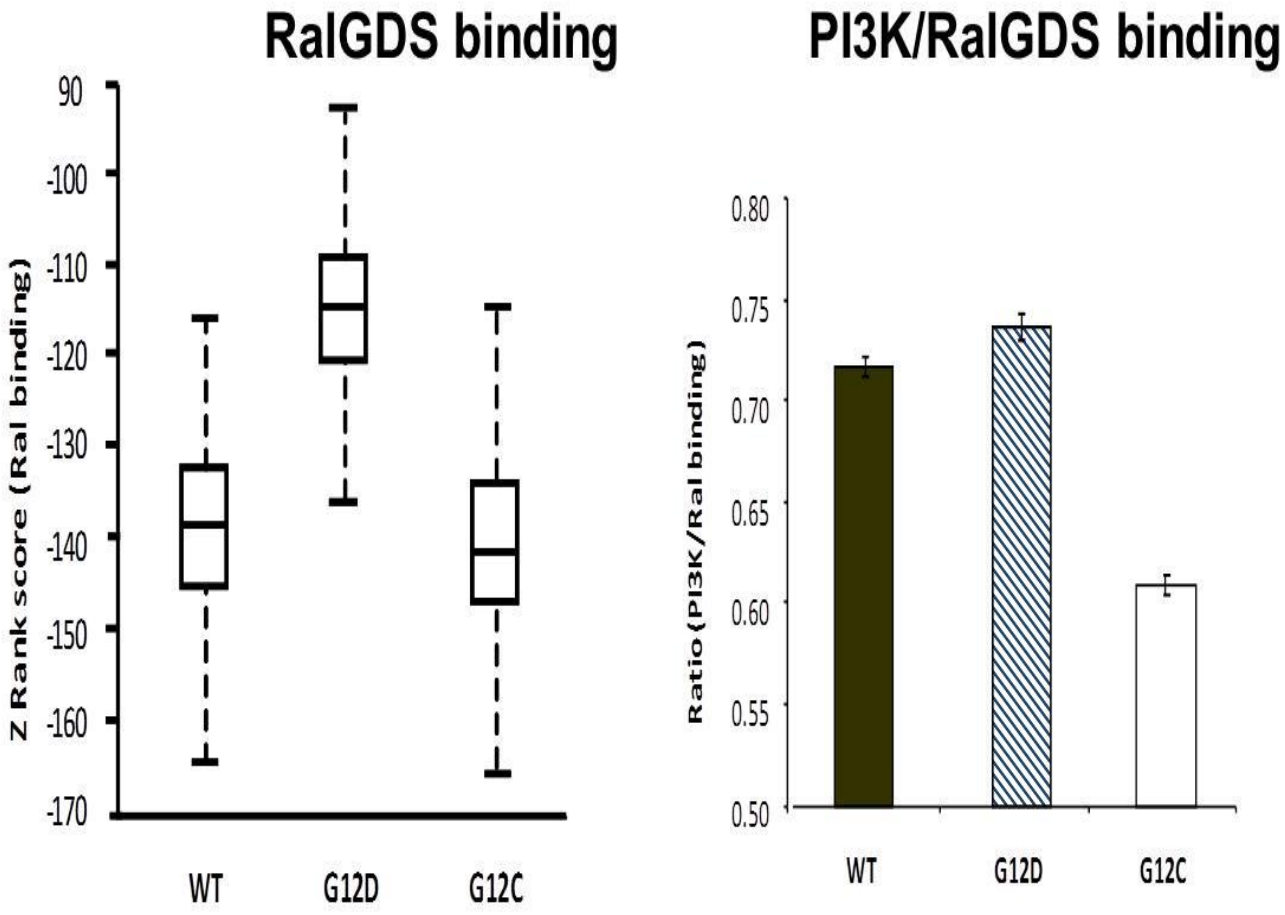

Figure 18: Scoring of different forms of mutant KRas bound to effecters. Z ranking was used to determine the binding of KRas to different effecters. The highest Z rank score was found for binding of KRas G12D into the RalGDS binding model, while WT and G12C KRas showed similar scoring. Additionally, a comparison of PI3K and RalGDS binding revealing that G12C showed more favorable binding to RalGDS than to PI3K accounting for our observations in cells. Reprinted with permission from [97].

Discussion

The recently completed BATTLE trial for patients with refractory NSCLC receiving either erlotinib, vandetanib, bexarotene and erlotinib, or sorafenib found that total mut-*KRAS* did not predict for overall survival for any of the treatments [94]. Reanalyzing the BATTLE data for the effect of different oncogenic KRas amino acid substitutions on patient survival revealed that a cysteine or valine substituted for glycine at codon 12 in KRas but not all forms of mutant KRas in a single group predicted for progression free survival. This is the first indication in NSCLC that different amino acids substitutions of in oncogenic KRas influence patient response to targeted therapy. A previous study in colon cancer patients reported that a cysteine or valine substitution at the codon 12 position in KRas is associated with rapid tumor progression and decreased patient survival when compared to other oncogenic KRas substitutions (mostly G12D) or wild type KRas[87,88]. Analysis of microarray transcriptome data in patient tumors from the BATTLE trial to find genes whose expression was significantly different between G12C or G12V KRas mutants and other KRas mutants identified cell cycle regulators such as Plk1 and Cyclin B1 as being down regulated in the oncogenic KRas G12C or G12V tumors and up regulated in the remaining mutt-KRas tumors. Dysregulation of the cell cycle is a well characterized feature of KRas mediated tumorgenesis [66]. RPPA analysis of a panel of genetically characterized NSCLC cell lines, comparing oncogenic KRas G12C or G12V to other oncogenic KRas mutants and wild type KRas showed decreased phospho-Akt in mut-KRas G12C or G12V cells, and elevated phospho-Akt in the remaining cells harboring an oncogenic KRAS relative to those cells expressing wild type KRas. Transfection of immortalized, p53 deficient human bronchial epithelial cells (HBEC *siP53*) with different forms of oncogenic KRAS showed that cells expressing oncogenic KRas G12C decreased phospho-Akt but elevated levels of Ral A/B in the GTP-bound active form. In contrast, cells expressing oncogenic KRas G12D showed increased phospho-Akt levels and decreased Ral activation, compared to wild type KRas cells. All the *KRAS* transfected cells grew at a similar rate in

culture but those with any form of *KRAS* transfected showed post-confluent growth. In contrast oncogenic KRas G12C cells with lower Akt signaling but elevated Ral signaling exhibited increased anchorage –independent growth in a colony formation assay compared to oncogenic KRasG12D cells or cells expressing the vector control or a wild type KRas . These findings agree with previous studies that found that Ral preferentially induces anchorage-independent growth in human cells, while Akt or Mek activation has few discernible effects [104]. The pattern of signaling is also consistent that previously observed when the same mutations were introduced into the lungs of mice, where oncogenic KRas G12D induced Raf and Akt activation [60]as opposed to KRas G12C which resulted in only Raf and Ral activation, with minimal Akt activation regardless of expression level [92,101]. Many NSCLC cell lines with minimal Akt activation displayed high activation of the mTOR effecter proteins p70nS6K and 4EBP. Inhibition of mTOR with rapamycin in cells with oncogenic KRas G12C resulted in the inhibition of p70S6K and a concurrent increase in Akt activation. The translational regulator mTOR is known to be activated by Akt signaling, in addition to the Mapk and Ral pathways [105]. Additionally, p70 S6K an output of mTOR has been shown to exert feedback to restrict growth factor signaling to the Akt pathway. Our results suggest that KRas driven mTOR signaling is inhibiting Akt activation which would otherwise occur through growth factor stimulation [103].

KRas is known to interact with different downstream effecters by undergoing large conformational changes in the switch I and switch II regions of the protein surrounding the codon 12 and 13 amino acids[6]. Our molecular modeling studies showed that oncogenic KRas G12C weakens the interaction with PI3K while the bulky aspartate of oncogenic KRas G12D causes steric interference of RalGDS homodimer formation and RalGDS activation which is not seen with the Cys of oncogenic KRas G12C. Both molecular dynamic and protein-protein docking data show the results of these changes, with a KRas G12C substitution having a higher affinity for RalGDS, and KRas G12D a higher affinity for PI3K. These modeling results are in agreement with the results of our cellular studies of the effects of the different oncogenic KRas amino acid substitutions on signaling activities. The findings of our study are

summarized in **Figure 19** showing different mechanisms for signaling through wildtype KRas, oncogenic KRas G12D and KRas G12C. The observation that the substitution of different amino acids induces heterogeneous behavior in the KRas protein resulting in different signaling outputs has profound implications for identifying and treating KRas driven tumors Subsequent studies on a lung cell line with different forms of activated *KRAS* expressed from a plasmid showed that different *KRAS* mutants conferred different sensitivities to both cytotoxic and molecularly targeted agents in cell growth assays [106]. The clear implication is that it may be possible to better treat oncogenic *KRAS* driven by a particular activating amino acid through an inhibitor to the particular pathways or to combine these agents in a rational fashion.

Figure 19

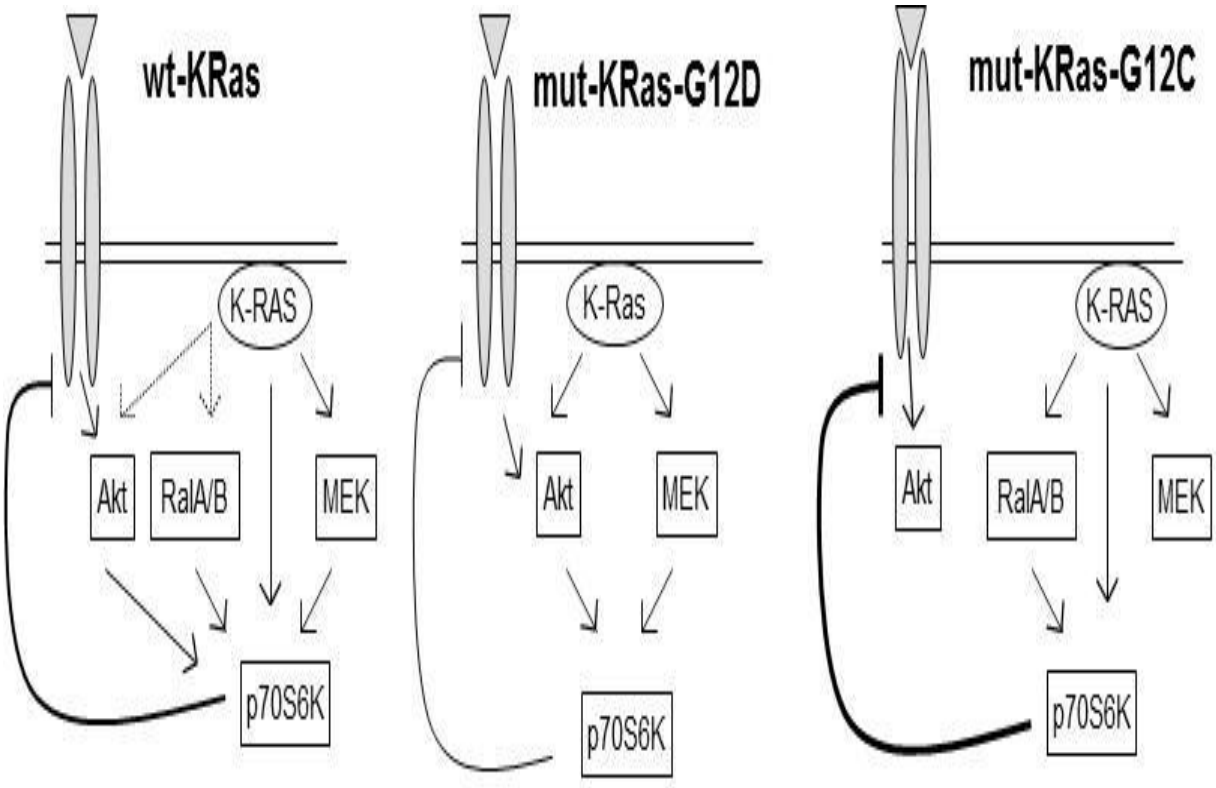

Figure 19: Scheme of signaling by different forms of KRas. WT-KRas and Akt are activated by growth factors and can activate the Akt, Ral, and Mek pathways which can then engage mTOR signaling and the mTOR effecter p70 S6K which then acts as a "feedback" to shut off growth factor mediated signaling. Mut-KRas G12D activates Mek, Akt and mTOR signaling independently of growth factors. Mut-KRas G12C actives Mek, Ral, and mTOR signaling independently of growth factors and inhibits growth factor mediated activation of Akt signaling. Reprinted with permission from [97].

Targeting *KRAS* mutant tumors by inhibition of downstream effecters

4.1 Introduction

Since the clinical failure of the FTI's, a majority of attempts to inhibit *KRAS* oncogene driven tumors have not focused on the inhibition of KRas itself but have explored methods to target mutant KRas indirectly [70]. The first is to inhibit KRas downstream effecter signaling that may be critical for the growth and survival of tumor cells with an activated KRas. The two most studied effecter pathways for which agents are clinically available, Raf/Mek and PI3K/Akt, have so far given equivocal results as to whether the approach will be successful. The notable exception is that of B-Raf inhibitors in melanoma which have been shown to activate Mapk signaling in cells with active Ras signaling [107]. Mek has been identified as both a KRas effecter critical for the Ras driven tumorgenesis [108] and, paradoxically, KRas has been identified as a marker of resistance to Mek inhibitors[109]. In a similar fashion PI3K has been identified as both critical for maintenance in tumors with oncogenic *KRAS*[110] and oncogenic *KRAS* has been identified as a resistance factor predicting lack of response to PI3K inhibitors[80]. The observations presented in the previous chapter [97] suggest that the type of amino acid substitution that actives KRas may influence which agents may be effective for treatment, a concept that has been demonstrated both in cell culture models[106] and in clinical trials where in CRC KRas G13D mutation tumors are uniquely sensitive to the EGFR inhibitor cetuximab [111]. Alternatively, studies have also shown that the presence of additional oncogenic lesions found frequently in human tumors, such as LKB1 loss in NSCLC, may complicate the analysis. A transgenic mouse model with a mutant KRas G12D conditionally expressed in the lung showed a response to a Mek inhibitor regimen, but the concurrent knockout of LKB1 reversed this sensitivity. To address the possibility that different activating *KRAS* mutations were causing these discrepancies we utilized a set of isogenic colon cell lines for which the parental line has a wild type *KRAS*, but gene editing had been used at the endogenous loci to create an oncogenic KRas G12D, G12C, and G12V, and screened these cells against clinically relevant inhibitors of Mek and Akt.. This approach eliminates artifacts which may

arise with the transfection of an expression vector, such as dramatic overexpression, and interactions with the endogenous protein. Additionally we looked for correlations between the methods of KRas activation in a 30 NSCLC cell line panel where additional high frequency lesions are often present.

The second approach to discover a novel a treatment for *KRAS* driven cancer has utilized broad siRNA and shRNA screening for synthetic lethal targets which inhibit the growth of *mutant KRAS* cells. This approach in the hands of others has identified TBK1 as a downstream effecter of RalB [112] , components of the cell cycle [96], and STK33, although it should be noted some of these results have failed to be reproduced [113].

4.2 Results

4.2.1 Isogenic KRas G12C/D/V treated with targeted therapies

To determine if there is a single targeted therapy that could be effective against a specific mutant *KRAS* we screened a large panel of cell lines against individual targeted therapies already in clinical use. They were the Mek inhibitors AZ6244 and GSK1120212, and the Akt inhibitors MK2206 and GSK 60693, using a panel of colon cancer cell lines with both a wild type KRas, as found in the parental SW48 cell line, and the mutant KRas G12D, G12C, and G12V substitutions created by gene editing at the endogenous loci. As the agents are targeting the Mek-Erk and PI3K-Akt pathways, the levels of active Erk and active Akt were measured by western blotting. Consistent with our observations in HBEC cells the SW48 cells with wild type or a KRas G12D substitution had higher levels of active Akt than those with KRas G12C or G12V substitution **(Figure 20)**.Additionally, the SW48 KRas G12D cells had higher levels of active Erk signaling which was not seen in our HBEC cells suggesting that some effects of introducing different forms of activated *KRAS* may be cell type specific, or differs when mutant KRas is expressed ectopically or at the endogenous location. Treatment with the AZD6244 Mek inhibitor showed no clear trend in response, but treatment with the Mek inhibitor GSK1120212 showed more consistent effects with the parental SW48 being the most sensitive, followed by the mutant KRas G12C and G12V variants with SW48 KRas G12D

being the least sensitive **(Figure 21)**. The Akt inhibitor GSK60693 showed only weak effect against the whole panel of cells with only the parental cell approaching 50% growth inhibition. In contrast MK2206 an allosteric Akt inhibitor showed clear differences (**Figure 22)**, inhibiting SW48 wild type KRas growth the most followed closely by SW48 mutant KRas G12D then G12C and G12V which never reached an IC50 value (shown in **Table 1**). This data indicates that while each inhibitor will have unique efficacy, likely based on potency and pharmacology that differences exist in the sensitivity of cells based on the substitution that activates KRas, with mut-KRas G12C/V showing increased cell growth inhibition with Mek inhibition and mut-KRas G12D showing a greater response to Akt inhibitors.

Figure 20

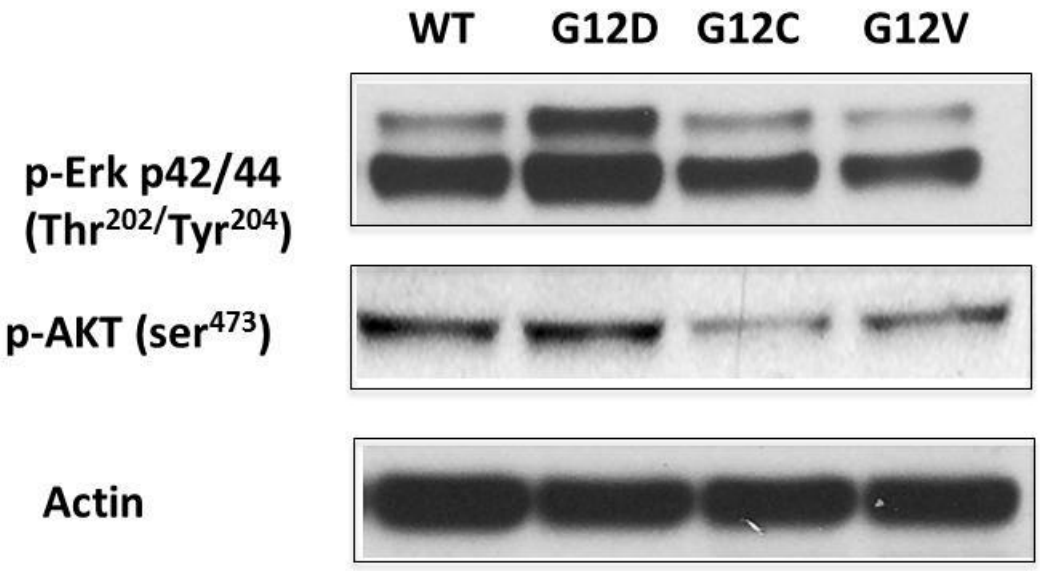

Figure 20: Signaling through the Mapk and Akt pathways in SW48 colon cancer cells with *KRAS* mutations substituted at the endogenous loci. The SW48 colon cancer cell line had a WT *KRAS* allele substituted with a mutation resulting in a KRas G12D, G12C or G12V protein. As we had observed in of HBEC cells KRas G12D activated Akt signaling while KRas G12C or G12V showed weaker activation. In these cells KRas 12D also showed stronger activation of the Mapk pathway.

Figure 21

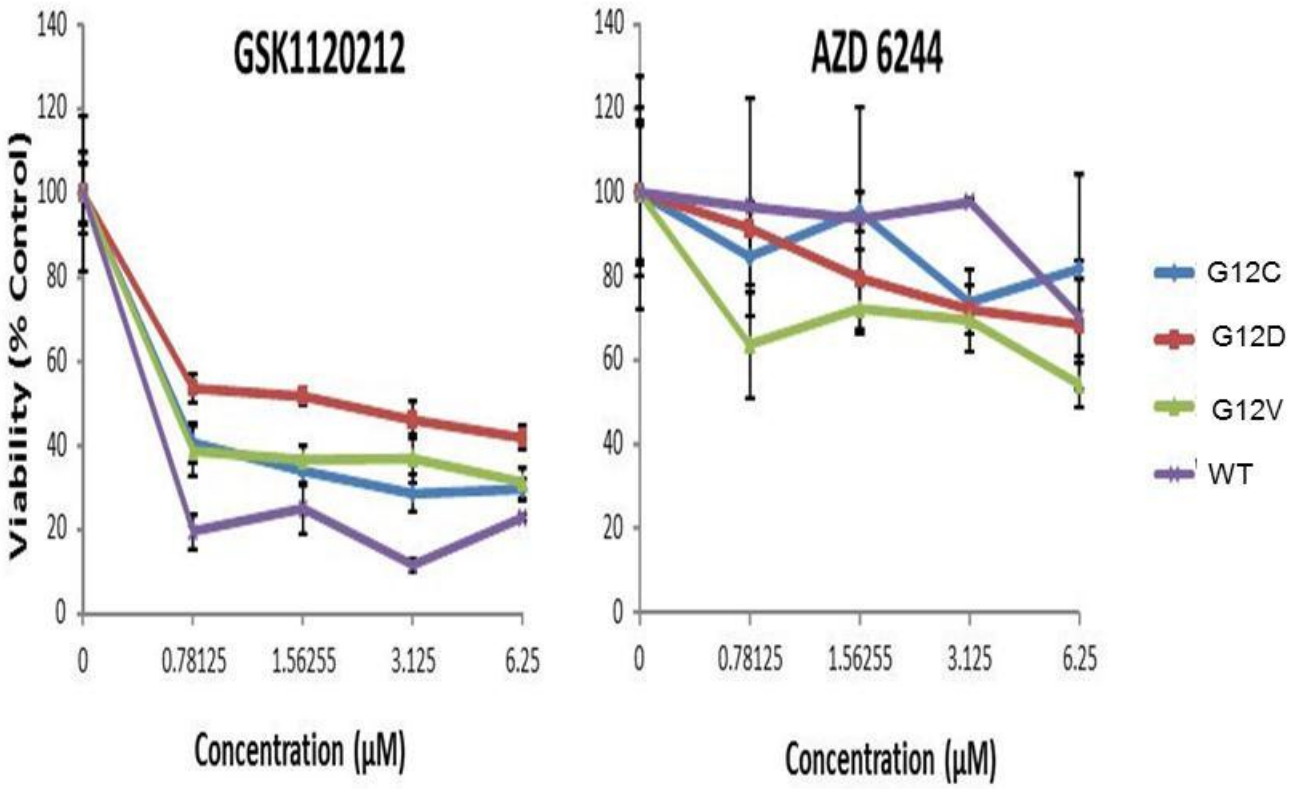

Figure 21: SW48 isogenic cell lines treated with Mek inhibitors. SW48 cells with WT KRas substituted with KRas G12D, G12C, or G12V expressed from the endogenous loci were treated with the indicated concentrations of the Mek inhibitors GSK1120212 or AZD6244 for 72 hours. In GSK1120212 treated cells wild type SW48 cells showed the greatest sensitivity followed by KRas G12C/V while KRas G12D showed the least sensitivity. No clear pattern emerged with AZ6244 indicating specific effects of these agents.

Figure 22

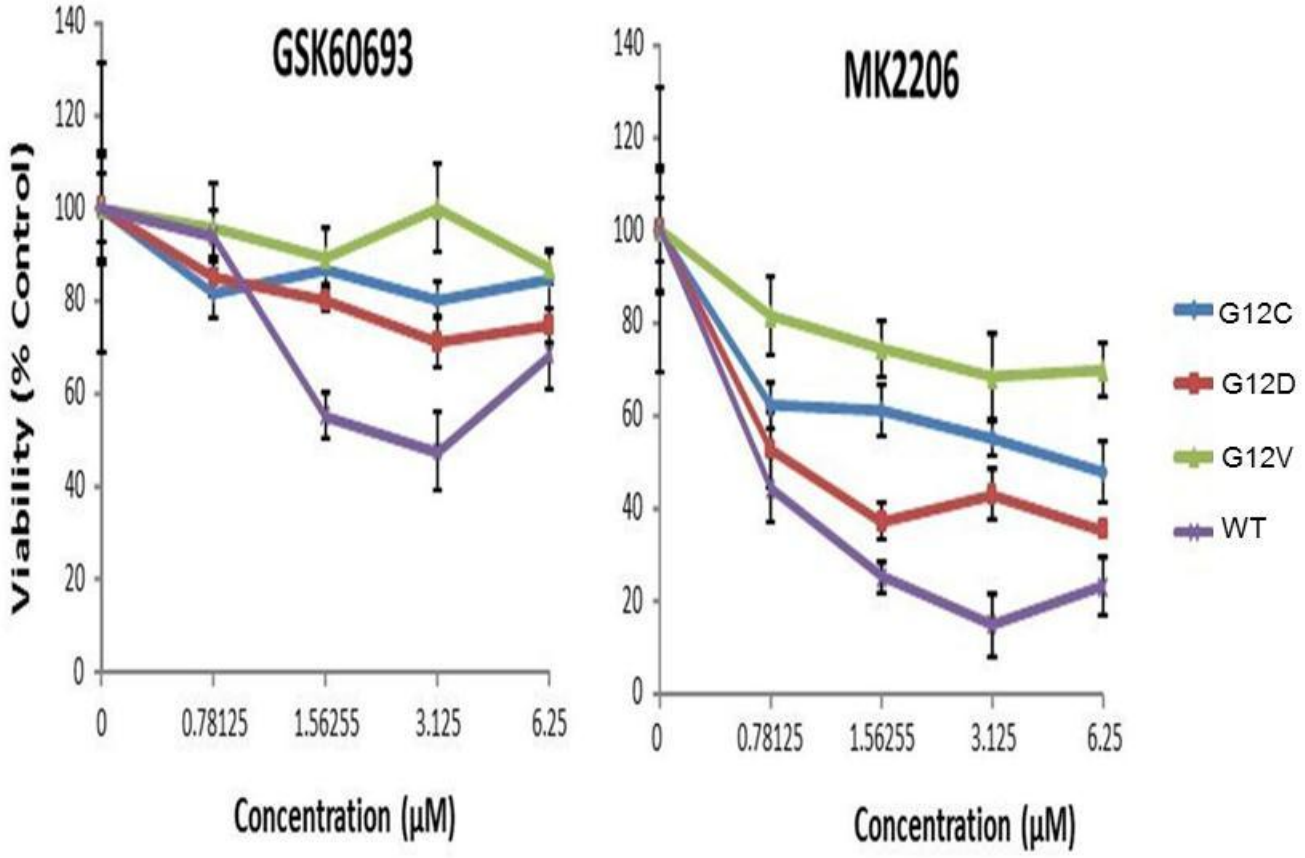

Figure 22: SW48 isogenic cell lines treated with Akt inhibitors. SW48 cells with WT KRas substituted with KRas G12D, G12C, or G12V substituted at the endogenous loci were treated with the indicated concentrations of the Akt inhibitors GSK60693 or MK2206 for 72 hours. In GSK60693 no clear pattern emerged. In MK2206 treated cells wild type SW48 cells showed the greatest sensitivity followed by G12D, then G12C and G12V constant with the Akt pathway activation observed in these cells. Again, agent specific effects were observed indicating non-equivalent pathway inhibition.

Table 1

Cell Line	GSK1120212	GSK60693	MK2206	AZD6244
Wild type	1.53 μM	3.92 μM	1.92 μM	43.6 μM
12C	1.91 μM	None	7.82 μM	None
12D	3.91 μM	None	3.41 μM	136 μM
12V	1.82 μM	None	None	7.59 μM

Table 1: IC50 values for agents targeted to the KRas effecter pathways. All agents tested against the SW48 isogenic lines had an IC50 >1 μM. SW48 KRas G12D was the least sensitive to the Mek inhibitor GSK1120212 and the most sensitive to the Akt inhibitor MK2206 consistent with patterns of Akt signaling observed in the HBEC cell line in Chapter 3 and the SW48 isogenic lines. GSK60693 and AZ6244 didn't show this clear trend but also had greatly reduced IC50's for cell growth inhibition.

4.2.2 Panel of lung cancer cells treated with targeted therapies

We also ran the Mek inhibitor AZ6244 and the Akt inhibitor MK2206 against a panel of 30 characterized NSCLC lines and looked for associations between type of activating KRAS mutant and response to these agents. No clear response pattern was seen in either the isogenic lines or the panel of NSCLC cells for the Mek inhibitor AZ6244 **(Figure 23).** The sensitivity of cell lines with activating substitutions in *KRAS* ranged from 3.4 µM to greater than 50 µM. Of the three lines most sensitive to AZ6244 (IC50<10µM) with oncogenic *KRAS*, the two cell lines harboring KRas G12C had concurrent inactivating mutations in the tumor suppressor *STK11* (LKB1), previously identified in a mouse model to confer resistance to tumor cells harboring oncogenic *KRAS* to this inhibitor[69]. Of the four cell lines most sensitive to MK2206 (IC50 < 3µM) two had an inactivating LKB1 mutation without a concurrent *KRAS* mutation (the only two on the panel) and H2122 a cell line with a KRas G12C substitution coexisting with a LKB1 mutation showed sensitivity to MK2206 while other LKB1 mutant cells with concurrent mut-KRas showed a marked resistance towards Akt inhibition **(Figure 24)**. The function of LKB1 in normal physiology is to stabilize and activate TSC2, which prevents mTOR mediated translation under low energy (low ATP) conditions **(Figure 26)**. The Mek and Akt pathways are both capable of degrading TSC2 to promote transcription, but LKB1 activation prevents this [99]. Measuring protein levels in LKB1 mutant cells sensitive to Akt inhibition showed MK2206 treatment restored TSC2 levels suggesting Akt is responsible for its degradation. In cell lines resistant to MK2206 the Mek inhibitor restored TSC2; however these lines were not sensitive to Mek inhibition **(Figure 25)**. This data suggests that unlike our isogenic colon lines in NSCLC cell lines interplay between LKB1 loss and KRas activation must be accounted for when attempting to predict response to targeted therapies and this may be reflective of a number of secondary mutations.

Overall, the data suggest that at the present time our knowledge of the interplay of signaling pathways activated by mutant KRas is inadequate to explain the differences in drug sensitivities for these downstream signaling pathways, except perhaps when LKB1 loss of

function and mutant KRas occur as independent lesions, as in our controlled models. Additionally, two dimensional growth on plastic surfaces may be unable to pick the dependence of mut-KRas cells on particular effecter pathways that are seen under conditions of in anchorage independent conditions or in the tumor environment. We have already seen this with the HBEC cells transfected with different mutant forms of KRas which show no difference in growth on plastic but dramatic differences in anchorage-independent growth in a clonogenic assay. The interaction between the pathways described in shown in **Figure 26**.

Figure 23

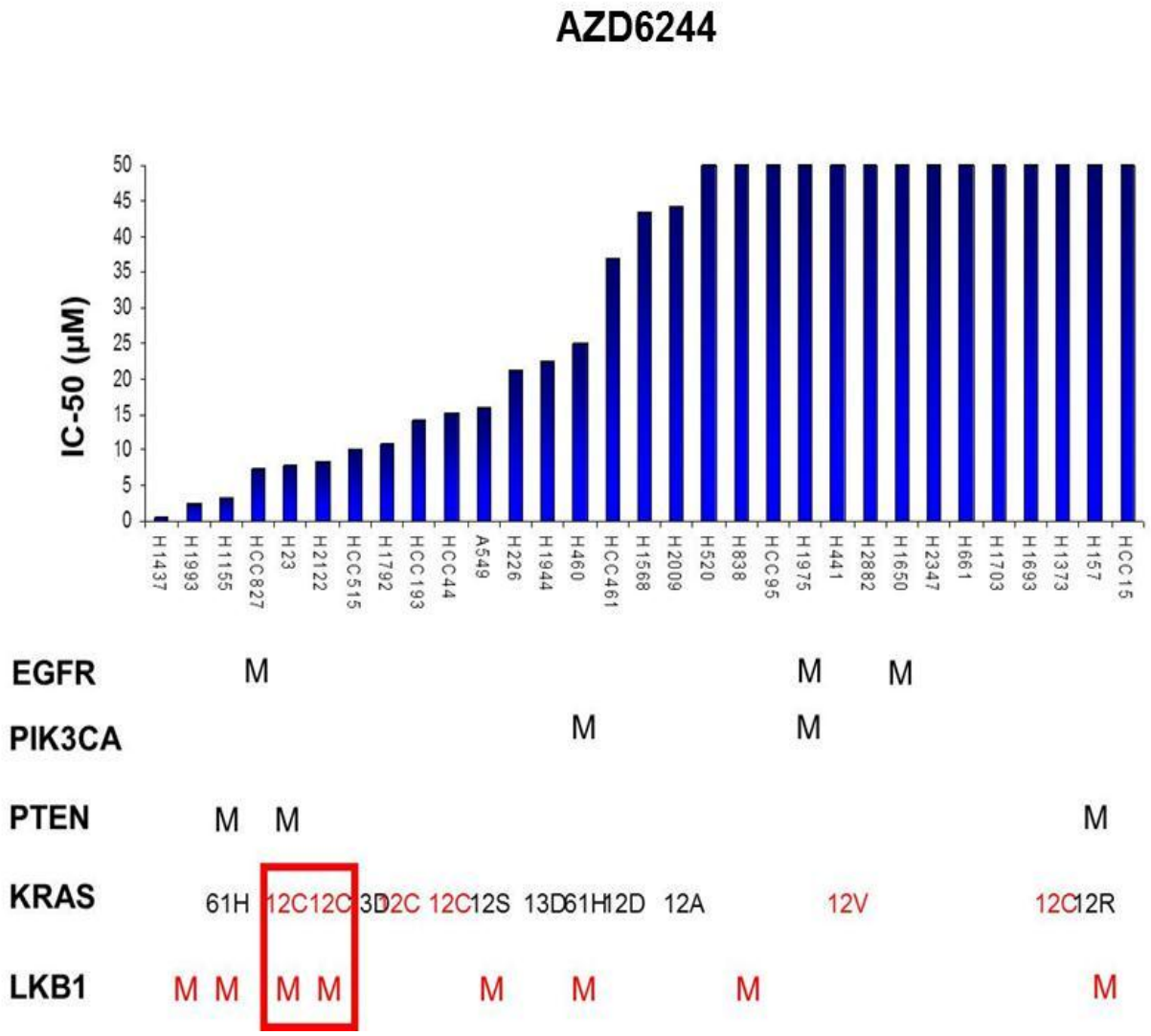

Figure 23: Mek inhibition across a cell panel of NSCLC lines. No clear pattern was seen in respect to IC50 of cell growth inhibition with AZ6244 in relationship to KRas activation except when LKB1 loss of function was included. The two mut-KRas G12C lines with a concurrent inactivating LKB1 mutation were the most sensitive to Mek inhibition (IC50 <10µM).

Figure 24

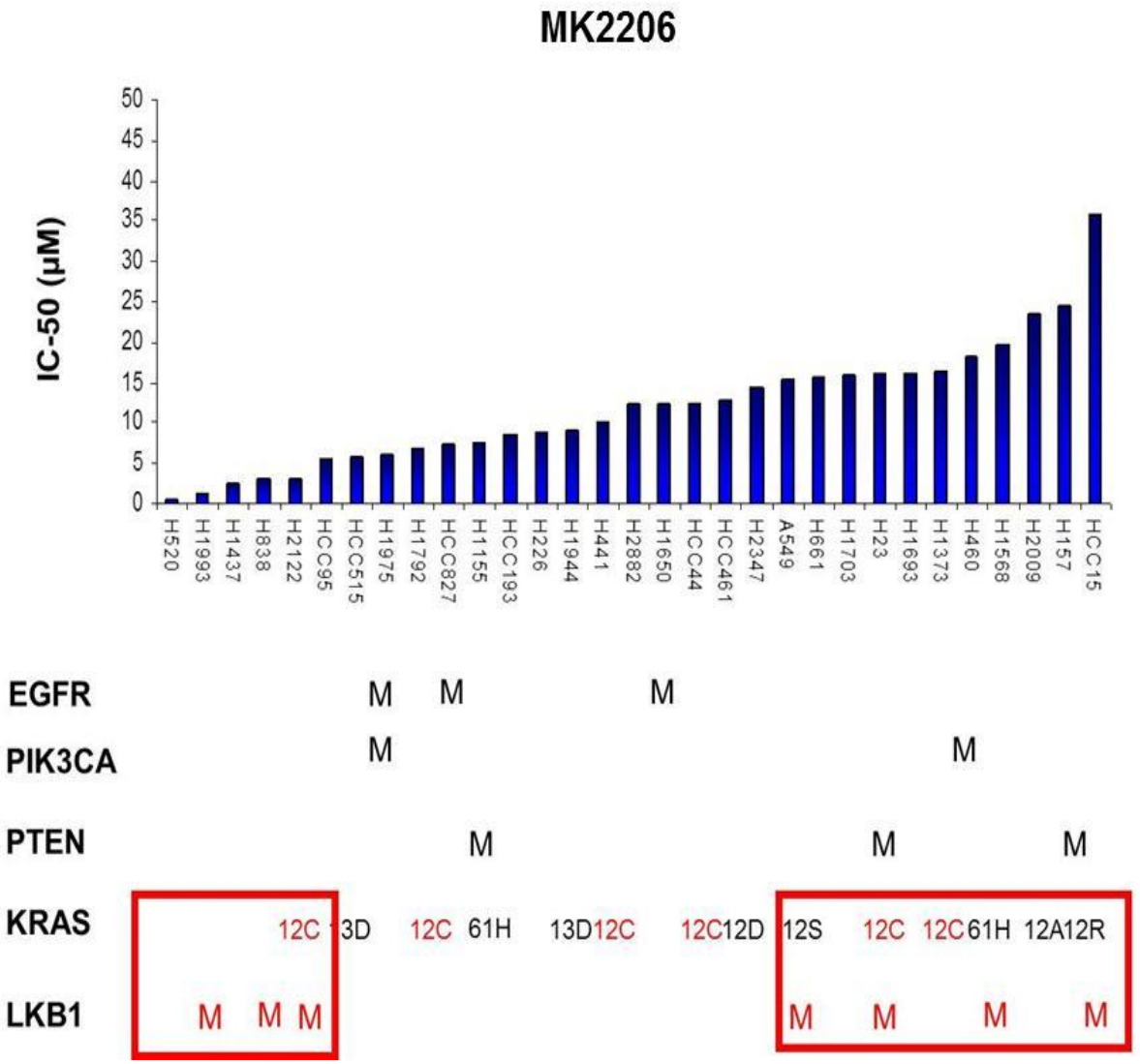

Figure 24: Akt inhibition across a panel of NSCLC cell lines. No clear pattern was seen in respect to IC50 of cell growth inhibition with regards to KRas activation. Those with LKB1mutations fell into two distinct groups. One group sensitive to Akt inhibition (IC50<4μM) which included two lines without concurrent mutant KRAS (the only two screened) and one with a concurrent KRas G12C mutation. The second group of LKB1 mutants was resistant to Akt inhibition (IC50>15μM) which all had a concurrent KRas mutation.

Figure 25

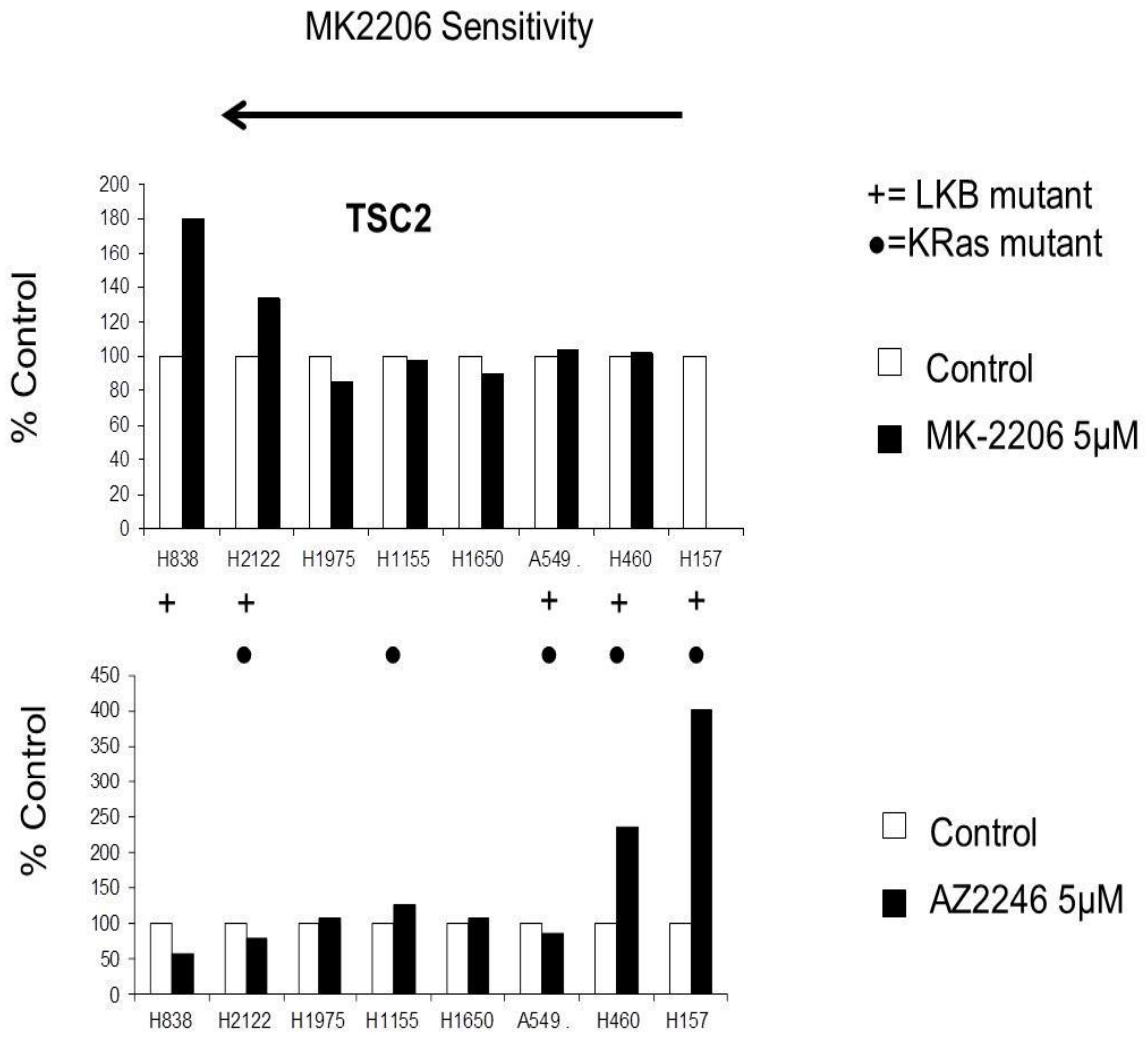

Figure 25: TSC2 stabilization after treatment with KRas effecter pathway inhibition. Measurement of TSC2 levels,degraded by Mek or Akt signaling and stabilized by LKB1 under low energy, after treatment with either control (DMSO) or an AKT (MK2206) or MEK (AZ6244) inhibitor. In LKB1 mutant lines sensitive to Akt inhibition treatment with 5μM MK2206 resulted in an increased expression of TSC2 (black lines) over control (white lines) not seen in resistant lines. Conversely, LKB1 mutant lines resistant to MK2206 showed stabilization of TSC2 with Mek inhibition although this did not correlate with sensitivity to this agent. Stabilized TSC2 represses mTOR signaling and translation.

Figure 26

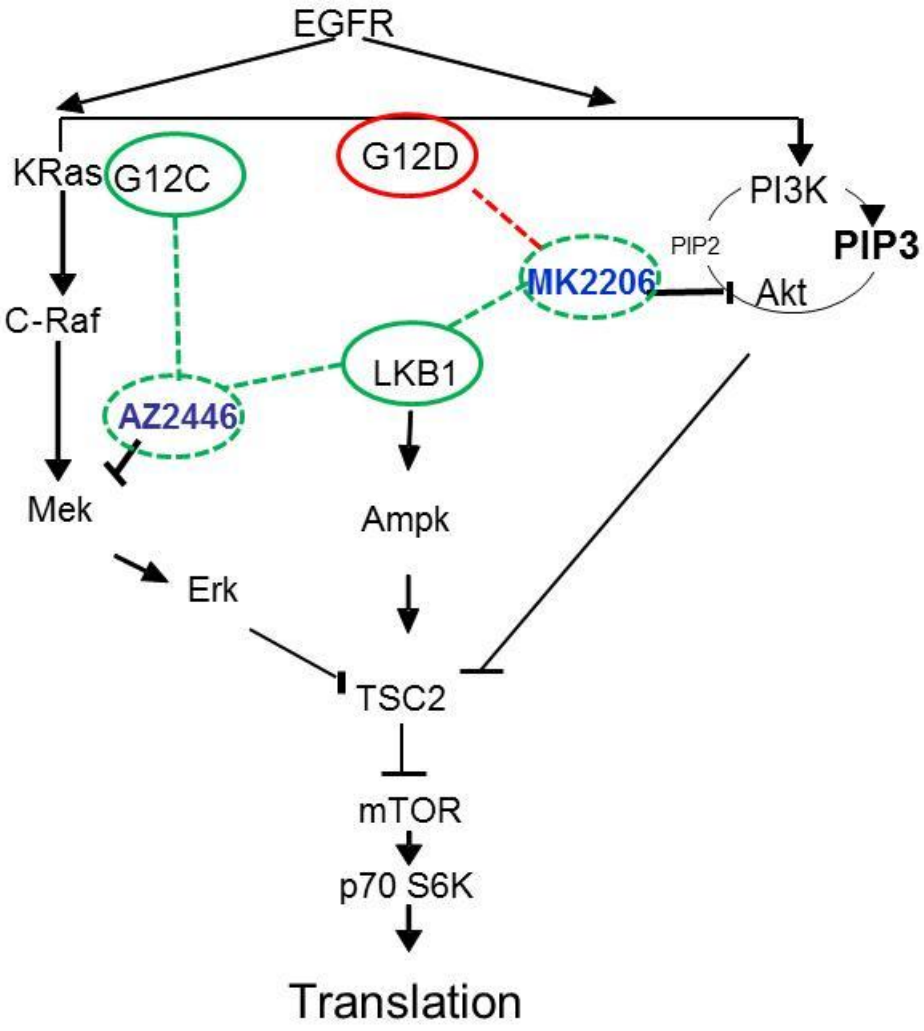

Figure 26: LKB1 plays a role in sensitivity to inhibition of Akt or Mek pathways. In our isogenic cell lines, the degree of growth inhibition by inhibitors of KRas effecter signaling was related to the activating mutation of KRas, while in a panel of NSCLC cell lines, the presence of inactivating mutations in LKB1 was found to influence response to these agents. KRas G12C lines with concurrent LKB1 inactivation being the most sensitive. Additionally LKB1 mutation alone conferred sensitivity of Akt inhibition, while in a majority of cell lines a concurrent KRas mutation conferred resistance. This effect was dependent on the ability of Akt inhibition to restore TSC2 expression.

4.3 siRNA treatment of isogenic lines with mutant KRas G12C

In chapter 3 it was determined that patients who harbored a mutant KRas G12C were resistant to multiple types of targeted therapy. To find new methods to treat these cells a genome wide siRNA screen was performed in the Mia Pa Ca-2 pancreatic cancer cell line which harbors a KRas G12C allele and an isogenic line with this allele deleted dubbed M27. The scheme for this screen is depicted in **Figure 27**.

4.3.1 Evaluation of direct KRas effecters

The validated KRas effecters described in **Figure 3** were the first set of data analyzed. siRNA directed towards these effecters had little effect of either the parental line or the M27 clone. Knockdown of BRaf, the Raf isoform primarily responsible for activating Mek/Erk signaling[38], inhibited growth in the M27 significantly more ($p=0.03$) than in the parental although by only 16% **(Figure 28)**. This finding may reflect recent findings elucidating a complex interplay of dimerization between Raf isoforms that can be modified by the activation of Ras isoforms in a melanoma model [114]. This data may indicate that the different isoforms of effecters or the effecters themselves are redundant, have feedback that negates the effect of their inhibition, or that KRas G12C mutants are using an effecter pathway that has not fully been characterized.

Figure 27

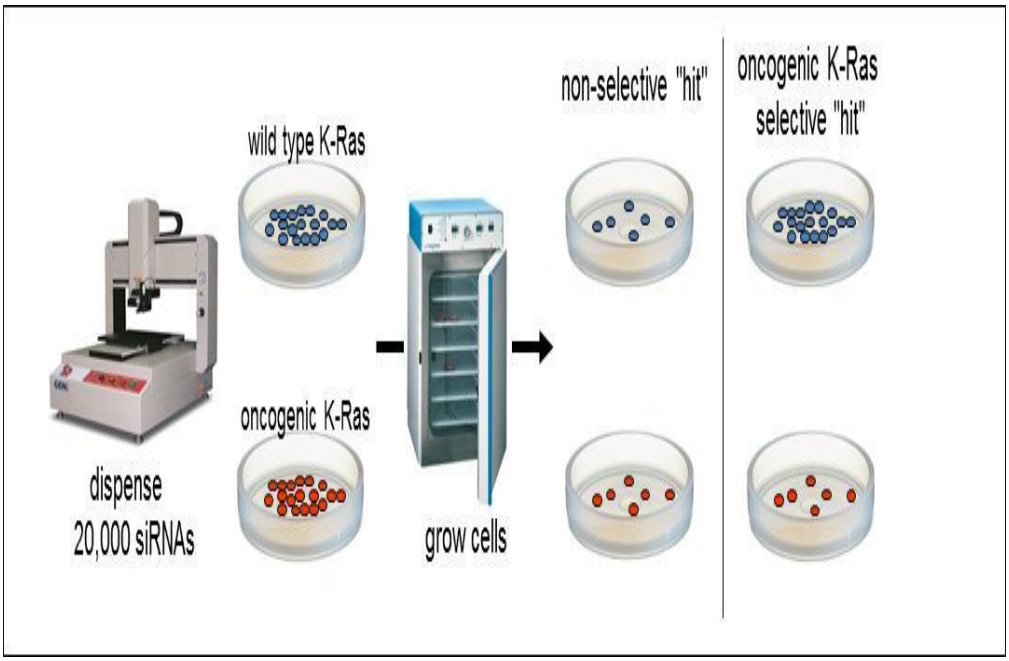

Figure 27: siRNA screen of the Mia Pa Ca-2 cell line (KRas G12C) and the isogenic clone with KRas deleted by homologous recombination. Each cell line was plated in 384 well plates with a pool of siRNA's targeting one gene already printed. Cells were allowed to growth for 72 hours and then cell viability was read. Each siRNA treatment was expressed as a fraction of the non-targeting control in the two cell lines. Finally these viabilities were compared to compare the effects of each gene knockdown in the cell line with and without mut-KRas G12C.

Figure 28

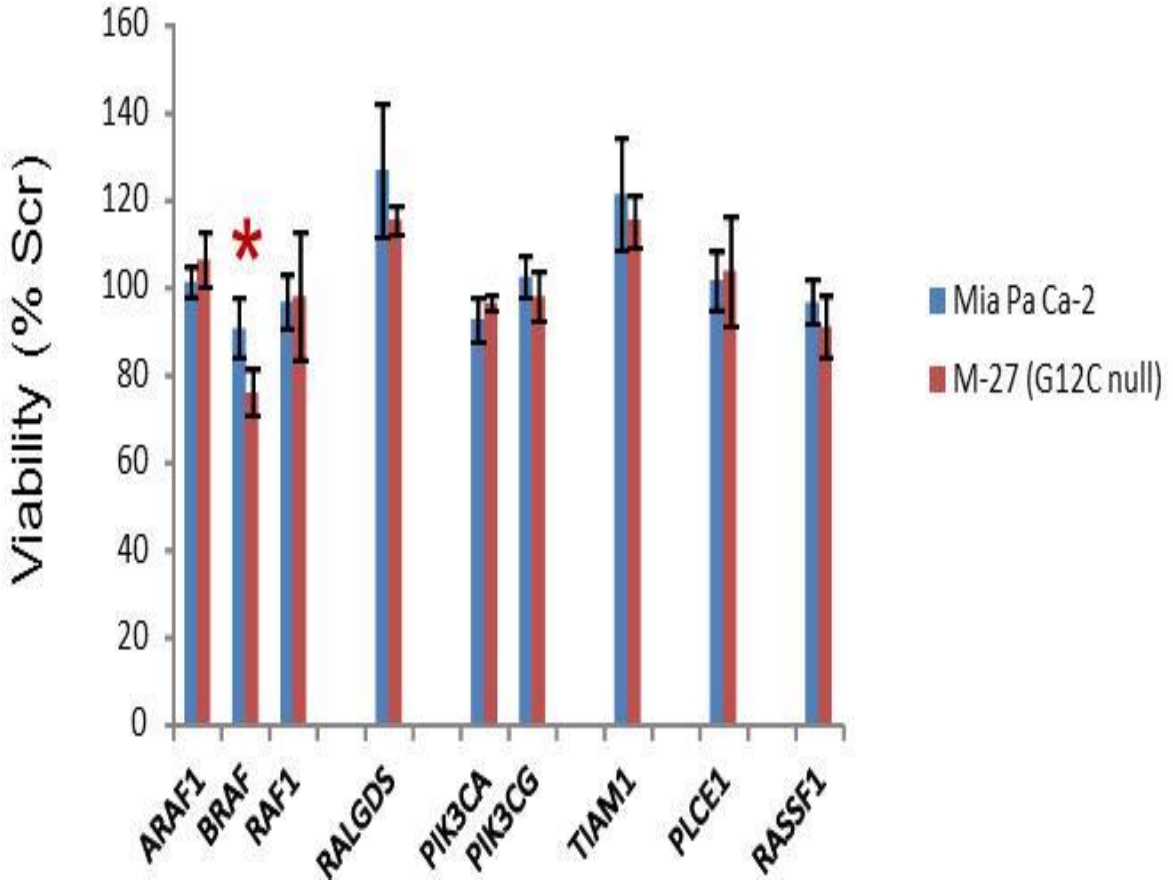

Figure 28: Analysis of the canonical KRas effecter pathways. The six best characterized KRas effecter pathways described in chapter 1 were analyzed. Cell viability was only reduced below 90% of non-targeting control in the M27 mut-KRas null clone with the deletion of *BRAF* while the parental Mia Pa Ca-2 cell line was not affected by this knockdown. Knockdown of any other of these KRas effecters failed to reduce viability lower than 90% compared with non-targeting control.

4.3.2 Determination and validation of siRNA hits

We selected “hits’ from the global siRNA screen based on their ability to selectively inhibit growth in Mia Pa Ca-2 mutant KRas G12C cells but not the wild type- KRas M27 clone. Once these “hits” were selected they validated using four second manufacturers siRNA’s in both the Mia Pa Ca-2/M27 isogenic line and the HCT-116 colon cancer line with an activating glycine to aspartate mutation in codon 13 and the HKH2 line the mutant *KRAS* allele deleted. In these lines 7 of 10 of the hits from our screen validated by our criteria that 3 of 4 of the individual siRNAs reflected the results seen in the initial screen. These results are shown in **Figure 29**. siRNA screening in mutant *KRAS* null/positive has been reported by several other groups and has yielded several “synthetic lethal” targets including *COPB2*, *TBK1* and *STK33* although the latter failed to reproduce in subsequent studies [96,112,113]. We utilized our a similar technique but shifted the focus of our analysis from siRNAs that simply inhibited the growth of cells with mutant *KRAS* to a greater extent than those with wild-type *KRAS* regardless of the viability, to focus specifically on targets which had no or minimal effect on the growth of our wild type cells while having a significant effect on cells with mutant *KRAS*.

Figure 29

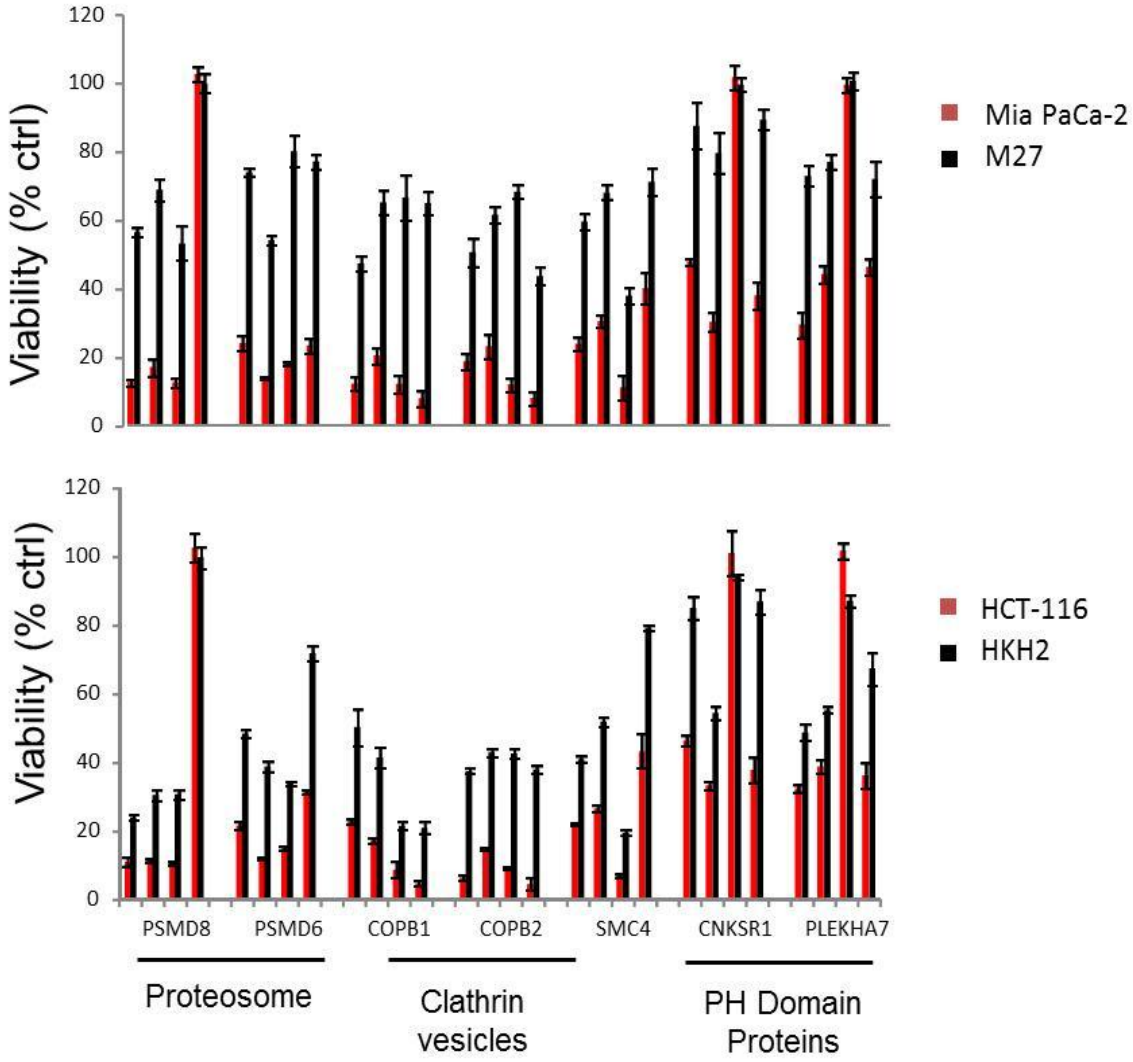

Figure 29: siRNA's which selectively reduced the viability of cells with mut-*KRAS*. siRNA's selected from the screen which reduced the viability of cell lines with a mut-*KRAS* (Mia Pa Ca-2, top/ HCT-116 bottom) but had no effect of the viability of isogenic lines with this mutant *KRAS* deleted (M27,top/HKH2, bottom). The four samples per target represent individual siRNA's to the same gene. Hits were considered validated if 3 out of 4 of these siRNA's produced a selective growth inhibition in the mut-*KRAS* line.

4.4 Discussion

Using a set of isogenic colorectal cell lines expressing KRas WT, G12C or G12D from the endogenous loci we have shown that the presence and type of activating mutation affect the response of cells to inhibitors of the PI3K and Raf effecter pathways of KRas. In all treatments that showed appreciable responses WT KRas cells were the most sensitive, reinforcing previous studies showing that mut-*KRAS* acts as a marker of resistance to inhibitors of the Raf-Mek and PI3K effecter pathways [80,109]. I have shown previously that mut-KRas 12C/V selectively activate the Raf-Mek inhibitor and RalGDS effecter pathways and inhibited PI3K signaling, conversely, mut-KRas G12D activated the Mek and PI3K effecter pathways but not the RalGDS pathway. Reflecting this, in colorectal cells engineered to express mut- KRas G12C/V the strongest growth inhibition was seen with the Mek inhibitor GSK1120212 while a weaker response was seen in KRas G12D expressing cells. In contrast, treatment with the Akt inhibitor MK-2206 resulted in a stronger response in mut-KRas G12D than in the mut-KRas G12C/V lines was observed reflecting the signaling pathways active in these cells. Although notably different agents targeting the same enzyme gave different results, indicating each particular agent evaluated may play a role in interpreting results. Subsequent studies on a lung cell line with different forms of activated KRas expressed from a plasmid showed that different *KRAS* mutants conferred different sensitivities to both cytotoxic and molecularly targeted agents in cell growth assays [106]. We next screened a Mek and Akt inhibitor across a panel of 30 NSCLC cell lines to attempt to correlate response to these inhibitors to differences in activating KRas mutations. However, to our surprise, no correlation was observed. To address this, we integrated analysis of other genes that are frequently mutated in NSCLC, many concurrently with *KRAS*, into our study. Loss of function mutations in LKB1, a tumor suppressor protein responsible for inhibiting translation though the stabilization of TSC2 under low energy conditions, is a common event in NSCLC[115], and frequently co-occurs with mut-*KRAS*[116]. Those pathways activated by LKB1 inactivation are known to interact with KRas effecter pathways and cause changes in cellular signaling, cellular

behavior, and response to targeted therapy. This reanalysis suggested that when these events were evaluated together trends emerge with LKB1 inactivation in the absence of mut-*KRAS* serving as a marker of response to the Akt inhibitor MK2006. Additionally one mut-LKB1/mut-*KRAS* cell line showed a degree of sensitivity to MK2206 while others with this genotype showed marked resistance. Both the Mek and Akt activation can induce the degradation of TSC2 resulting in mTOR mediated translation. LKB1 serves as a regulator of this process, activating in response to low intracellular energy levels and stabilizing TSC2 and inhibiting translation, a high energy process, until intracellular energy levels can be restored. Measuring protein levels in a panel of cells treated with MK2206 we found that those with LKB1 mutations that displayed growth inhibition had increased TSC2 levels post exposure. This included both a line with and a line without mut-*KRAS* mutation. All lines with mut- LKB1 and no response to MK2206 displayed concurrent mut- *KRAS* and displayed no increase in TSC2 after MK2206 treatment. In contrast, this group of cells displayed increased TSC2 levels when treated with AZ6244, although this did not correlate with response to this agent. Taken together this indicates that the presence of LKB1 with a mut-KRAS may confound attempts to inhibit KRAS though inhibition of the PI3K and Raf effecter pathways and the interactions of these pathways may be variable perhaps reflecting a third unknown determinant or the order of acquisition of these lesions.

Additionally, the Mia Pa Ca-2 line with and without the mut-KRAS 12C mutation was evaluated against a genome wide siRNA screen. We found that none of the canonical effecter pathways of KRAS had an important influence on the viability of these cells in the presence or absence of mut-KRAS 12C. However we found a set of genes that when inhibited showed increased growth inhibition in cells with mut-KRas 12C when compared to those cells with WT KRas. These included components of the proteasome and clatherin complex described previously[96] and two PH domain containing proteins, uniquely identified by our screen, one of which is a known component of the KRas nanocluster, necessary for KRas signaling. *CNKSR1* (protein product is CNK1) is described in Chapter 5.

Targeting KRas signaling through inhibition of the Ras nanocluster protein CNK1

5.1 Introduction

Many of the studies describing the activity of the Ras isoforms have been conducted on the protein itself; however, it is known that Ras proteins do not exist on membranes with only with their effecters, but rather as part of a “nanocluster” of scaffold and other accessory proteins. These nanoclusters govern such functions as selective Ras isoform recruitment. An example of this was seen in the G Protein signaling 14 (GPS14) receptor, found to selectively activate HRas [117]. When evaluated in *in vitro* assays GPS14 bound Ras-like proteins promiscuously, however in cells there was HRas selective recruitment to the nanocluster, facilitated by accessory proteins. Potential accessory proteins include gelectin family members are known to associate selectively in different Ras nanoclusters, with gelectin1 [118] associating with HRas, and gelectin 3 associating with KRas [119]. Nucleolin has also been identified as a selective KRas interacting protein, associating KRas with EGFR [119], although a different study found over expressed nucleolin associated all active Ras isoforms with EGFR [120]. The discrepancies suggest a possible dynamic protein interaction. Our studies described below have shown that the scaffold protein CNK1 can be classified as an essential component of the KRas nanocluster, associating KRas with its effecter proteins. Furthermore we hypothesized that inhibition of CNK1 by disrupting its proper localization represents a promising new stragedy to inhibit KRas driven cancers.

5.2 CNKSR1 as a component of KRas signaling

CNK1 is a multi-domain protein that was first discovered through genetic studies that identified *Drosophila* CNK (dCNK) as essential for the deranged eye phenotype induced by a constitutively active Ras mutant [121]. The N terminus of dCNK1 consists of a sterile alpha motif (SAM) domain, a conserved region in CNK1 (CRIC) domain, a PSD-95/DLG-1/ZO-1 (PDZ) domain and a C terminal proline-rich region containing a serine phosphorylation site and a pleckstrin homology (PH) domain. dCNK1 has an extended C terminus not present in human

CNK1 containing a Raf-inhibitory region (RIR) and a YELI site. Human CNKSR1 also has a conserved region among chordates (CRAC) domain implicated in protein binding. In *Drosophila*, growth factor receptor activation causes the YELI domain to bind dSrc reconfiguring the RIR, thus allowing dRaf binding to dRas, while the N-terminus SAM domain binds HYPEN (HYP) recruits Kinase Suppressor of Ras (dKSR).The resultant dKSR/dRaf dimer allows dMek phosphorylation and initiates the Mapk signaling cascade[122]. *Drosophila* has one Raf isoform, whereas mammals have three, (A-Raf B-Raf and C-Raf). B-Raf is frequently found with a phosphorylation-mimicking mutation rendering it independently active, whereas oncogenic KRas has been shown to selectively use the C-Raf isoform and accordingly C-Raf is required for the initiation of lung cancer by K-Ras[123]. Studies with mammalian CNK1 have shown a direct interaction between CNK1 and human HYP, B-Raf, and C-Raf. Drosophila models also suggested that CNK1 may be involved in dRAL signaling and subsequent studies showed direct binding between human CNK1 and RalGDS and the GTPase RhoA. Finally these studies showed the CNK1 directly bound the PI3K effecter Akt in human cell lines and was membrane localized. **Figure 30** summarizes the KRas signaling nanocluster found in *Drosophila* and humans. Together these studies suggest that *CNKSR1* plays a role in multiple downstream pathways in KRas signal transduction. As described below we performed an siRNA screen looking for gene that would selectively inhibit the growth of cells with an oncogenic KRas while having no effect on an isogenic cell line with the mutated *KRAS* allele silenced and identified human *CNKSR1*.

5.3 Results

5.3.1 Growth of NSCLC cell lines after *CNKSR1* knockdown

We studied the ability of *CNKSR1* knockdown to inhibit the growth of a panel of wild type and mutant KRas NSCLC cell lines finding that in cells with an activating *KRAS* mutation, si*CNKSR1* had a growth inhibitory effect of 45% or greater **(Figure 31)**. Additionally a growth inhibitory effect was seen in the H1993 cell line with a wild type *KRAS*, a likely explanation is that this wild type KRas cell has “mutant Ras-like properties” as previously been reported for

NSCLC cell lines [124]. Four other cell lines we tested with a wild type *KRAS* showed no significant response to the knockdown of *CNKSR1* suggesting they utilize of alternative pathways to elicit cell growth and survival. The ability of si*CNKSR1* to inhibit CNK1 expression is represented in three NSCLC cell lines with wild type *KRA*S (two of which showed no CNK1 expression) and three NSCLC cell lines with mutant *KRAS* in **Figure 32**.

Figure 30

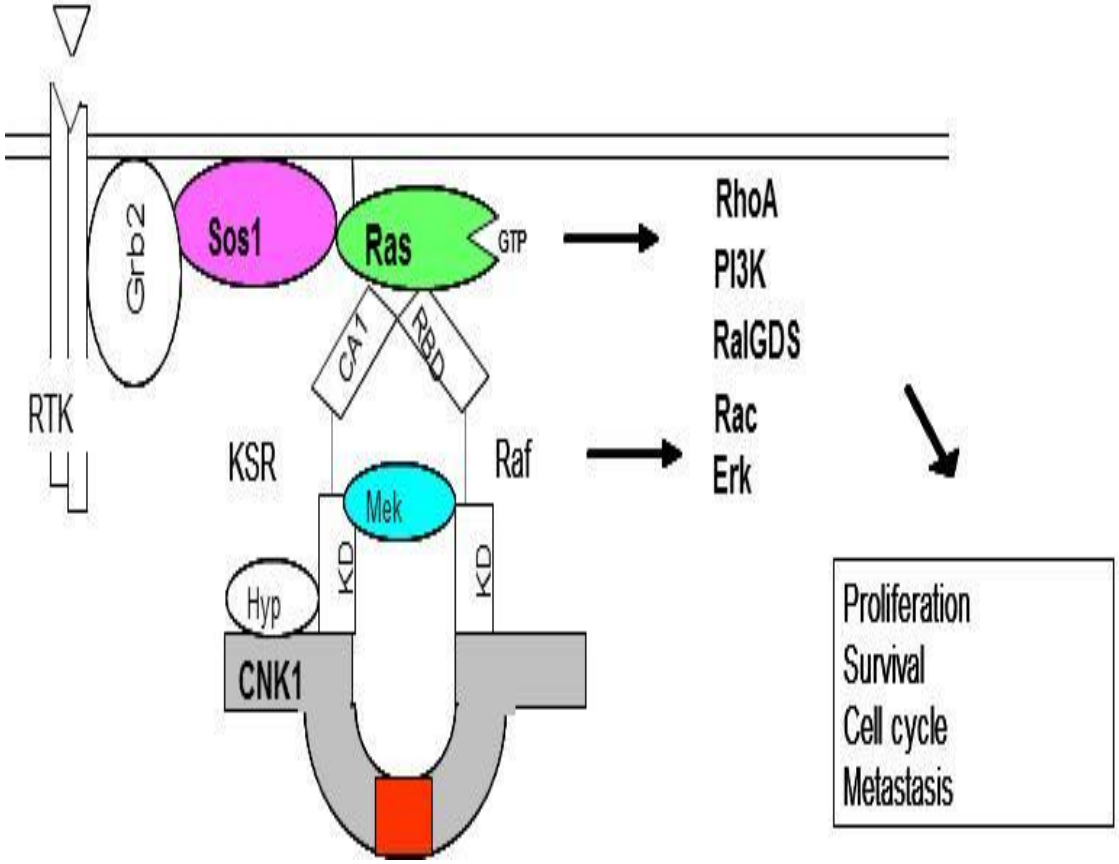

Figure 30: CNK1 nanocluster signaling. The CNK1 protein was initially described in *Drosophlia* as a scaffold for dRas signaling through the Mapk pathway by direct binding of dRaf, dHYP and dKSR. The human CNK1 has also been implicated in the direct binding of Raf but also the Ras effecters RhoA, RalGDS and PI3K. **Figure 30** adapted from [125] .

Figure 31

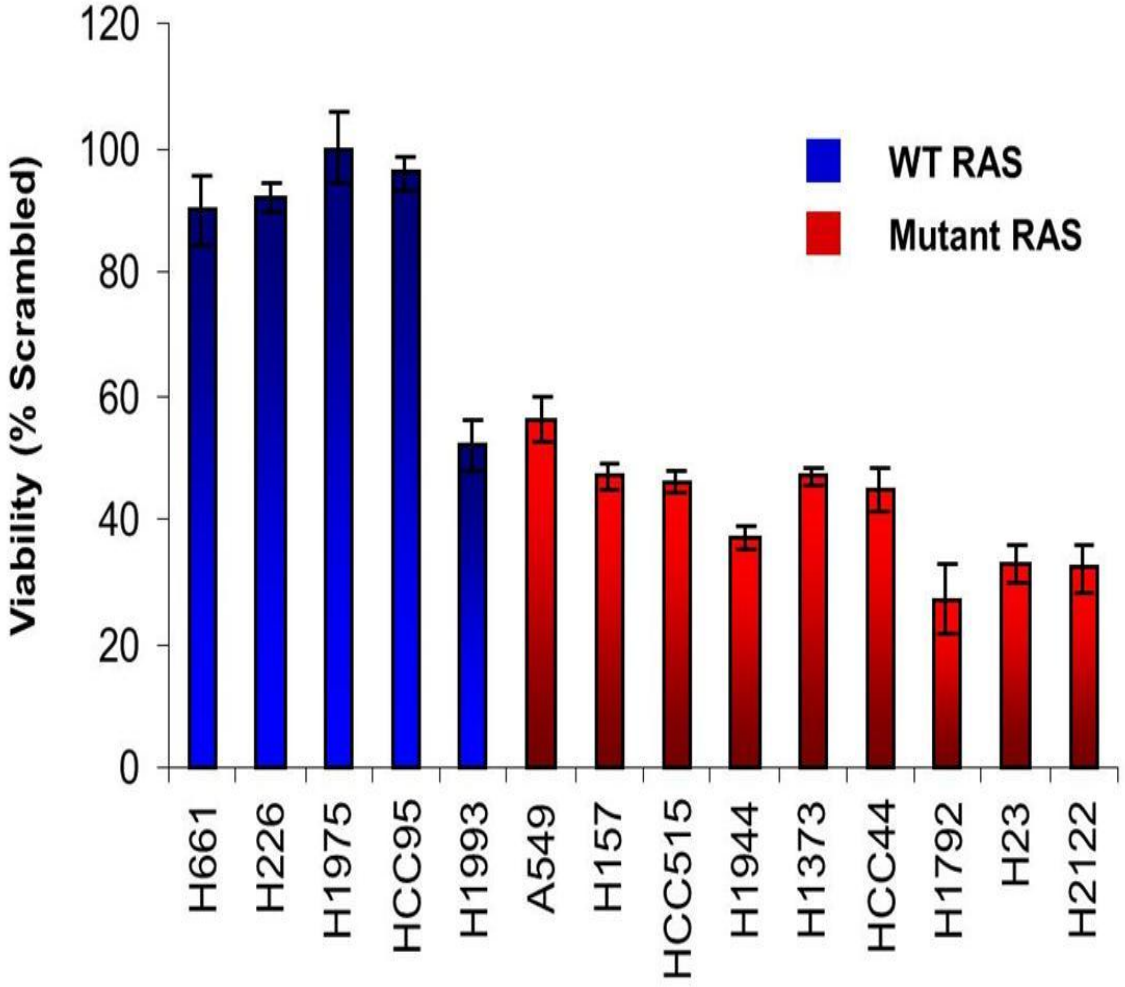

Figure 31: Viability of NSCLC cells after treatment with si*CNKSR1*. Cells were treated with si*CNKSR1* or non-targeting siRNA for 72 hours and cell proliferation was measured. A marked decrease in viability was seen in all the mut-*KRAS* cells and one WT-*KRAS* line when compared to cells treated with non-targeting siRNA. Other the WT-*KRAS* cells were unaffected.

Figure 32

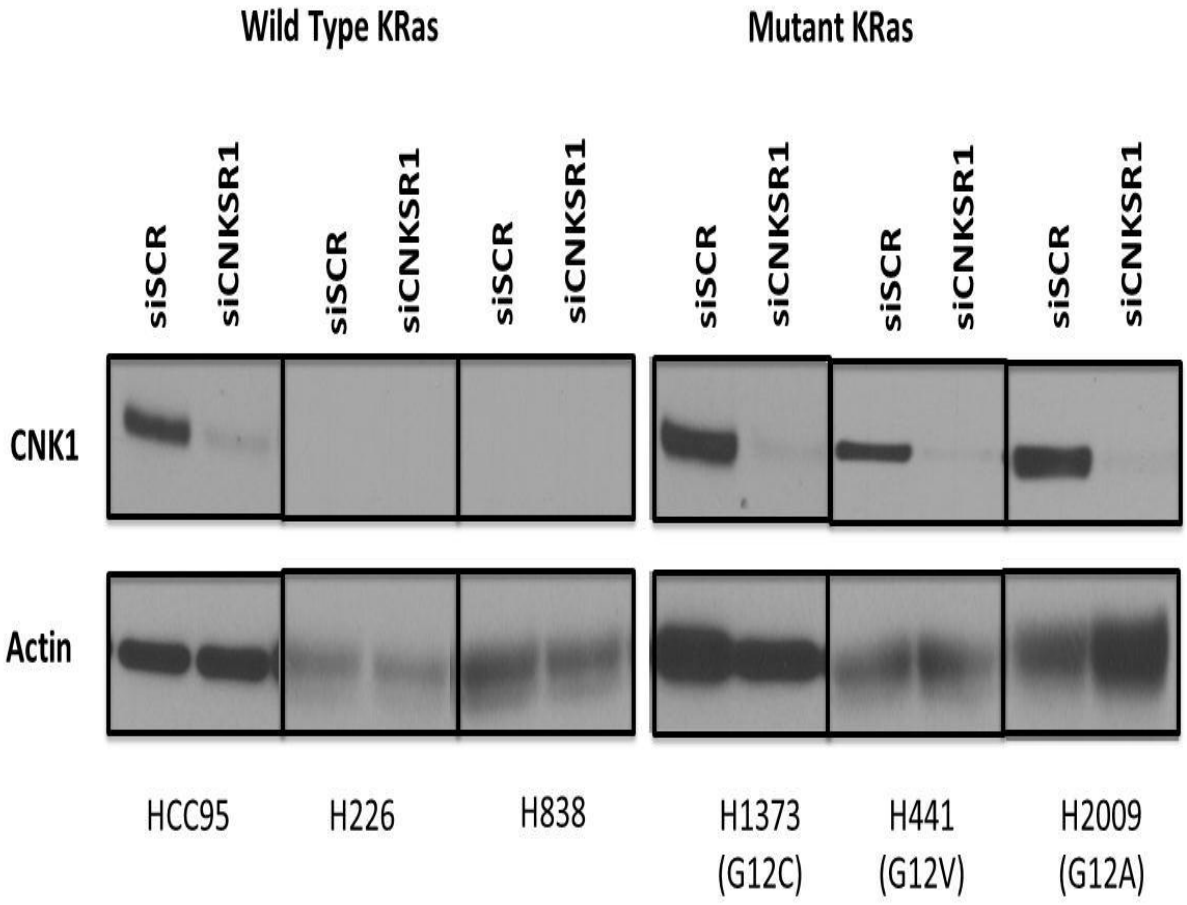

Figure 32: Knockdown of CNK1 with si*CNKSR1*. Three NSCLC cell lines with wild type *KRAS* and three lines with mutant *KRAS* (KRas G12C, G12V and G12A) were treated with si*CNKSR1* or non-targeting siRNA for 48 hours and protein expression was measured. Two of the three wild type cell lines displayed no CNK1 expression while one line had CNK1 expression but showed no viability decrease (**Figure 31**) despite no CNK1 being detectable after si*CNKSR1* treatement. In mutant *KRAS* lines CNK1 was detectable in all lines tested and *siCNKSR1* resulted in undetectable CNK1 in all lines tested. Actin served as a loading control

5.3.2 Effect of oncogenic *KRAS* and *CNKSR1* deletion on spheroid formation

Initial studies characterizing HCT-116 and the HKH2 line with a deleted mut-*KRAS* allele found that the HKH2 clone grew at half the rate of the parental line in adherent 2D conditions, similar to what we observed with *CNKSR1* knockdown in **Figure 29**. The initial studies additionally characterizing the HKH2 line showed more dramatic effects in 3-D assays such as colony formation or xenograft formation[126]. We explored this using a spheroid formation assay we investigated the ability of HCT-116 and HKH2 to form spheroids under non-adherent conditions. While HCT-116 formed large (>300 μM) spheroids, HKH2 cells aggregated together but failed to grow **(Figure 33)**. We next determined if this phenotype could be reproduced by knockdown of *CNKSR1*. We treated HCT-116 with a non-targeting siRNA and an si*KRAS* to serve as a negative and positive control, respectively. HCT-116 treated with siSCR grew similar to untreated cells while *siKRAS* inhibited spheroid formation in a similar fashion to HKH2 **(Figure 34)**. HCT-116 cells treated with *siCNKSR1* formed aggegerates similar to those created by HKH2 and HCT-116 cells.

5.3.3 *CNKSR1* deletion induces anoikis in a *KRAS* dependent manner.

Activated KRas has been shown to inhibit anoikis, apoptosis caused by detachment from a matrix, in cancer cells[127]. To determine if *CNKSR1* deletion restores anoikis, we treated HCT-116 and HKH2 cells with non-targeting siRNA, si*CNKSR1* or si*KRAS*. We found that siRNA to *CNKSR1* and si*KRAS* selectively induces anoikis in HCT-116 but not HKH2 cells as shown in **Figure 35**.

Figure 33

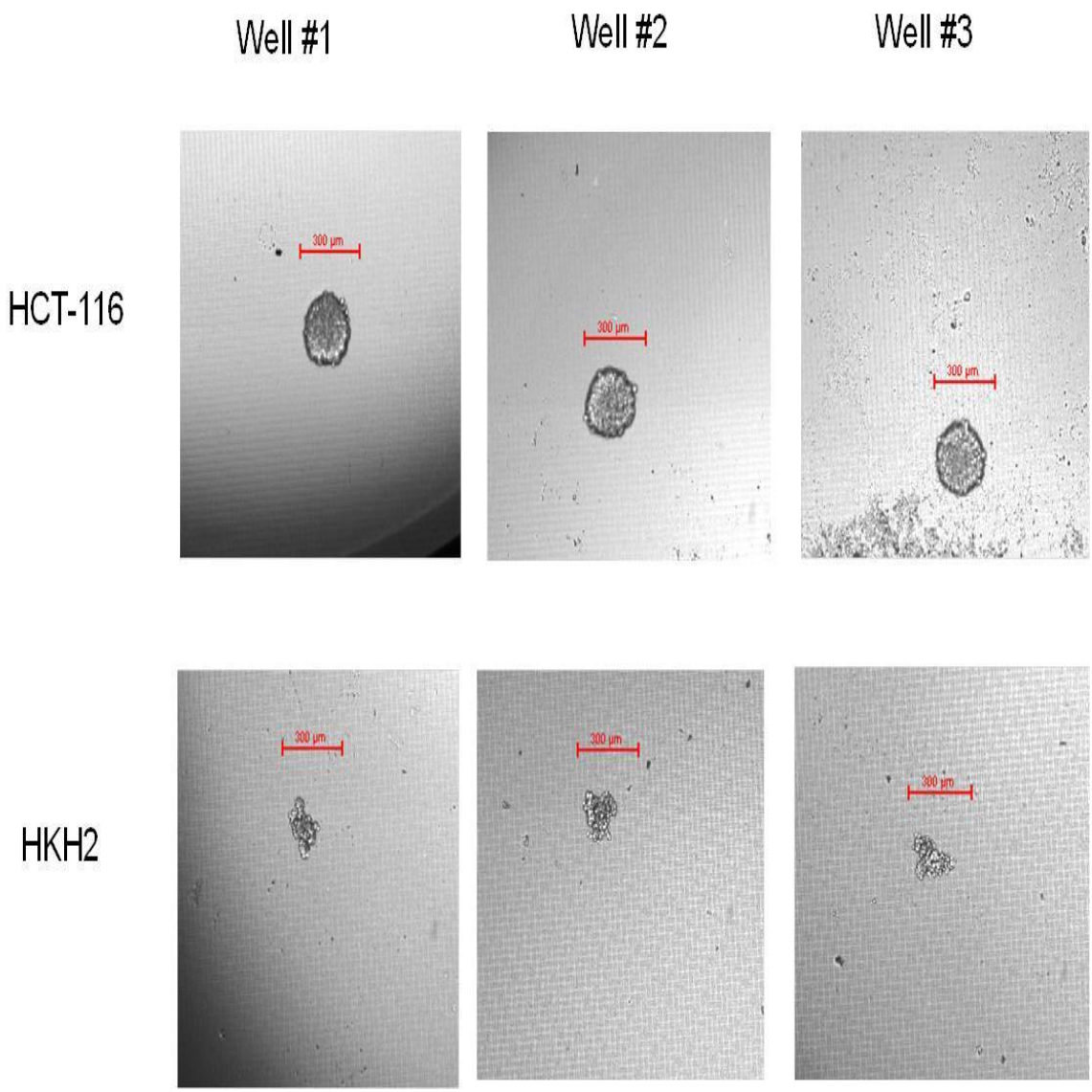

Figure 33: Spheroid formation in the presence or absence of mut-KRas. 20,000 HCT-116 or HKH2 cells were put into a hanging drop in a 3-D meshed plate. HCT-116 with a mut-*KRAS* allele formed spheroids greater the 300µM in size. In contrast, the isogenic clone of HCT-116, HKH2, with the mut-*KRAS* allele deleted formed only small aggregates which failed to proliferate.

Figure 34

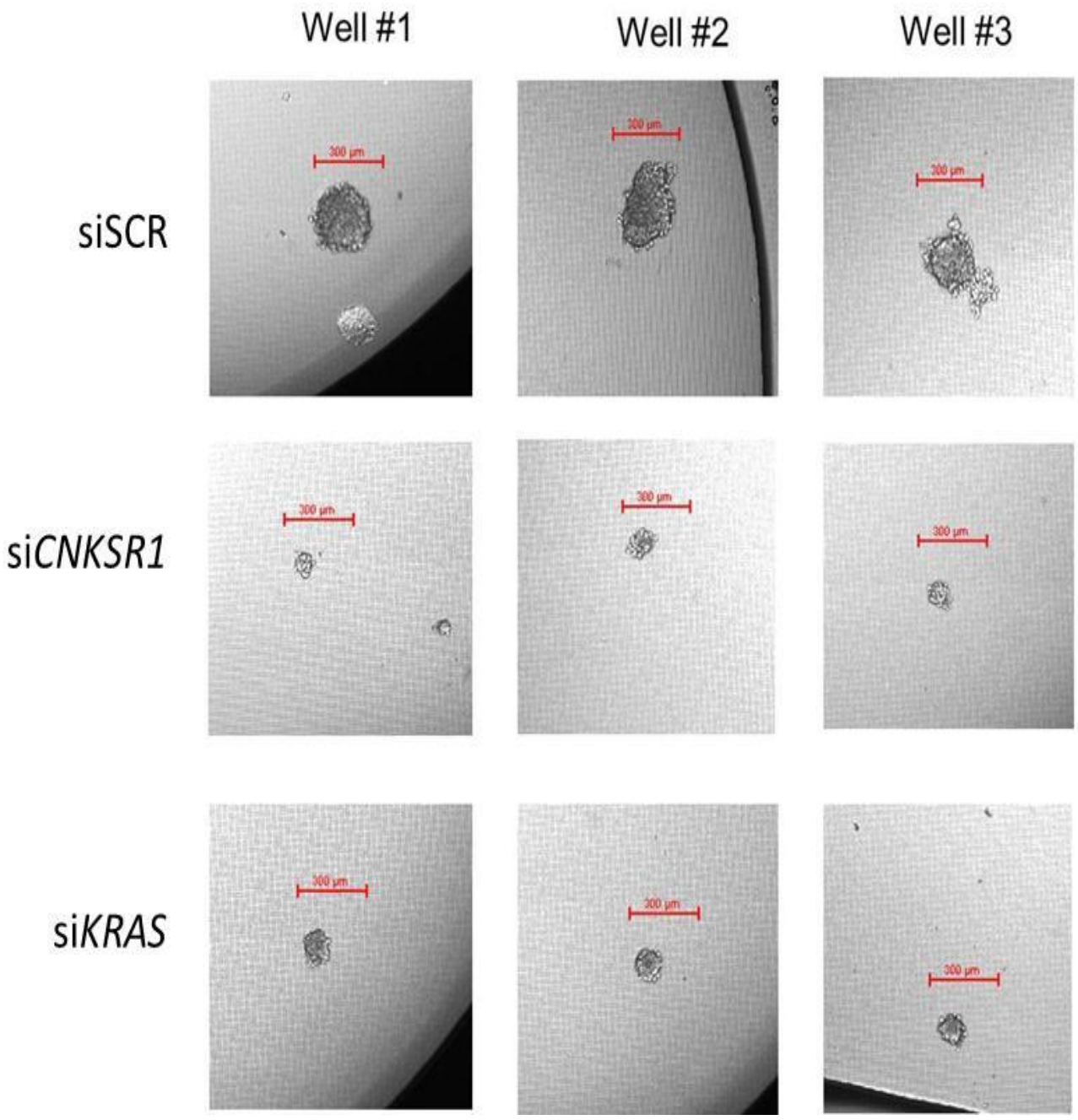

Figure 34: Spheroid formation in in HCT-116 cells after treatment with si*CNKSR1* or si*KRAS*. HCT-116 cells were treated with non-targeting siRNA or si*CNKSR1* 48 hours before plating in hanging drops. The HCT-116 cells treated with non-targeting siRNA formed spheroids greater than 300 µM similar to untreated HCT-116 cells **(Figure 32)**. HCT-116 cells treated with si*CNKSR1* or si*KRAS* displayed a phenotype similar to HKH2 cells forming small aggregates which fail to proliferate **(Figure 32)**.

Figure 35

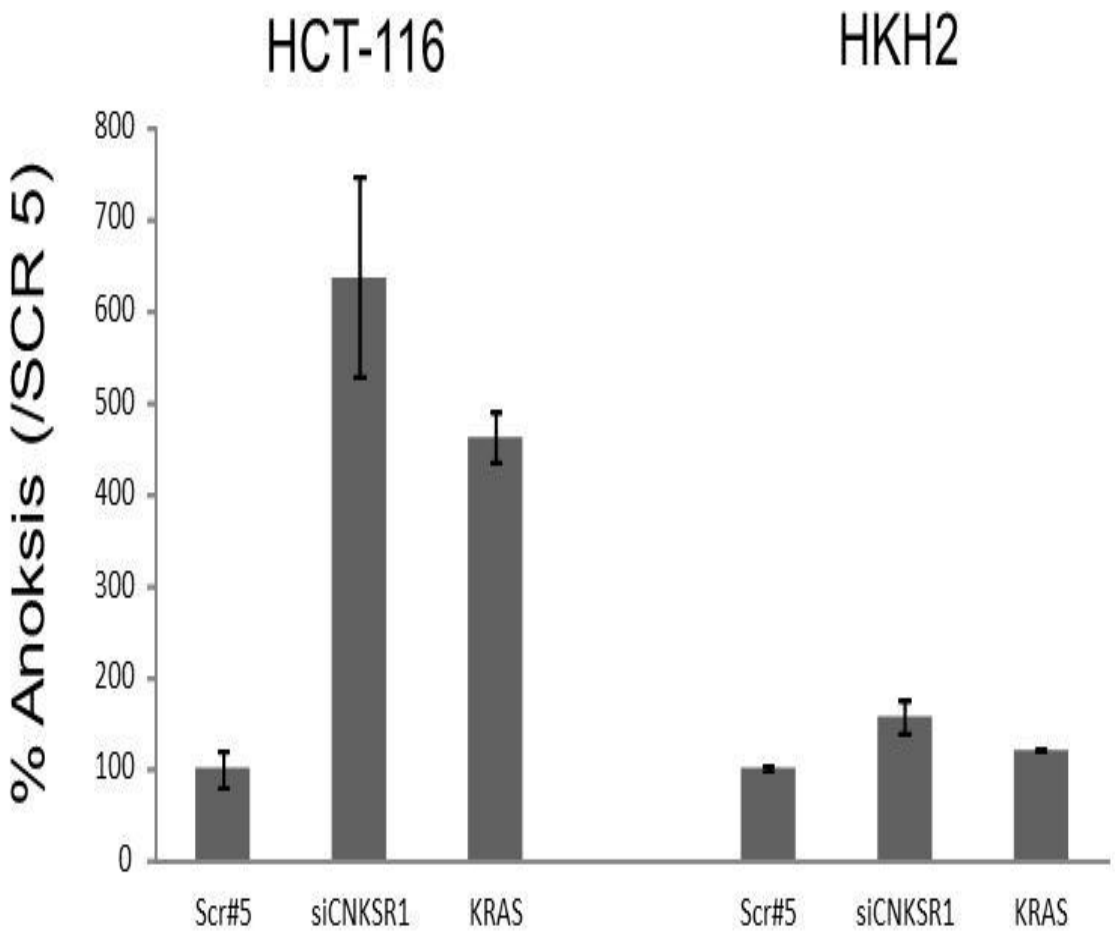

Figure 35: Anoikis in HCT-116 and HKH2 cells. HCT-116 and the HKH2 variant cells were treated with non-targeting siRNA (SCR5), si*CNKSR1* or si*KRAS*. These cells were then put in non-adherent, single cell conditions for 24 hours and apoptosis was measured. It was found that si*CNKSR1* or si*KRAS* significantly increased anoikis in HCT-116 cells while having minimal effect on HKH2 cells, indicating that signaling by both mut-KRas G13D and CNK1 were inhibiting anoikis in HCT-116 cells.

5.3.4 Analysis of signaling responsible for growth inhibition

To determine the molecular mechanism by which the knockdown of *CNKSR1* mimicked the absence of oncogenic *KRAS* we subjected both the mutant KRas HCT-116 and wild type KRas HKH2 cell lines, and a panel of wild type and mutant KRas NSCLC cell lines to RPPA analysis after treatment with non-targeting control or si*CNKSR1*. To first determine the optimal time to measure the effects of *CNKSR1* knockdown, siSCR (non-targeting siRNA) or si*CNKSR1* was added to the cells and levels of the CNK1 protein were measured after different times **(Figure 36)**. After treatment with si*CNKSR1*, CNK1 protein began to decline at 24 hours and was undetectable at 48 hours and remained inhibited at 72 hours. We next observed the proteins showing largest charge in HCT-116 when treated with si*CNKSR1* and compared those to levels in HCT-116 and HKH2, the isogenic line for mut-*KRAS* in an attempt to characterize the mechanisms responsible the observations in our siRNA screening results **(Figure 37)**. *CNKSR1* knockdown caused a large decrease in both Cyclin B and phosphorylated Rb in both the isogenic KRas cells and the cell line panel. Cdk1, which couples with Cyclin B to make the mitosis promoting factor necessary for cell cycle progression into mitosis, was also down regulated in both conditions. This is notable as a previous study on these isogenic lines with an shRNA library found that HCT-116 was more sensitive to deletion of several components of mitotic signaling including Plk1 than its isogenic partner [96]. Additionally, Rb phosphorylation at the site responsible for its inactivation and resulting in cell cycle progression, was significantly inhibited in a manner similar to that seen in MEFs created with an absence of Ras signaling[128]. To test whether this effect was specific to the HCT-116 cell line or broadly applicable, we additionally performed RPPA on a collection of pancreatic, colon and lung cancer cell lines and found that all lines tested showed knockdown of Cyclin B and Cdk1 ($p<0.01$) additionally the phosphorylation of Rb1 at the serine [807] site was significantly downregulated ($p<0.05$) **(Figure 38)**. Additionally Fak ($p<0.01$) and Chk1 ($p<0.05$) were significantly down-regulated in this cell line panel after si*CNKSR1* knockdown (data not shown), also observed with the deletion of the mut-*KRAS* allele. These changes occurred after

CNKSR1 deletion regardless of the type of amino acid substitution responsible for activating KRas indicating a universal mechanism for inhibition of KRas signaling. A significant difference between si*CNKSR1* and the deletion of mut-*KRAS* allele was that while phosphorylated YB-1 was up regulated after si*CNKSR1* treatment ($p<0.05$) in this panel, deletion of the mut-*KRAS* allele resulted conversely in down regulation of this phosphorylation site **(Figure 37)**, indicating si*CNKSR1* is not an exact phenocopy of the deletion of a mut-*KRAS* allele.

Figure 36

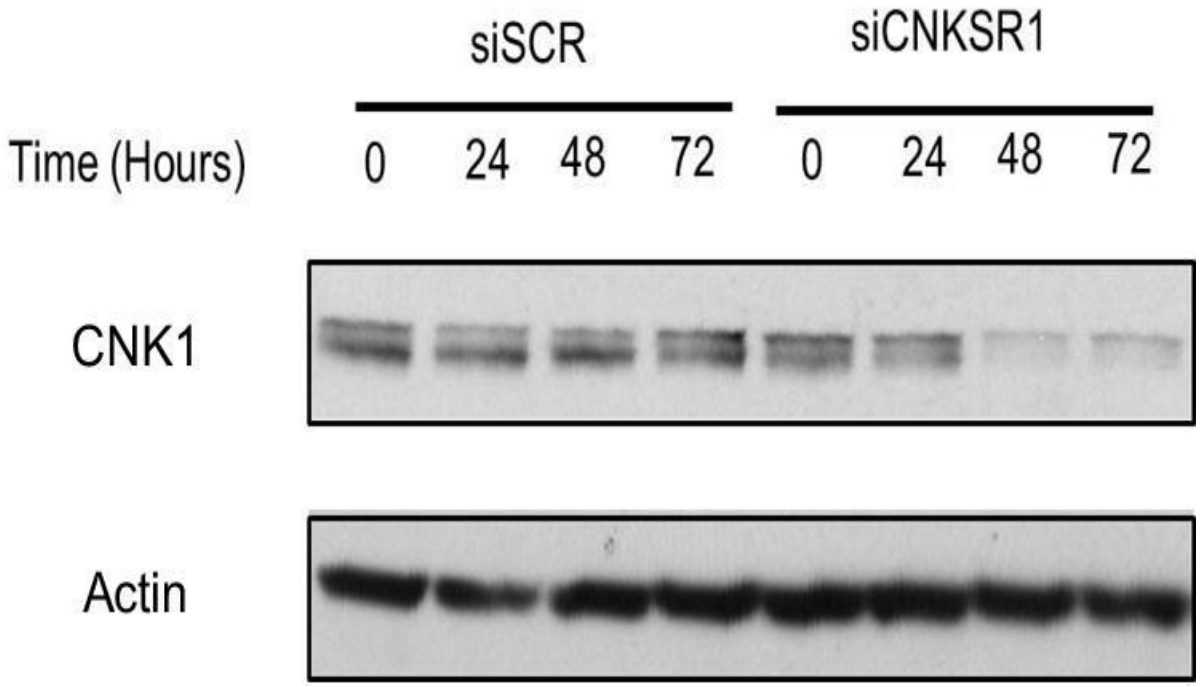

Figure 36: Time course for knockdown of CNK1 with si*CNKSR1*. Non-targeting siRNA or si*CNKSR1* was applied to cells at indicated time points before lysing and probing for CNK1 with a specific antibody. Actin served as a loading control.

Figure 37

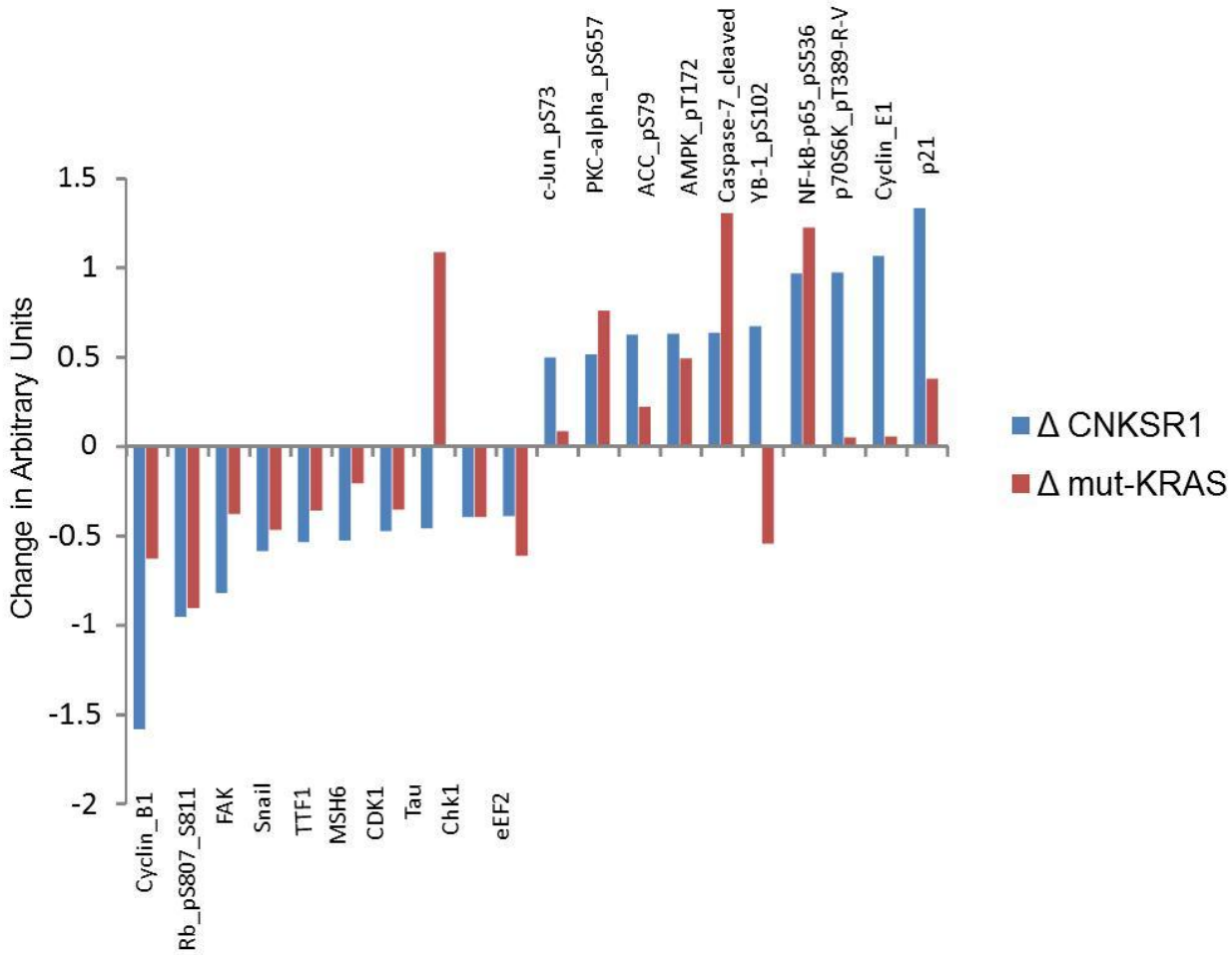

Figure 37: Comparison of HCT-116 treated with si*CNKSR1* to a mut-*KRAS* null clone by RPPA. The change (in arbitrary units) in the ten most down regulated proteins by si*CNKSR1* when compared with non-targeting siRNA (blue) compared to the change between HCT-116 and the HKH2 clone (red). Several cell cycle proteins including Cyclin B, phosphorylated Rb, Cdk1 and Chk1 were down regulated in both conditions.

Figure 38

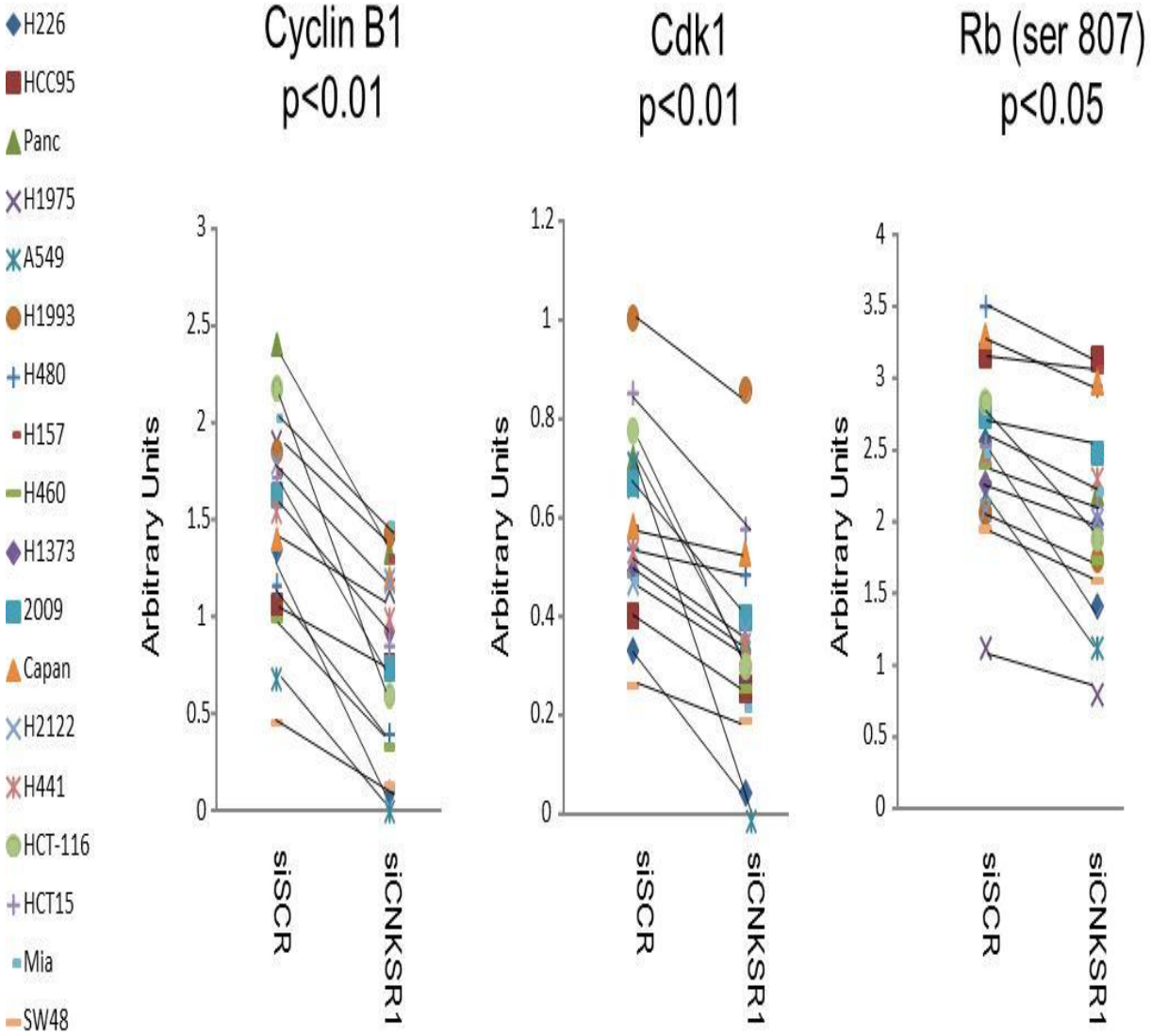

Figure 38: Cell cycle proteins significantly changed in a panel of cells after treatment with a non-targeting control and si*CNKSR1* as determined by RPPA. Cyclin B and Cdk1 form the mitosis promoting factor and were both significantly down-regulated after si*CNKSR1* treatment. Phosphorylated Rb was also down-regulated after si*CNKSR1* treatment. Notably this was the same phenotype seen in Rasless MEFs[128].

5.3.5 Cell Cycle analysis after *CNKSR1* knockdown

A decrease of Cyclin B and Cdk1 indicates the ability of cells to form the Mitosis Promoting Factor and a failure to progress through the cell cycle while the phosphorylation of Rb is essential for progression past the G1 stage. To determine whether the changes in cell cycle proteins seen with the knockdown of *CNKSR1* had functional consequences we subjected our cells to cell cycle analysis. We found that HKH2 cells without mutant KRas showed an increase of cells in the G1 phase of the cell cycle compared to HCT-116 cells with mutant KRas. Thus, knockdown of *CNKSR1* has a modest effect in HKH2 cells, but strongly induces G1 arrest in HCT-116 cells **(Figure 39)**. We next compared the cell cycle of a mut-KRas G12V cell line which showed decreased viability with to *CNKSR1* (H441) knockdown to a cell line with wild type *KRAS* which expresses CNK1(**Figure 32**) but showed no response to *CNKSR1* knockdown (HCC95). As expected H441 accumulated in the G1 phase of the cell cycle while the HCC95 resistant line showed little effect of *CNKSR1* knockdown **(Figure 40)**. These results strongly suggest that the decreased proliferation seen in our panel of NSCLC cell lines is a result of the cells accumulating in G1. Additionally since the HCT-116 line has a mut-KRas G12D and H441 an activated KRas G12V the findings suggest that the G1 arrest is independent of the amino acid substitution responsible for KRas activation.

Figure 39

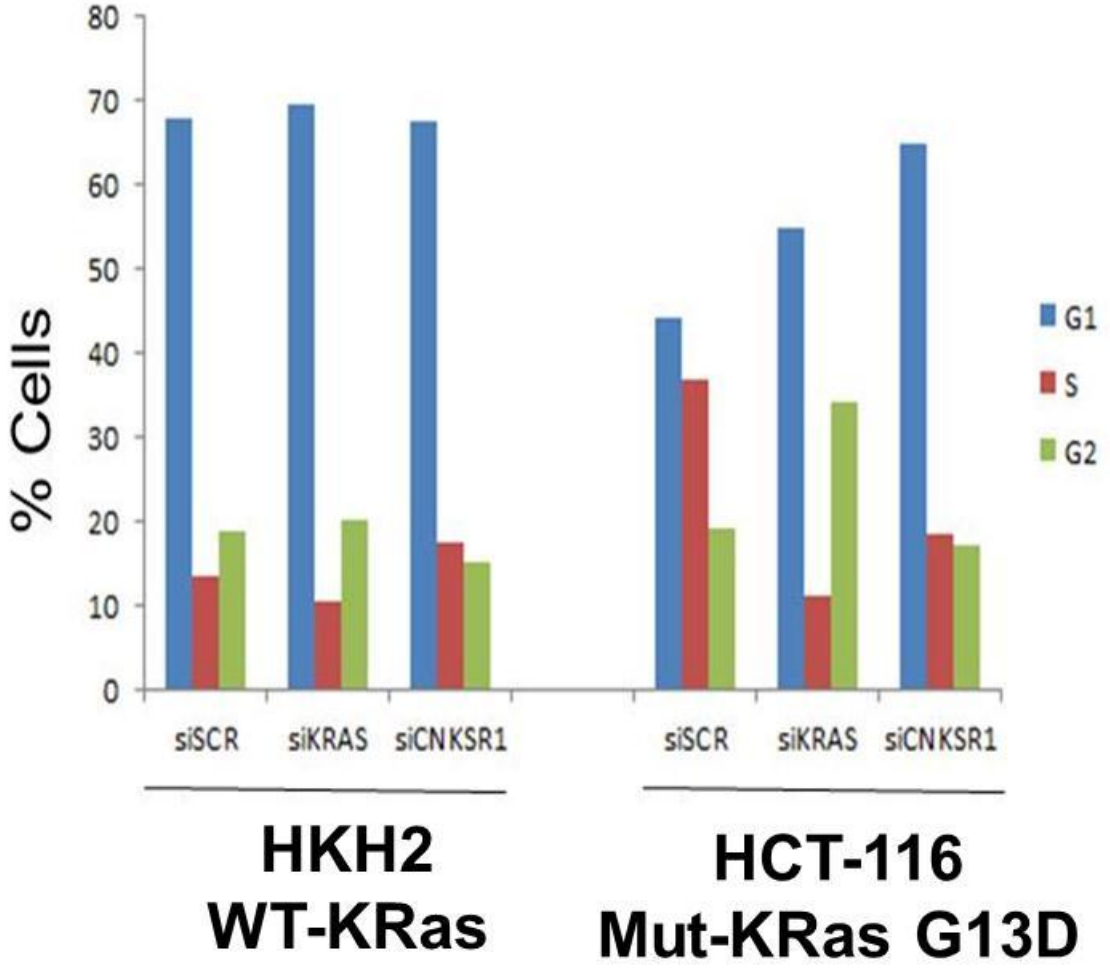

Figure 39: Cell cycle analysis of HCT-116 and HKH2 cells treated with si*KRAS* or si*CNKSR1*. HCT-116 cells lacking the mut-*KRAS* allele (HKH2) show a higher proportion of cells in the G1 phase of the cell cycle which is unchanged by the addition of si*KRAS* or si*CNKSR1*. HCT-116 (mut-KRas G13D) cells show a greater distribution of cells through the cell cycle than HKH2 but show an increase in cells in the G1 phase with both si*KRAS* and si*CNKSR1*.

Figure 40

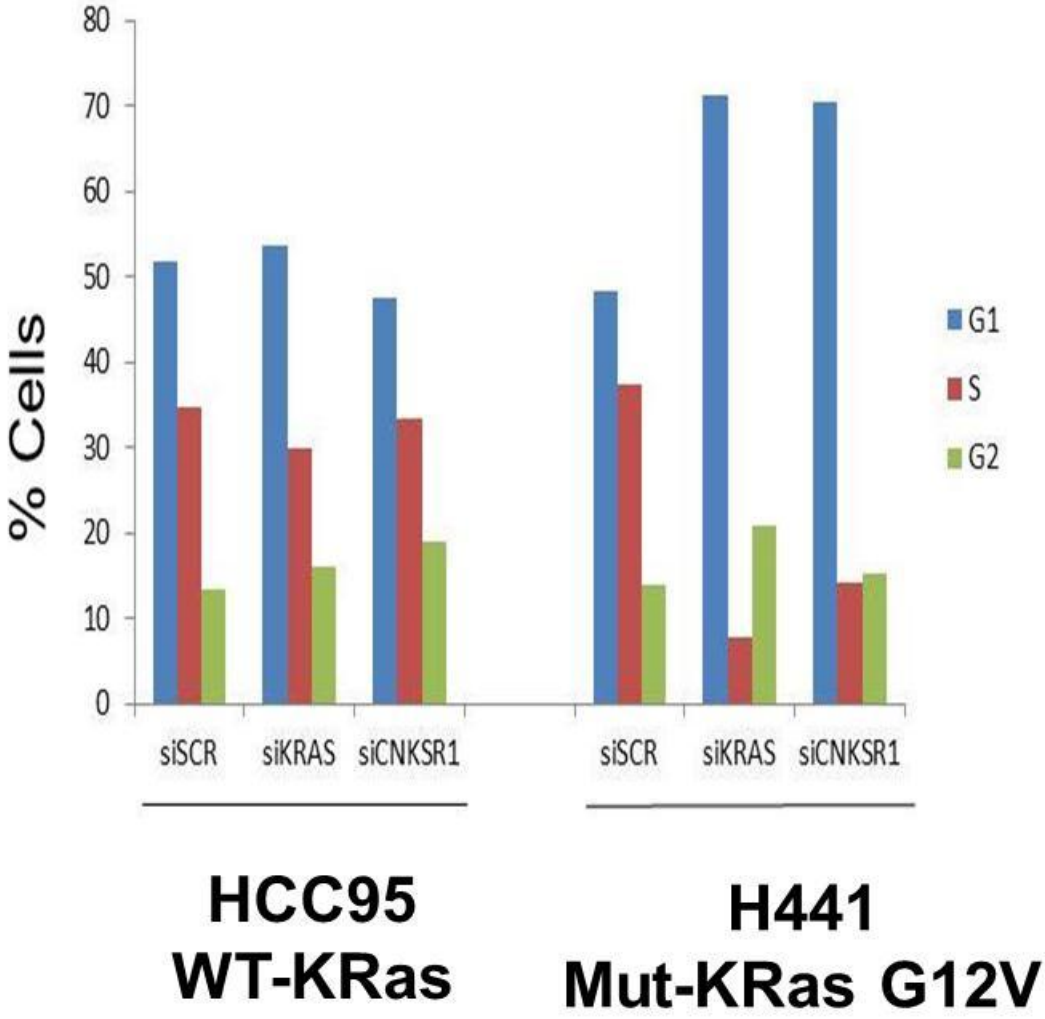

Figure 40: Cell cycle analysis of NSCLC cells. HCC95 (WT *KRAS*) and H441 (mut-*KRAS*) showed a similar distribution through the cell cycle. Treatment of HCC95, which showed no viability change with si*CNKSR1*, with si*KRAS* or si*CNKSR1* showed no effect on the cell cycle distribution of these cells. H441, which showed decreased viability with si*CNKSR1* treatment, showed an increase in the G1 phase of the cell cycle after treatment with both si*KRAS* and si*CNKSR1*.

5.3.6 CNK1 localization with mutant KRas

In the *Drosophila* studies dCNK and dRas in drospohlia were found co-localized in the cellular membrane [121]. To address the question whether in mammalian cells there is a membrane association of fluorescent protein tagged CNK1 and KRas, we used confocal microscopy and a technique known as Fluorescence Lifetime Imaging Microscopy. The basis of FLIM is that upon excitation, if the protein GFP tag is within the critical distance of 10 nm of another protein with a red fluorescent protein RFP tag, FRET (Förster resonance energy transfer) occurs from the donor (GFP) to the acceptor (RFP). This results in a reduction of the emission lifetime of the donor GFP which is measurable and indicates a direct interaction within 10 nM. The use of FLIM to detect FRET has the advantage that only the GFP donor fluorescence needs to be measured. HEK293 cells were transfected with either a WT or a mutant KRAS 12D tagged with red fluorescent protein (RFP) and CNK1 tagged with green fluorescent protein (GFP) allowed to grow for 48 hours and fixed on slides.

In the cells transfected with wild type KRAS and CNK1, CNK1 was largely cytoplasmic and the WT KRAS was localized to the membrane, there was a small level of co-localization at the membrane, however, the lifetime of CNK1 GFP after excitation was similar to that of our cells transfected with only CNK1 GFP, indicating that there was colocalization (less than 500 nm) but no direct interaction (ie more than 10 nM) with the WT KRas RFP. HEK293 cells transfected with mut-KRAS 12D and CNKSR showed a markedly transformed phenotype with elongated cells and branching morphology. In these cells these two proteins were found colocalized at the cellular membrane in distinctive clusters **(Figure 41)**. Additionally, the lifetime of the GFP was reduced suggesting that they were in close proximity, with less than 10 nM separating them **(Figure 42)**.

Figure 41

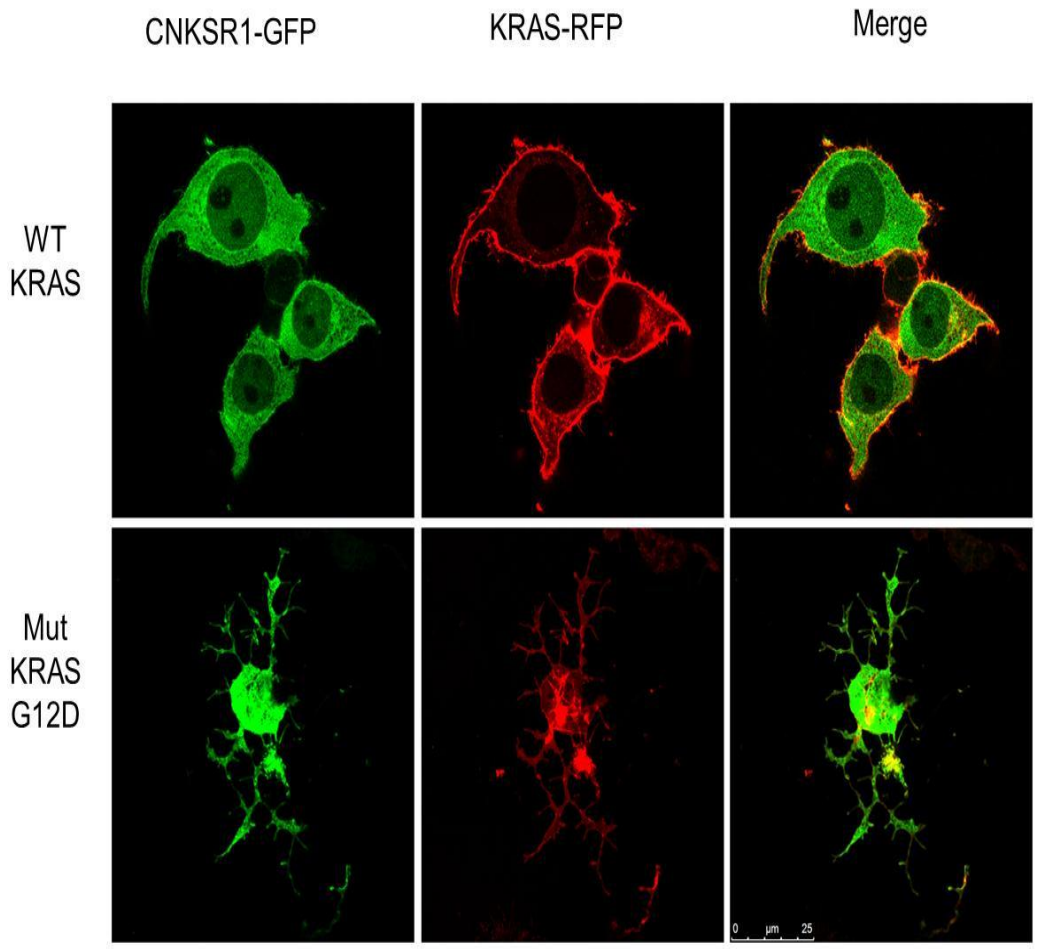

Figure 41: Confocal of CNK1 and KRas. CNK1 was tagged with GFP and either WT KRAS or mut-KRAS G12D were tagged with RFP. These fusion proteins were then co-transfected in HEK293 cells and serum starved overnight. In cells transfected with CNK1 GFP and WT KRAS GFP CNK1 protein was primarily cytoplasmic and KRas was mostly localized to the membrane, which no or little co-localization occurring. The cells transfected with mut-KRAS displayed a dramatic change in morphology with a fiberous appearance. These cells showed co-localization of CNK1 protein and mut-KRas at the membrane and at the tips of fibrous extensions.

Figure 42

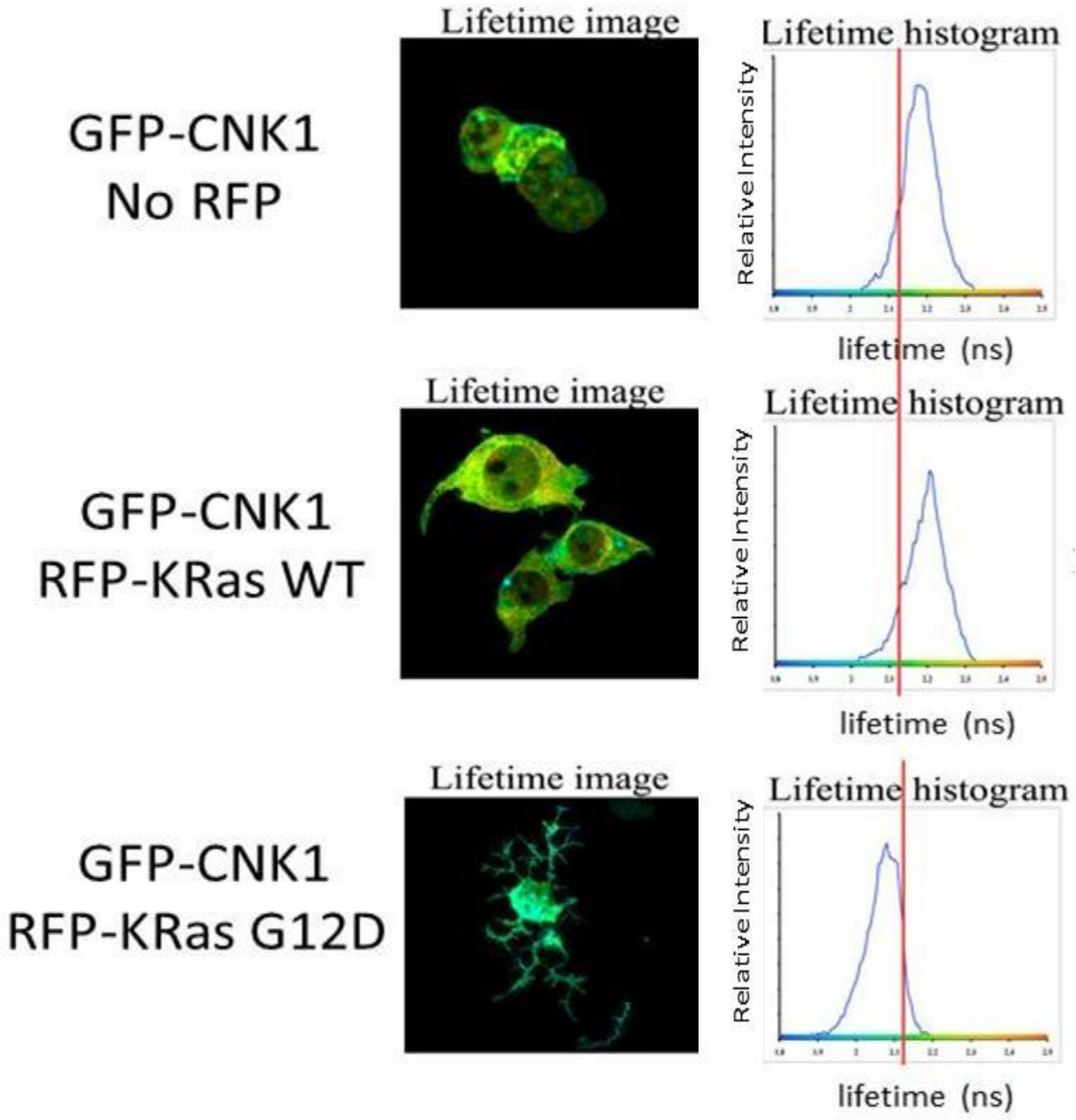

Figure 42: FLIM analysis of CNK1and KRas. Fluorescence Lifetime Imaging Micorscopy was used to analyze interaction between CNK1 and either WT KRas or Mut-KRas G12D. Cells transfected with CNK1-GFP alone served as a control. When co-transfection of CNK1 and WT KRas was performed, the lifetime of GFP after excitation was similar to what was seen in our CNK1-GFP alone sample. In contrast, a dramatic decrease was seen in this lifetime with the co-transfection of CNK1 and mut-KRas G12D indicating that electrons were being transferred to RFP, meaning the two fusion proteins are within 10nM of each other.

5.4 Rationale for CNK1 as a target for cancer therapy

siRNA to *CNKSR1* inhibits growth in all the oncogenic KRas cancers we have tested, regardless of the activating mutations or tissue origin. However since CNK1 is not an active (ATP utilizing) enzyme it is unclear how to approach CNK1 as a target for cancer therapy. The PH domain of CNK1 binds to the same negatively charged phospholipids as the polybasic domain in the KRas hypervariable region [129] but with higher affinity to membrane phosphatidylinostol-2- and 3-phosphates (PIP_2, PIP_3) and is critical for the proper localization of CNK1. As small molecules which bind to the PH domains of the Akt and PDK1 kinases have previously been developed[130], we postulated that it should be possible to use this paradigm as a way to inhibit CNK1 by inhibiting its proper localization with mutant KRas.

5.4.1 Viability of NSCLC cells with treated of a dominant negative PH domain

To test the hypothesis that binding molecules to the PH domain would be an effective method to inhibit the activity of CNK1, we expressed only the PH domain of CNK1 without any other portions of the protein present. This PH domain fragment retained the ability to bind PIP_2 and PIP_3 with KD's of 144 and 146 nM respectively. This PH domain occupied the $PIP_{2/3}$ lipids on the membrane but had none of the other domains important for signaling. As such it has characteristics of a dominant negative and blocked the growth of mutant KRas cells. We transfected the NSCLC line H1373 whose growth is inhibited by si*CNKSR1* with either the PH domain of CNK1 or a vector controland found transfection efficacy to be ~99% as measured by the presence or absence of GFP expressed independly by the vector or fused to our GFP construct. The viability of these cells was then measured after 72 hours. We found a significant ($p<0.05$) 48% reduction in viability similar to the 49% reduction in viability seen by si*CNKSR1* in **Figure 43**.

Figure 43

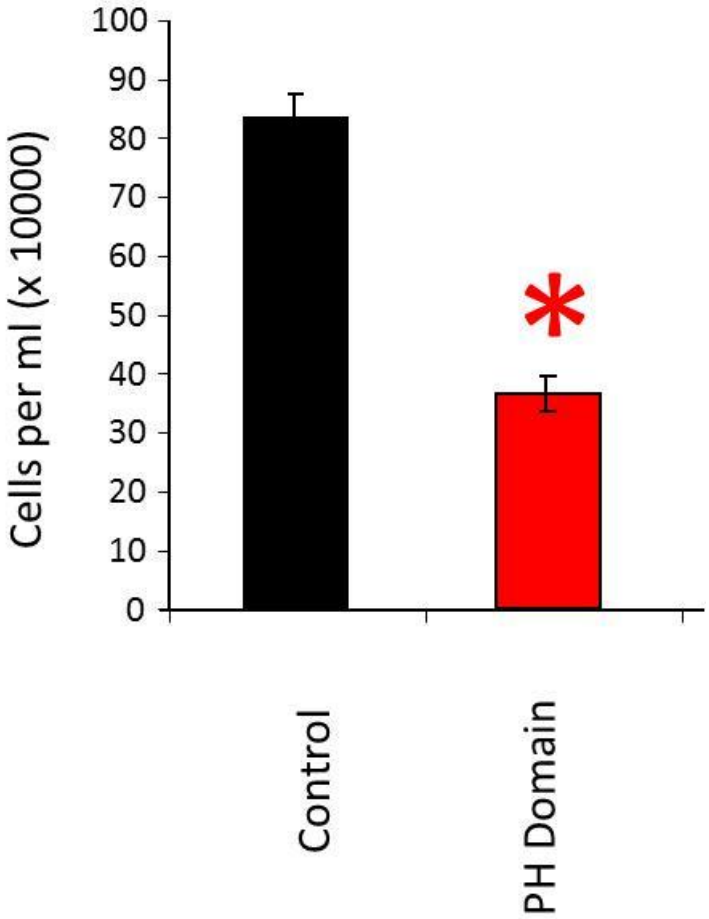

Figure 43: Expression of a dominant negative PH domain in NSCLC cells. A GFP only expressing vector control and the CNK1 PH domain- GFP fusion lacking any other protein domains was inserted in H1373 NSCLC cells, known to be sensitive to CNKSR1 knockdown. Transfection efficiency was measured by the presence of GFP and found to be ~99%.The empty vector had no effect on the proliferation of the cells, but the cells transfected with the PH domain showed a significant decrease in viability ($p<0.05$) after 72 hours.

5.4.2 Identification of agents inhibiting CNK1

A homology model for the PH domain was developed in collaboration with the Dr. Zhang in the Computer Modeling Core at the Center for Targeted Therapy at MD Anderson. The first set of analogs was screened for the selective inhibition of growth in HCT-116 (mutant *KRAS*) and HKH2 (wild type *KRAS*) cells for 72 hours. While compound 1 showed non-selective killing of both cell lines, compound 4 and 7 in the series showed selective inhibition of the growth of the mut-*KRAS* cells and less activity against WT-*KRAS* cells **(Figure 43)**. The compounds that showed activity were then screened against a set of lung cancer lines with known sensitivities to si*CNKSR1*, four with WT-*KRAS* that are insensitive to *CNKSR1* knockdown and four with mut-*KRAS* that showed sensitivity to si*CNSKR1* knockdown. In these lines compound1 showed dramatic growth inhibition against all lines tested. In contrast compound 4 and compound 7 showed growth inhibition in only the four lines with mut-*KRAS* that had been found sensitive to si*CNKSR1* **(Figure 44)**. Finally, all compounds were tested for direct binding to the recombinant CNK1 PH domain and the Akt PH domain using Surface Plasmon Resonance (SPR) spectroscopy to determine if the binding was specific. Compound 1 and 4 had undetectable binding. Compound 7 however bound with a K_D of 3.2 µM to the CNK1 PH domain and 17 µM to the Akt PH domain. Finally, several analogs of compound 7 were created. Two of these 7.3 and 7.5 showed improved affinity to the CNK1 PH domain while still retaining selectivity **(Table 2)**.

Figure 44

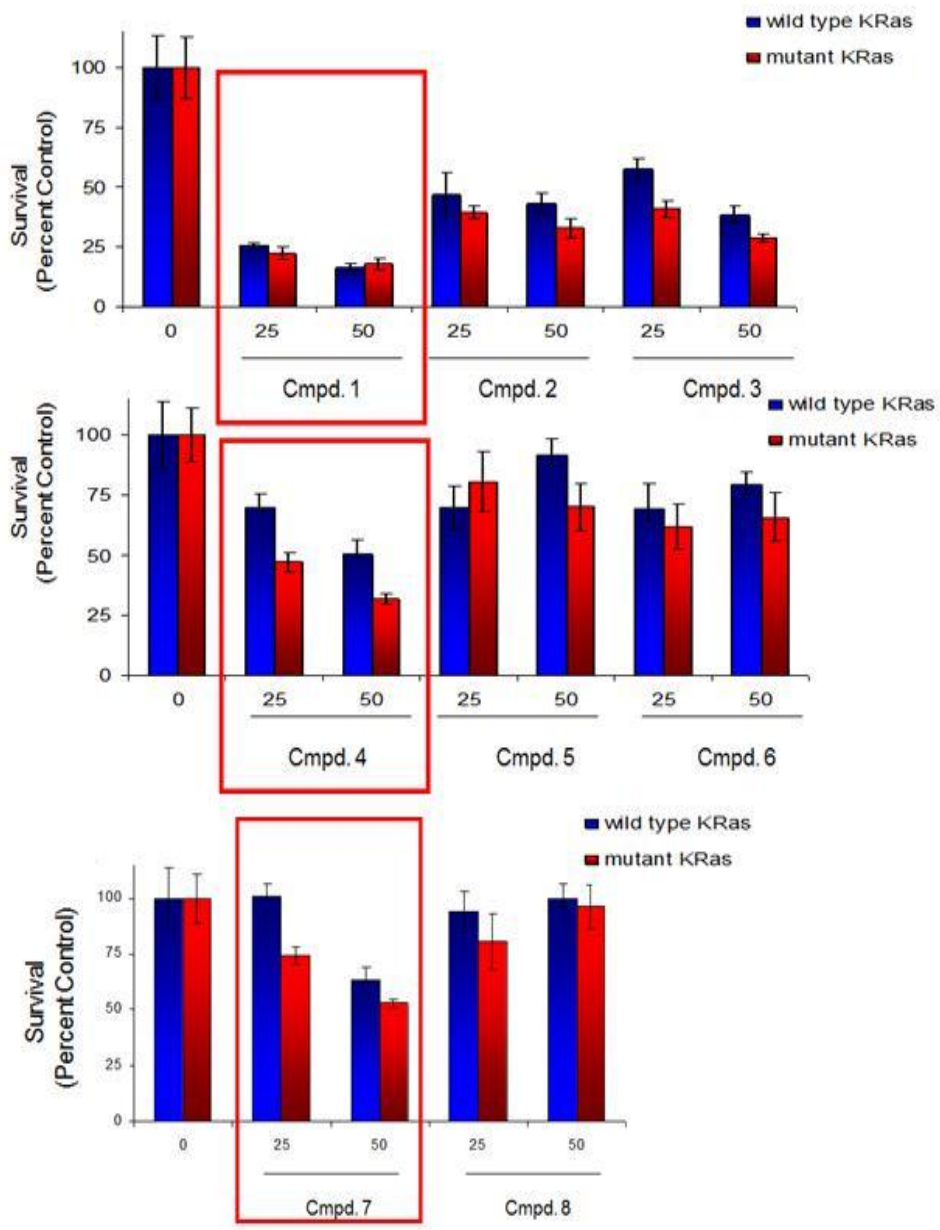

Figure 44: Screening of agents targeting the CNK1 PH domain against isogenic lines. Compounds identified in an in-silico screen were tested at 25 and 50μM concentrations in HCT-116 and the isogenic HKH2 cell line. In **Figure 29** we showed that knockdown of CNKSR1 inhibited the viability of HCT-116 cells while having minimal effects on the HKH2 clone, thus we selected agents which showed the greatest effects against HCT-116 while having minimal effects against HKH2. Compounds 4 and 7 showed the greatest selective effect. Additionally Compound 1 showed potent cell killing against both lines.

Figure 45

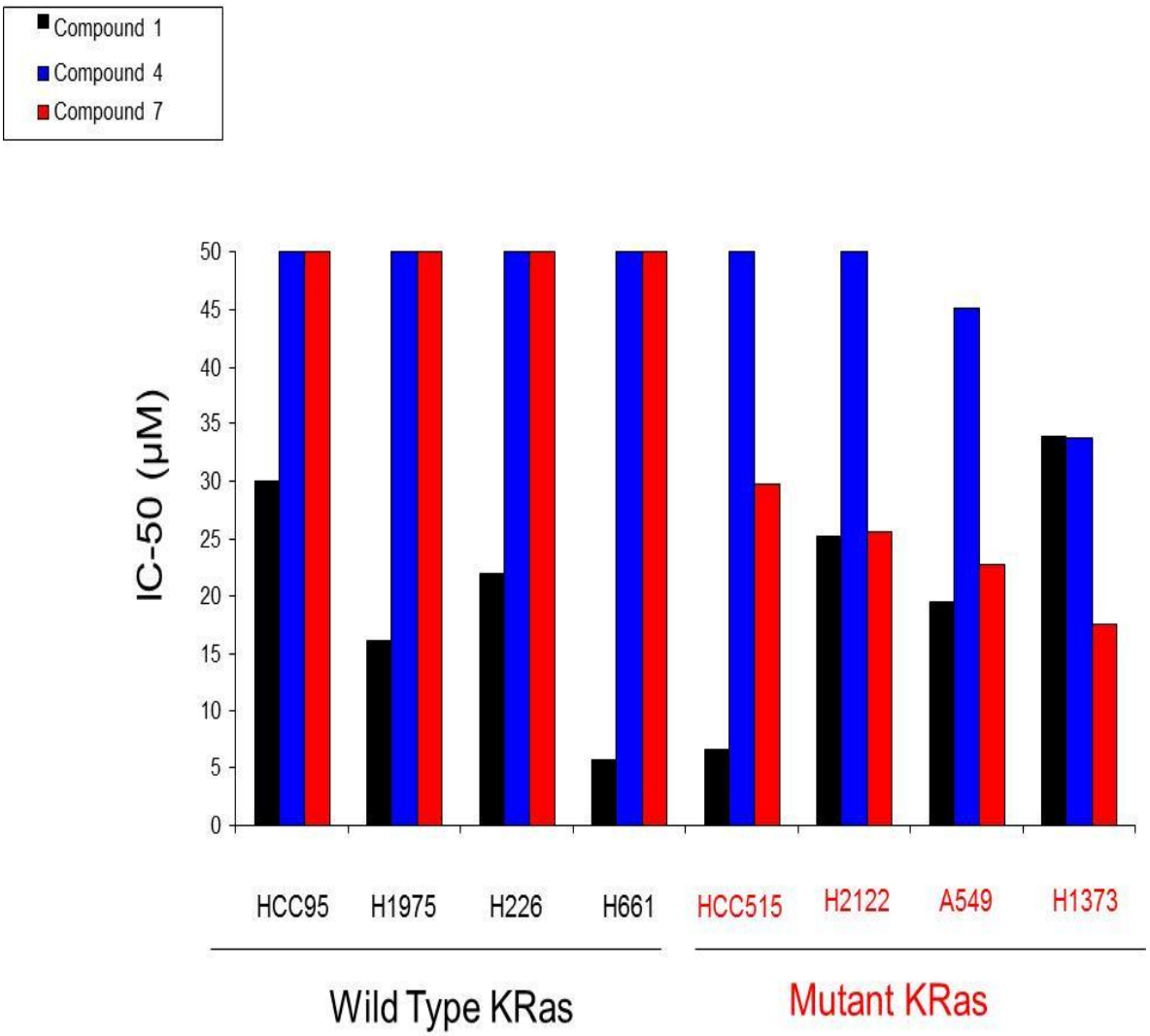

Figure 45: Screening of lead compound hits in a panel of NSCLC cell lines. As compounds 1,4, and 7 showed activity against our isogenic lines, we evaluated the activity of these agents in a panel of NSCLC cancer cells with known *KRAS* status and sensitivity to *CNKSR1* inhibition and determined the IC50 values. As we had seen in our initial screen, Compound 1 inhibited the viability of all the cell lines tested. Compound 4 decreased viability in some but not all of the mut-*KRAS* cell lines which also showed sensitivity to *CNKSR1* knockdown. Compound 7 didn't effect proliferation in any of the WT *KRAS* lines but inhibited proliferation in the mut-*KRAS* lines tested.

Table 2

Compound	Protein	
	CNK1	Akt
1	N.B.	N.B.
4	N.B.	N.B.
7	3.2	17
7A	N.B.	N.B.
7.3	0.02	66
7.4	insoluble	insoluble
7.5	0.4	2.5

Table 2. SPR to determine binding of lead compounds and analogs to the PH domain of CNK1 and Akt. SPR was used to determine binding of the lead compounds to the recombinant PH domains of Akt or CNK1. N.B. indicates no detectable binding. Compound 1 or 4 failed to give a binding value indicating no or weak binding. Compound 7 gave a K_D of 3.2 µM and 17µM to the recombinant CNK1 and Akt PH domain respectively. Additionally a series of analogs was made to compound 7 which showed increased binding to the CNK1 PH domain while still retaining selectivity towards the Akt PH domain.

5.5 Discussion

We identified *CNKSR1* as a gene that selectively inhibited the growth of cells with a mutant-*KRAS*. Here we screened a panel a NSCLC lines against a putative small molecule inhibitor of the PH domain of CNK1 and found that the growth of all the mut-*KRAS* was inhibited while a majority of the WT-*KRAS* did not show any inhibition of growth. Notably, one WT-*KRAS* line did show a response to inhibition indicating that there may be a sub-population of wild type KRas lines with a KRas-like phenotype that may be responsive to *CNKSR1* inhibition. Using RPPA analysis we found that deletion of *CNKSR1* mimicked deletion of the mut-*KRAS* allele in the down regulation of phosphorylated Rb and the components of the mitosis promoting factor, Cyclin B and Cdk1. This finding was validated across a large panel of cell lines, with every line treated showing a decrease in these proteins. Our isogenic lines and NSCLC lines with and without mut-*KRAS* were then used to show that treatment with si*CNKSR1* induced an increase in the G1 phase of the cell cycle. This is intriguing for several reasons, the first being that mice engineered to express activated NRas or KRas in the colon showed that while NRas increased resistance to apoptosis, KRas activation caused uncontrolled proliferation. Similarly, MEFs engineered to be devoid of any Ras activity mimicked the phenotype seen in our *CNKSR1* knockout, expressing Cdk4 and Cyclin D, but finding no activity at the Rb ser^{807} which is known to phosphorylate and not expressing Cdk1 or Cyclin B[128]. Finally, using the same set of isogenic lines in which we did many of our studies, a shRNA screen found that the Mut-*KRAS* cells were sensitive to inhibition of mitosis when compared to cells with just the wild type allele [96]. To our surprise, despite these dramatic changes in cell cycle, no consistent change was seen by RPPA in the canonical Mapk or Akt effecter pathways (data not shown). Studies have found that C-Raf promotes mitosis in a Mek and ATP-dependent fashion[131] and similarly binds to Rb[132] and that C-Raf is necessary for KRas driven tumor development independently of Mek signaling [66,133]. Given the well characterized role of CNK1 and Raf in *Drosophlia* signaling [121], it is tempting to speculate that increased Mek independent C-Raf signaling may be the mechanism responsible for CNK1

driving KRas mediated growth. Supporting this idea, our studies showed that while WT-Ras and CNK1 had little or no co-localization, mut-KRas and CNK1 had a highly focal localization in clusters and FLIM microscopy revealed that these two proteins were with 10 nm of each other at the cellular membrane indicating the presence of an analogous association of proteins as is seen in *Drosophila*. *Drosophila* has one Raf isoform while mammals have three, and the association of CNKSR1 may be specific for C-Raf and act in a Mek independent fashion. An additional hypothesis is that a less characterized KRas effecter may drive the effects of CNK1 deletion. The observation that C-Raf knockdown failed to have a selective effect in the isogenic lines strengthens this idea. A proposed model of how CNK1 drives KRas driven cell cycle progression is shown in **Figure 46**. The knockout of *CNKSR1* had similar effects to deletion of the mut-*KRAS* allele or si*KRAS* in a 3-D spheroid formation assay and an anoikis assay, indicating that knockout of *CNKSR1* had similar consequences on phenotype both in 2-D and 3-D assays, thus, validating what we saw in our siRNA screen and validating its importance in KRas driven tumors Finally, we showed that either a dominant negative PH domain or small molecules development has begun on to inhibit the PH domain had similar consequences to knockout of *CNKSR1* with siRNA.

Figure 46

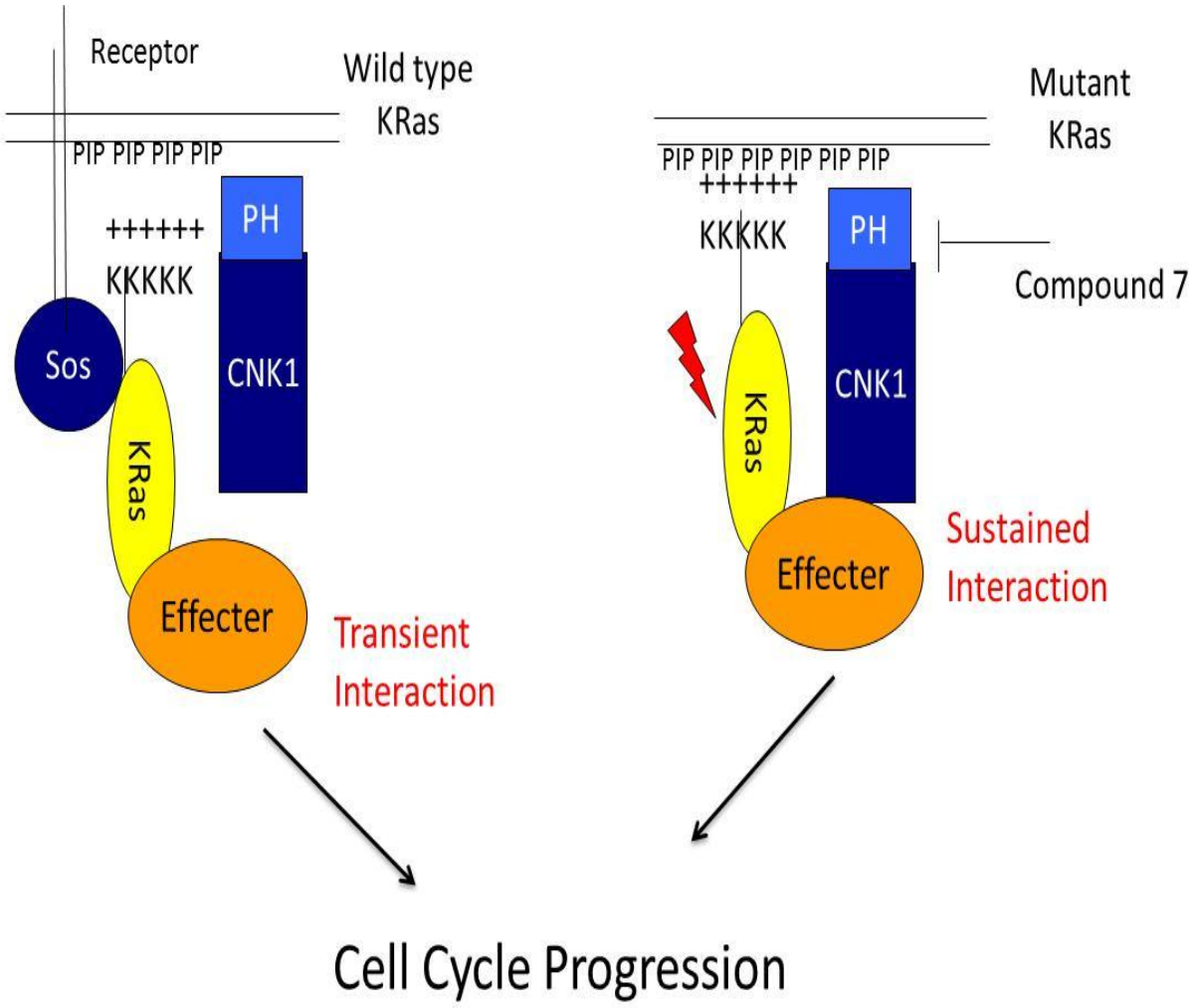

Figure 46: CNK1 and KRas cooperate to drive progression through the cell cycle. CNK1 and KRas interact in the nanocluster, brought together by membrane lipids, to facilitate KRas signaling through effecters and resulting in cell cycle progression. This interaction is promoted in cells with mutant KRas resulting in a sustained interaction between the two proteins. We have identified a lead compound with binds to the PH domain of compound 7 inhibits its interaction with membrane lipids and thus disrupts the nanocluster.

Chapter 6 Summary and future directions

6.1 Future directions regarding differing KRas effecter utilization

In chapter 3 it was discovered that the the identity of the amino acid activating KRas at codon 12 influences which effecter pathways the KRas enzyme will utilize to promote tumorigensis. Two major implications immediately arise from this discovery. The first relates to scientific studies which have previously and continue to define the properties of KRas. Historically, studies performed with different amino acid substitutions utilized to activate KRas have been cross-referenced. My new results indicate that these experiments may be fundamentally different as the KRas enzyme will behave differently depending on how it is activated, thus a study performed with a mut-KRas G12D model must be compared to another KRas G12D model and cannot be directly compared with a study which has used a G12V substitution to activate KRas. Additionally, as we have shown that KRas G12D behaves differently than a KRas G12C, the widespread use of a mouse model harboring a conditionally activated KRas G12D to study lung cancer[79], as opposed to a G12C activating substation predominantly found in this disease, may warrant reevaluation. Thus the mouse model with a KRas G12C activating mutation which has been described in the literature[92] should become the defaut to characterize NSCLC.

The second is the analysis of both traditional and targeted therapies in tumors in relationship to *KRAS* status. Rather than evaluate *KRAS* mutation as a homogenous group, it is more precise to look at individual *KRAS* activating mutations particularilty in, but not limited to, inhibitors of KRas effecter signaling. These studies will likely be limited by low patient numbers as we encountered in the BATTLE trial and ultimately may require large scale studies as was performed in the RASCAL[87] and RASCAL II[88] trials or retrospective combined analysis of several trials. Finally, recent years have seen numerous attempts to find genes patterns ('signatures') which define cancers driven by mut-*KRAS* or display "*KRAS*-like" properties[124].

Attempts to build these signatures may be hindered by the grouping of the KRas enzyme activated by different amino acids. In light of this, tailoring signatures to individual KRas mutations and comparing these to wild type KRas models may be more informative and allow use of these signatures for classification, treatment decisions, and the identification of future therapeutic targets

6.2 Future directions in targeting KRas effecters

Chapter 3 suggested that the amino acid substation by which KRAS is activated in cells would play a role in the response of these cells to the inhibition of different KRas effecter proteins, an idea validated in chapter 4. However while different levels of response were seen to inhibitors of the Mapk or PI3K pathways, none of these agents showed reponses greater than 80% growth inhibition even at concentrations well above those required to inhbit the target enzymes. Chapter 3 indicated responses are likely mitigated by feedback pathways derepressed with effecter inhibition and growth factor signaling reactivation and this is a topic which warrents further exploration.This has been addressed in experimental models by the similtaneous inhibition of both the Raf and PI3K KRas effecters, thus eliminating potential redundancy or feedback between these pathways in KRas signaling. This stragedy is now in clinical trials for mutant KRas tumors in many different cancer types. Despite some promising responses, early data is indicating that the combination may also have unacceptable toxicity[134]. However, as multiple agents are in clinical trials targeting different nodes in these pathways and adminsitered in different scheduling regimines, an acceptable combination may be found.

Should agents be found which show promise either alone or in combination in KRas mutant tumors, chapter 4 highlighted the importance of looking at multiple known oncogenic lesions when determining treatment efficacy in contrast to looking at *KRAS* mutation as a single marker. This was explored with concurrent *KRAS* activating and LKB1 inactivating

mutations, occurring frequently in lung cancers in chapter 4 and similar observations have been made with *KRAS* activating and *PIK3CA* activating mutations which occur frequently in colorectal cancer[135]. While a majority of studies have focused on the presence of two mutations as a marker of resistance to an inhibitior of one on these individual targets, it is notable that at least one study has found the co-occurance of *KRAS* and LKB1 inactivating lesions in lung cancer to be a predictor of single agent activity of a Mapk inhibitor[136]. Our data in chapter 4 supported this, with G12C and LKB1 mutant tumors showing increased sensitivity to AZ6244. Thus by not looking at the co-occurance of two oncogenic lesions as independent events but understanding how these lesions interact in cellular signaling pathways it may be possible to predict a single agent which may be utilized for therapeutic benefit, negating increased toxicity from the combination of multiple agents.

6.3 Future directions for CNK1

In chapter 5, the deletion of *CNKSR1* was shown to selectively inhibit the growth of isogenic cells with an activated KRas allele and inhbit the growth of cells in a panel which harbored any form of activated KRas. This is likely due to a physical association between CNK1 and KRas in the “nanocluster” of proteins which occurs at the cell membrane and faciliatates KRas effecter signal transduction. Additionally, CNK1 harbors a PH domain which localizes this protein with KRas at the membrane and serves as a drugabble point to inhibit this interaction. We found KRas utilizes CNK1 to drive cells cycle progression but the precise pathway by which this occurs in human cells needs to be eluciadated. Previous studies in both human and *drosophlia* cells suggest that a Mapk independant CRaf/RhoA pathway is a likely candidate. This would contrast the the drospholia CNK which utilizes Mapk and why these differences occur is a point of interest likely relating to the precence of a single Raf isoform in Drosophlia and the evolution of three distinct Raf isoforms in humans.

As a therapeutic target, it is notable that CNK1 deletion in our *in vitro* settings results in cell cycle arrest but shows no indication of induction of apoptosis. The deletion has never been performed in an *in-vivo* setting where factors such as tumor stress occur and may yield different results and these experiements must be performed. If cell cycle arrest is the only consequence of *CNKSR1* deletion, addition agents may need to been combined with CNK1 inhibiitors to achieve not only an arrest of tumor growth but to achieve the induction of apoptosis currently thought necessary for tumor regression. If these combinations prove effective, the increased toxicity that may result from these combinations must be considered as with Mek and Akt inhibitors but the unique association between CNK1 and mutant KRas encourages the idea a favorable profile will exist. Finally, while the class of agents we have developed to inhibit CNK1 localization are promising in our *in-vitro* experiements, continued study will be necessary to determine if inhibition of localization is equivalent to deletion of protein expression. Finally, if these agents continue to show promise in an *in-vitro* setting, experiments in animals will be necessary for further development. This will require these agents show acceptable pharmacokinetic and pharmacodynamics properities or modifications may be necessary. If these hurdles are overcome, the inhibition of CNK1localization will emerge as an exciting new therapeutic option for patients with tumors harboring the *KRAS* oncogene.

References

1 K. Wennerberg, K. L. Rossman, and C. J. Der, "The Ras superfamily at a glance," J Cell Sci **118** (Pt 5), 843-846 (2005).

2 J. J. HARVEY, "AN UNIDENTIFIED VIRUS WHICH CAUSES THE RAPID PRODUCTION OF TUMOURS IN MICE," Nature **204**, 1104-1105 (1964).

3 E. H. Chang, M. A. Gonda, R. W. Ellis, E. M. Scolnick, and D. R. Lowy, "Human genome contains four genes homologous to transforming genes of Harvey and Kirsten murine sarcoma viruses," Proc Natl Acad Sci U S A **79** (16), 4848-4852 (1982).

4 E. H. Hurowitz, J. M. Melnyk, Y. J. Chen, H. Kouros-Mehr, M. I. Simon, and H. Shizuya, "Genomic characterization of the human heterotrimeric G protein alpha, beta, and gamma subunit genes," DNA Res **7** (2), 111-120 (2000).

5 J. Colicelli, "Human RAS superfamily proteins and related GTPases," Sci STKE **2004** (250), RE13 (2004).

6 M. V. Milburn, L. Tong, A. M. deVos, A. Brünger, Z. Yamaizumi, S. Nishimura, and S. H. Kim, "Molecular switch for signal transduction: structural differences between active and inactive forms of protooncogenic ras proteins," Science **247** (4945), 939-945 (1990).

7 M. E. Fortini, M. A. Simon, and G. M. Rubin, "Signalling by the sevenless protein tyrosine kinase is mimicked by Ras1 activation," Nature **355** (6360), 559-561 (1992); T. Satoh, M. Endo, M. Nakafuku, S. Nakamura, and Y. Kaziro, "Platelet-derived growth factor stimulates formation of active p21ras.GTP complex in Swiss mouse 3T3 cells," Proc Natl Acad Sci U S A **87** (15), 5993-5997 (1990).

8 I. R. Vetter and A. Wittinghofer, "The guanine nucleotide-binding switch in three dimensions," Science **294** (5545), 1299-1304 (2001).

9 M. A. Simon, G. S. Dodson, and G. M. Rubin, "An SH3-SH2-SH3 protein is required for p21Ras1 activation and binds to sevenless and Sos proteins in vitro," Cell **73** (1), 169-177 (1993).

10 R. D. Rogge, C. A. Karlovich, and U. Banerjee, "Genetic dissection of a neurodevelopmental pathway: Son of sevenless functions downstream of the sevenless and EGF receptor tyrosine kinases," Cell **64** (1), 39-48 (1991).

11 E. J. Lowenstein, R. J. Daly, A. G. Batzer, W. Li, B. Margolis, R. Lammers, A. Ullrich, E. Y. Skolnik, D. Bar-Sagi, and J. Schlessinger, "The SH2 and SH3 domain-containing protein GRB2 links receptor tyrosine kinases to ras signaling," Cell **70** (3), 431-442 (1992).

12 H. Kouhara, Y. R. Hadari, T. Spivak-Kroizman, J. Schilling, D. Bar-Sagi, I. Lax, and J. Schlessinger, "A lipid-anchored Grb2-binding protein that links FGF-receptor activation to the Ras/MAPK signaling pathway," Cell **89** (5), 693-702 (1997).

13 E. Y. Skolnik, C. H. Lee, A. Batzer, L. M. Vicentini, M. Zhou, R. Daly, M. J. Myers, J. M. Backer, A. Ullrich, and M. F. White, "The SH2/SH3 domain-containing protein GRB2 interacts with tyrosine-phosphorylated IRS1 and Shc: implications for insulin control of ras signalling," EMBO J **12** (5), 1929-1936 (1993).

14 L. C. Robinson, J. B. Gibbs, M. S. Marshall, I. S. Sigal, and K. Tatchell, "CDC25: a component of the RAS-adenylate cyclase pathway in Saccharomyces cerevisiae," Science **235** (4793), 1218-1221 (1987).

15 W. Wei, R. D. Mosteller, P. Sanyal, E. Gonzales, D. McKinney, C. Dasgupta, P. Li, B. X. Liu, and D. Broek, "Identification of a mammalian gene structurally and functionally related to the CDC25 gene of Saccharomyces cerevisiae," Proc Natl Acad Sci U S A **89** (15), 7100-7104 (1992).

16 L. Chen, L. J. Zhang, P. Greer, P. S. Tung, and M. F. Moran, "A murine CDC25/ras-GRF-related protein implicated in Ras regulation," Dev Genet **14** (5), 339-346 (1993).

17 M. Trahey and F. McCormick, "A cytoplasmic protein stimulates normal N-ras p21 GTPase, but does not affect oncogenic mutants," Science **238** (4826), 542-545 (1987).

18 M. Trahey, G. Wong, R. Halenbeck, B. Rubinfeld, G. A. Martin, M. Ladner, C. M. Long, W. J. Crosier, K. Watt, and K. Koths, "Molecular cloning of two types of GAP complementary DNA from human placenta," Science **242** (4886), 1697-1700 (1988).

19 G. A. Martin, D. Viskochil, G. Bollag, P. C. McCabe, W. J. Crosier, H. Haubruck, L. Conroy, R. Clark, P. O'Connell, and R. M. Cawthon, "The GAP-related domain of the neurofibromatosis type 1 gene product interacts with ras p21," Cell **63** (4), 843-849 (1990).

20 H. Resat, T. P. Straatsma, D. A. Dixon, and J. H. Miller, "The arginine finger of RasGAP helps Gln-61 align the nucleophilic water in GAP-stimulated hydrolysis of GTP," Proc Natl Acad Sci U S A **98** (11), 6033-6038 (2001).

21 I. A. Prior and J. F. Hancock, "Ras trafficking, localization and compartmentalized signalling," Semin Cell Dev Biol **23** (2), 145-153 (2012).

22 I. A. Prior, A. Harding, J. Yan, J. Sluimer, R. G. Parton, and J. F. Hancock, "GTP-dependent segregation of H-ras from lipid rafts is required for biological activity," Nat Cell Biol **3** (4), 368-375 (2001).

23 A. Apolloni, I. A. Prior, M. Lindsay, R. G. Parton, and J. F. Hancock, "H-ras but not K-ras traffics to the plasma membrane through the exocytic pathway," Mol Cell Biol **20** (7), 2475-2487 (2000).

24 H. Umanoff, W. Edelmann, A. Pellicer, and R. Kucherlapati, "The murine N-ras gene is not essential for growth and development," Proc Natl Acad Sci U S A **92** (5), 1709-1713 (1995).

25 L. Johnson, D. Greenbaum, K. Cichowski, K. Mercer, E. Murphy, E. Schmitt, R. T. Bronson, H. Umanoff, W. Edelmann, R. Kucherlapati, and T. Jacks, "K-ras is an essential gene in the mouse with partial functional overlap with N-ras," Genes Dev **11** (19), 2468-2481 (1997).

26 S. J. Plowman, D. J. Williamson, M. J. O'Sullivan, J. Doig, A. M. Ritchie, D. J. Harrison, D. W. Melton, M. J. Arends, M. L. Hooper, and C. E. Patek, "While K-ras is essential for mouse development, expression of the K-ras 4A splice variant is dispensable," Mol Cell Biol **23** (24), 9245-9250 (2003).

27 L. M. Esteban, C. Vicario-Abejón, P. Fernández-Salguero, A. Fernández-Medarde, N. Swaminathan, K. Yienger, E. Lopez, M. Malumbres, R. McKay, J. M. Ward, A. Pellicer, and E. Santos, "Targeted genomic disruption of H-ras and N-ras, individually or in combination, reveals the dispensability of both loci for mouse growth and development," Mol Cell Biol **21** (5), 1444-1452 (2001).

28 N. Potenza, C. Vecchione, A. Notte, A. De Rienzo, A. Rosica, L. Bauer, A. Affuso, M. De Felice, T. Russo, R. Poulet, G. Cifelli, G. De Vita, G. Lembo, and R. Di Lauro, "Replacement of K-Ras with H-Ras supports normal embryonic development despite inducing cardiovascular pathology in adult mice," EMBO Rep **6** (5), 432-437 (2005).

29 N. Yamauchi, A. A. Kiessling, and G. M. Cooper, "The Ras/Raf signaling pathway is required for progression of mouse embryos through the two-cell stage," Mol Cell Biol **14** (10), 6655-6662 (1994).

30 K. A. Rauen, L. Schoyer, F. McCormick, A. E. Lin, J. E. Allanson, D. A. Stevenson, K. W. Gripp, G. Neri, J. C. Carey, E. Legius, M. Tartaglia, S. Schubbert, A. E. Roberts, B. D. Gelb, K. Shannon, D. H. Gutmann, M. McMahon, C. Guerra, J. A. Fagin, B. Yu, Y. Aoki, B. G. Neel, A. Balmain, R. R. Drake, G. P. Nolan, M. Zenker, G. Bollag, J. Sebolt-Leopold, J. B. Gibbs, A. J. Silva, E. E. Patton, D. H. Viskochil, M. W. Kieran, B. R. Korf, R. J. Hagerman, R. J. Packer, and T. Melese, "Proceedings from the 2009 genetic syndromes of the Ras/MAPK pathway: From bedside to bench and back," Am J Med Genet A **152A** (1), 4-24 (2010).

31 S. Schubbert, M. Zenker, S. L. Rowe, S. Böll, C. Klein, G. Bollag, I. van der Burgt, L. Musante, V. Kalscheuer, L. E. Wehner, H. Nguyen, B. West, K. Y. Zhang, E. Sistermans, A. Rauch, C. M. Niemeyer, K. Shannon, and C. P. Kratz, "Germline KRAS

mutations cause Noonan syndrome," Nat Genet **38** (3), 331-336 (2006); A. E. Roberts, T. Araki, K. D. Swanson, K. T. Montgomery, T. A. Schiripo, V. A. Joshi, L. Li, Y. Yassin, A. M. Tamburino, B. G. Neel, and R. S. Kucherlapati, "Germline gain-of-function mutations in SOS1 cause Noonan syndrome," Nat Genet **39** (1), 70-74 (2007); M. Tartaglia, E. L. Mehler, R. Goldberg, G. Zampino, H. G. Brunner, H. Kremer, I. van der Burgt, A. H. Crosby, A. Ion, S. Jeffery, K. Kalidas, M. A. Patton, R. S. Kucherlapati, and B. D. Gelb, "Mutations in PTPN11, encoding the protein tyrosine phosphatase SHP-2, cause Noonan syndrome," Nat Genet **29** (4), 465-468 (2001).

32 M. Tartaglia, B. D. Gelb, and M. Zenker, "Noonan syndrome and clinically related disorders," Best Pract Res Clin Endocrinol Metab **25** (1), 161-179 (2011).

33 M. Cully and J. Downward, "SnapShot: Ras Signaling," Cell **133** (7), 1292-1292.e1291 (2008).

34 B. Dickson, F. Sprenger, D. Morrison, and E. Hafen, "Raf functions downstream of Ras1 in the Sevenless signal transduction pathway," Nature **360** (6404), 600-603 (1992).

35 M. Han, A. Golden, Y. Han, and P. W. Sternberg, "C. elegans lin-45 raf gene participates in let-60 ras-stimulated vulval differentiation," Nature **363** (6425), 133-140 (1993).

36 J. M. Kyriakis, H. App, X. F. Zhang, P. Banerjee, D. L. Brautigan, U. R. Rapp, and J. Avruch, "Raf-1 activates MAP kinase-kinase," Nature **358** (6385), 417-421 (1992).

37 C. Peyssonnaux and A. Eychène, "The Raf/MEK/ERK pathway: new concepts of activation," Biol Cell **93** (1-2), 53-62 (2001).

38 F. Kern, E. Doma, C. Rupp, T. Niault, and M. Baccarini, "Essential, non-redundant roles of B-Raf and Raf-1 in Ras-driven skin tumorigenesis," Oncogene (2012).

39 E. Nekhoroshkova, S. Albert, M. Becker, and U. R. Rapp, "A-RAF kinase functions in ARF6 regulated endocytic membrane traffic," PLoS One **4** (2), e4647 (2009).

40 P. Rodriguez-Viciana, P. H. Warne, R. Dhand, B. Vanhaesebroeck, I. Gout, M. J. Fry, M. D. Waterfield, and J. Downward, "Phosphatidylinositol-3-OH kinase as a direct target of Ras," Nature **370** (6490), 527-532 (1994).

41 N. T. Ihle and G. Powis, "The biological effects of isoform-specific PI3-kinase inhibition," Curr Opin Drug Discov Devel **13** (1), 41-49 (2010).

42 S. Gupta, A. R. Ramjaun, P. Haiko, Y. Wang, P. H. Warne, B. Nicke, E. Nye, G. Stamp, K. Alitalo, and J. Downward, "Binding of ras to phosphoinositide 3-kinase p110alpha is required for ras-driven tumorigenesis in mice," Cell **129** (5), 957-968 (2007).

43 A. Kikuchi, S. D. Demo, Z. H. Ye, Y. W. Chen, and L. T. Williams, "ralGDS family members interact with the effector loop of ras p21," Mol Cell Biol **14** (11), 7483-7491 (1994).

44 J. M. Lambert, Q. T. Lambert, G. W. Reuther, A. Malliri, D. P. Siderovski, J. Sondek, J. G. Collard, and C. J. Der, "Tiam1 mediates Ras activation of Rac by a PI(3)K-independent mechanism," Nat Cell Biol **4** (8), 621-625 (2002).

45 M. R. Wing, D. M. Bourdon, and T. K. Harden, "PLC-epsilon: a shared effector protein in Ras-, Rho-, and G alpha beta gamma-mediated signaling," Mol Interv **3** (5), 273-280 (2003).

46 T. E. O'Toole, K. Bialkowska, X. Li, and J. E. Fox, "Tiam1 is recruited to β1-integrin complexes by 14-3-3ζ where it mediates integrin-induced Rac1 activation and motility," J Cell Physiol **226** (11), 2965-2978 (2011).

47 A. Gérard, R. A. van der Kammen, H. Janssen, S. I. Ellenbroek, and J. G. Collard, "The Rac activator Tiam1 controls efficient T-cell trafficking and route of transendothelial migration," Blood **113** (24), 6138-6147 (2009).

48 D. Vavvas, X. Li, J. Avruch, and X. F. Zhang, "Identification of Nore1 as a potential Ras effector," J Biol Chem **273** (10), 5439-5442 (1998).

49 J. Avruch, R. Xavier, N. Bardeesy, X. F. Zhang, M. Praskova, D. Zhou, and F. Xia, "Rassf family of tumor suppressor polypeptides," J Biol Chem **284** (17), 11001-11005 (2009).

50 W. H. Kirsten, V. Schauf, and J. McCoy, "Properties of a murine sarcoma virus," Bibl Haematol (36), 246-249 (1970).

51 A. Jemal, R. Siegel, J. Xu, and E. Ward, "Cancer statistics, 2010," CA Cancer J Clin **60** (5), 277-300 (2010).

52 J. L. Bos, E. R. Fearon, S. R. Hamilton, M. Verlaan-de Vries, J. H. van Boom, A. J. van der Eb, and B. Vogelstein, "Prevalence of ras gene mutations in human colorectal cancers," Nature **327** (6120), 293-297 (1987).

53 S. Rodenhuis, M. L. van de Wetering, W. J. Mooi, S. G. Evers, N. van Zandwijk, and J. L. Bos, "Mutational activation of the K-ras oncogene. A possible pathogenetic factor in adenocarcinoma of the lung," N Engl J Med **317** (15), 929-935 (1987).

54 C. Almoguera, D. Shibata, K. Forrester, J. Martin, N. Arnheim, and M. Perucho, "Most human carcinomas of the exocrine pancreas contain mutant c-K-ras genes," Cell **53** (4), 549-554 (1988).

55 F. Luo, H. Ye, R. Hamoudi, G. Dong, W. Zhang, C. E. Patek, G. Poulogiannis, and M. J. Arends, "K-ras exon 4A has a tumour suppressor effect on carcinogen-induced murine colonic adenoma formation," J Pathol **220** (5), 542-550 (2010).

56 I. A. Prior, P. D. Lewis, and C. Mattos, "A comprehensive survey of Ras mutations in cancer," Cancer Res **72** (10), 2457-2467 (2012).

57 P. H. Seeburg, W. W. Colby, D. J. Capon, D. V. Goeddel, and A. D. Levinson, "Biological properties of human c-Ha-ras1 genes mutated at codon 12," Nature **312** (5989), 71-75 (1984).

58 A. Wittinghofer, S. M. Franken, A. J. Scheidig, H. Rensland, A. Lautwein, E. F. Pai, and R. S. Goody, "Three-dimensional structure and properties of wild-type and mutant H-ras-encoded p21," Ciba Found Symp **176**, 6-21; discussion 21-27 (1993).

59 M. Serrano, A. W. Lin, M. E. McCurrach, D. Beach, and S. W. Lowe, "Oncogenic ras provokes premature cell senescence associated with accumulation of p53 and p16INK4a," Cell **88** (5), 593-602 (1997).

60 D. A. Tuveson, A. T. Shaw, N. A. Willis, D. P. Silver, E. L. Jackson, S. Chang, K. L. Mercer, R. Grochow, H. Hock, D. Crowley, S. R. Hingorani, T. Zaks, C. King, M. A. Jacobetz, L. Wang, R. T. Bronson, S. H. Orkin, R. A. DePinho, and T. Jacks, "Endogenous oncogenic K-ras(G12D) stimulates proliferation and widespread neoplastic and developmental defects," Cancer Cell **5** (4), 375-387 (2004).

61 J. Lee, K. T. Jang, C. S. Ki, T. Lim, Y. S. Park, H. Y. Lim, D. W. Choi, W. K. Kang, K. Park, and J. O. Park, "Impact of epidermal growth factor receptor (EGFR) kinase mutations, EGFR gene amplifications, and KRAS mutations on survival of pancreatic adenocarcinoma," Cancer **109** (8), 1561-1569 (2007).

62 M. Zeng, H. Kikuchi, M. S. Pino, and D. C. Chung, "Hypoxia activates the K-ras proto-oncogene to stimulate angiogenesis and inhibit apoptosis in colon cancer cells," PLoS One **5** (6), e10966 (2010).

63 P. M. Campbell and C. J. Der, "Oncogenic Ras and its role in tumor cell invasion and metastasis," Semin Cancer Biol **14** (2), 105-114 (2004).

64 M. Malumbres and M. Barbacid, "RAS oncogenes: the first 30 years," Nat Rev Cancer **3** (6), 459-465 (2003).

65 A. J. Aguirre, N. Bardeesy, M. Sinha, L. Lopez, D. A. Tuveson, J. Horner, M. S. Redston, and R. A. DePinho, "Activated Kras and Ink4a/Arf deficiency cooperate to produce metastatic pancreatic ductal adenocarcinoma," Genes Dev **17** (24), 3112-3126 (2003).

66 K. M. Haigis, K. R. Kendall, Y. Wang, A. Cheung, M. C. Haigis, J. N. Glickman, M. Niwa-Kawakita, A. Sweet-Cordero, J. Sebolt-Leopold, K. M. Shannon, J. Settleman, M. Giovannini, and T. Jacks, "Differential effects of oncogenic K-Ras and N-Ras on

proliferation, differentiation and tumor progression in the colon," Nat Genet **40** (5), 600-608 (2008).

67 R. Meuwissen, S. C. Linn, M. van der Valk, W. J. Mooi, and A. Berns, "Mouse model for lung tumorigenesis through Cre/lox controlled sporadic activation of the K-Ras oncogene," Oncogene **20** (45), 6551-6558 (2001).

68 H. Ji, M. R. Ramsey, D. N. Hayes, C. Fan, K. McNamara, P. Kozlowski, C. Torrice, M. C. Wu, T. Shimamura, S. A. Perera, M. C. Liang, D. Cai, G. N. Naumov, L. Bao, C. M. Contreras, D. Li, L. Chen, J. Krishnamurthy, J. Koivunen, L. R. Chirieac, R. F. Padera, R. T. Bronson, N. I. Lindeman, D. C. Christiani, X. Lin, G. I. Shapiro, P. A. Jänne, B. E. Johnson, M. Meyerson, D. J. Kwiatkowski, D. H. Castrillon, N. Bardeesy, N. E. Sharpless, and K. K. Wong, "LKB1 modulates lung cancer differentiation and metastasis," Nature **448** (7155), 807-810 (2007).

69 Z. Chen, K. Cheng, Z. Walton, Y. Wang, H. Ebi, T. Shimamura, Y. Liu, T. Tupper, J. Ouyang, J. Li, P. Gao, M. S. Woo, C. Xu, M. Yanagita, A. Altabef, S. Wang, C. Lee, Y. Nakada, C. G. Peña, Y. Sun, Y. Franchetti, C. Yao, A. Saur, M. D. Cameron, M. Nishino, D. N. Hayes, M. D. Wilkerson, P. J. Roberts, C. B. Lee, N. Bardeesy, M. Butaney, L. R. Chirieac, D. B. Costa, D. Jackman, N. E. Sharpless, D. H. Castrillon, G. D. Demetri, P. A. Jänne, P. P. Pandolfi, L. C. Cantley, A. L. Kung, J. A. Engelman, and K. K. Wong, "A murine lung cancer co-clinical trial identifies genetic modifiers of therapeutic response," Nature **483** (7391), 613-617 (2012).

70 A. D. Cox and C. J. Der, "Ras history: The saga continues," Small GTPases **1** (1), 2-27 (2010).

71 A. D. Cox and C. J. Der, "Farnesyltransferase inhibitors: promises and realities," Curr Opin Pharmacol **2** (4), 388-393 (2002).

72 M. Sinensky, L. A. Beck, S. Leonard, and R. Evans, "Differential inhibitory effects of lovastatin on protein isoprenylation and sterol synthesis," J Biol Chem **265** (32), 19937-19941 (1990).

73 N. E. Kohl, S. D. Mosser, S. J. deSolms, E. A. Giuliani, D. L. Pompliano, S. L. Graham, R. L. Smith, E. M. Scolnick, A. Oliff, and J. B. Gibbs, "Selective inhibition of ras-dependent transformation by a farnesyltransferase inhibitor," Science **260** (5116), 1934-1937 (1993).

74 G. L. James, J. L. Goldstein, M. S. Brown, T. E. Rawson, T. C. Somers, R. S. McDowell, C. W. Crowley, B. K. Lucas, A. D. Levinson, and J. C. Marsters, "Benzodiazepine peptidomimetics: potent inhibitors of Ras farnesylation in animal cells," Science **260** (5116), 1937-1942 (1993).

75 D. B. Whyte, P. Kirschmeier, T. N. Hockenberry, I. Nunez-Oliva, L. James, J. J. Catino, W. R. Bishop, and J. K. Pai, "K- and N-Ras are geranylgeranylated in cells treated with farnesyl protein transferase inhibitors," J Biol Chem **272** (22), 14459-14464 (1997).

76 C. Mascaux, N. Iannino, B. Martin, M. Paesmans, T. Berghmans, M. Dusart, A. Haller, P. Lothaire, A. P. Meert, S. Noel, J. J. Lafitte, and J. P. Sculier, "The role of RAS oncogene in survival of patients with lung cancer: a systematic review of the literature with meta-analysis," Br J Cancer **92** (1), 131-139 (2005).

77 H. Linardou, I. J. Dahabreh, D. Kanaloupiti, F. Siannis, D. Bafaloukos, P. Kosmidis, C. A. Papadimitriou, and S. Murray, "Assessment of somatic k-RAS mutations as a mechanism associated with resistance to EGFR-targeted agents: a systematic review and meta-analysis of studies in advanced non-small-cell lung cancer and metastatic colorectal cancer," Lancet Oncol **9** (10), 962-972 (2008).

78 P. B. Chapman, A. Hauschild, C. Robert, J. B. Haanen, P. Ascierto, J. Larkin, R. Dummer, C. Garbe, A. Testori, M. Maio, D. Hogg, P. Lorigan, C. Lebbe, T. Jouary, D. Schadendorf, A. Ribas, S. J. O'Day, J. A. Sosman, J. M. Kirkwood, A. M. Eggermont, B. Dreno, K. Nolop, J. Li, B. Nelson, J. Hou, R. J. Lee, K. T. Flaherty, G. A. McArthur, and BRIM-3 Study Group, "Improved survival with vemurafenib in melanoma with BRAF V600E mutation," N Engl J Med **364** (26), 2507-2516 (2011).

79 J. A. Engelman, L. Chen, X. Tan, K. Crosby, A. R. Guimaraes, R. Upadhyay, M. Maira, K. McNamara, S. A. Perera, Y. Song, L. R. Chirieac, R. Kaur, A. Lightbown, J. Simendinger, T. Li, R. F. Padera, C. García-Echeverría, R. Weissleder, U. Mahmood, L. C. Cantley, and K. K. Wong, "Effective use of PI3K and MEK inhibitors to treat mutant Kras G12D and PIK3CA H1047R murine lung cancers," Nat Med **14** (12), 1351-1356 (2008).

80 N. T. Ihle, R. Lemos, P. Wipf, A. Yacoub, C. Mitchell, D. Siwak, G. B. Mills, P. Dent, D. L. Kirkpatrick, and G. Powis, "Mutations in the phosphatidylinositol-3-kinase pathway predict for antitumor activity of the inhibitor PX-866 whereas oncogenic Ras is a dominant predictor for resistance.," Cancer Res **69** (1), 143-150 (2009).

81 M. Sato, M. B. Vaughan, L. Girard, M. Peyton, W. Lee, D. S. Shames, R. D. Ramirez, N. Sunaga, A. F. Gazdar, J. W. Shay, and J. D. Minna, "Multiple oncogenic changes (K-RAS(V12), p53 knockdown, mutant EGFRs, p16 bypass, telomerase) are not sufficient to confer a full malignant phenotype on human bronchial epithelial cells," Cancer Res **66** (4), 2116-2128 (2006).

82 J. P. Sullivan, M. Spinola, M. Dodge, M. G. Raso, C. Behrens, B. Gao, K. Schuster, C. Shao, J. E. Larsen, L. A. Sullivan, S. Honorio, Y. Xie, P. P. Scaglioni, J. M. DiMaio, A. F. Gazdar, J. W. Shay, I. I. Wistuba, and J. D. Minna, "Aldehyde dehydrogenase activity selects for lung adenocarcinoma stem cells dependent on notch signaling," Cancer Res **70** (23), 9937-9948 (2010).

83 J. C. Phillips, R. Braun, W. Wang, J. Gumbart, E. Tajkhorshid, E. Villa, C. Chipot, R. D. Skeel, L. Kalé, and K. Schulten, "Scalable molecular dynamics with NAMD," J Comput Chem **26** (16), 1781-1802 (2005).

84 M. Seeber, M. Cecchini, F. Rao, G. Settanni, and A. Caflisch, "Wordom: a program for efficient analysis of molecular dynamics simulations," Bioinformatics **23** (19), 2625-2627 (2007).

85 B. Pierce and Z. Weng, "ZRANK: reranking protein docking predictions with an optimized energy function," Proteins **67** (4), 1078-1086 (2007).

86 S. M. Franken, A. J. Scheidig, U. Krengel, H. Rensland, A. Lautwein, M. Geyer, K. Scheffzek, R. S. Goody, H. R. Kalbitzer, and E. F. Pai, "Three-dimensional structures and properties of a transforming and a nontransforming glycine-12 mutant of p21H-ras," Biochemistry **32** (33), 8411-8420 (1993).

87 H. J. Andreyev, A. R. Norman, D. Cunningham, J. R. Oates, and P. A. Clarke, "Kirsten ras mutations in patients with colorectal cancer: the multicenter "RASCAL" study," J Natl Cancer Inst **90** (9), 675-684 (1998).

88 H. J. Andreyev, A. R. Norman, D. Cunningham, J. Oates, B. R. Dix, B. J. Iacopetta, J. Young, T. Walsh, R. Ward, N. Hawkins, M. Beranek, P. Jandik, R. Benamouzig, E. Jullian, P. Laurent-Puig, S. Olschwang, O. Muller, I. Hoffmann, H. M. Rabes, C. Zietz, C. Troungos, C. Valavanis, S. T. Yuen, J. W. Ho, C. T. Croke, D. P. O'Donoghue, W. Giaretti, A. Rapallo, A. Russo, V. Bazan, M. Tanaka, K. Omura, T. Azuma, T. Ohkusa, T. Fujimori, Y. Ono, M. Pauly, C. Faber, R. Glaesener, A. F. de Goeij, J. W. Arends, S. N. Andersen, T. Lövig, J. Breivik, G. Gaudernack, O. P. Clausen, P. D. De Angelis, G. I. Meling, T. O. Rognum, R. Smith, H. S. Goh, A. Font, R. Rosell, X. F. Sun, H. Zhang, J. Benhattar, L. Losi, J. Q. Lee, S. T. Wang, P. A. Clarke, S. Bell, P. Quirke, V. J. Bubb, J. Piris, N. R. Cruickshank, D. Morton, J. C. Fox, F. Al-Mulla, N. Lees, C. N. Hall, D. Snary, K. Wilkinson, D. Dillon, J. Costa, V. E. Pricolo, S. D. Finkelstein, J. S. Thebo, A. J. Senagore, S. A. Halter, S. Wadler, S. Malik, K. Krtolica, and N. Urosevic, "Kirsten ras mutations in patients with colorectal cancer: the 'RASCAL II' study," Br J Cancer **85** (5), 692-696 (2001).

89 F. Al-Mulla and E. M. MacKenzie, "Differences in in vitro invasive capacity induced by differences in Ki-Ras protein mutations," J Pathol **195** (5), 549-556 (2001).

90 M. V. Céspedes, F. J. Sancho, S. Guerrero, M. Parreño, I. Casanova, M. A. Pavón, E. Marcuello, M. Trias, M. Cascante, G. Capellà, and R. Mangues, "K-ras Asp12 mutant

neither interacts with Raf, nor signals through Erk and is less tumorigenic than K-ras Val12," Carcinogenesis **27** (11), 2190-2200 (2006).

91 S. Guerrero, A. Figueras, I. Casanova, L. Farré, B. Lloveras, G. Capellà, M. Trias, and R. Mangues, "Codon 12 and codon 13 mutations at the K-ras gene induce different soft tissue sarcoma types in nude mice," FASEB J **16** (12), 1642-1644 (2002).

92 H. S. Floyd, C. L. Farnsworth, N. D. Kock, M. C. Mizesko, J. L. Little, S. T. Dance, J. Everitt, J. Tichelaar, J. A. Whitsett, and M. S. Miller, "Conditional expression of the mutant Ki-rasG12C allele results in formation of benign lung adenomas: development of a novel mouse lung tumor model," Carcinogenesis **26** (12), 2196-2206 (2005).

93 Y. Zhou, W. M. Rideout, T. Zi, A. Bressel, S. Reddypalli, R. Rancourt, J. K. Woo, J. W. Horner, L. Chin, M. I. Chiu, M. Bosenberg, T. Jacks, S. C. Clark, R. A. Depinho, M. O. Robinson, and J. Heyer, "Chimeric mouse tumor models reveal differences in pathway activation between ERBB family- and KRAS-dependent lung adenocarcinomas," Nat Biotechnol **28** (1), 71-78 (2010).

94 E. S. Kim, R. S. Herbst, I. I. Wistuba, J. J. Lee, G. R. Blumenschein, A. Tsao, D. J. Stewart, M. E. Hicks, J. Erasmus, S. Gupta, C. M. Alden, S. Liu, X. Tang, F. R. Khuri, H. T. Tran, B. E. Johnson, J. V. Heymach, L. Mao, F. Fossella, M. S. Kies, V. Papadimitrakopoulou, S. E. Davis, S. M. Lippman, and W. K. Hong, "The BATTLE trial: personalizing therapy for lung cancer," Cancer Discov **1** (1), 44-53 (2011).

95 T. P. Zand, D. J. Reiner, and C. J. Der, "Ras effector switching promotes divergent cell fates in C. elegans vulval patterning.," Dev Cell **20** (1), 84-96 (2011).

96 J. Luo, M. J. Emanuele, D. Li, C. J. Creighton, M. R. Schlabach, T. F. Westbrook, K. K. Wong, and S. J. Elledge, "A genome-wide RNAi screen identifies multiple synthetic lethal interactions with the Ras oncogene," Cell **137** (5), 835-848 (2009).

97 N. T. Ihle, L. A. Byers, E. S. Kim, P. Saintigny, J. J. Lee, G. R. Blumenschein, A. Tsao, S. Liu, J. E. Larsen, J. Wang, L. Diao, K. R. Coombes, L. Chen, S. Zhang, M. F. Abdelmelek, X. Tang, V. Papadimitrakopoulou, J. D. Minna, S. M. Lippman, W. K.

Hong, R. S. Herbst, I. I. Wistuba, J. V. Heymach, and G. Powis, "Effect of KRAS oncogene substitutions on protein behavior: implications for signaling and clinical outcome," J Natl Cancer Inst **104** (3), 228-239 (2012).

98 R. J. Buchsbaum, B. A. Connolly, and L. A. Feig, "Interaction of Rac exchange factors Tiam1 and Ras-GRF1 with a scaffold for the p38 mitogen-activated protein kinase cascade," Mol Cell Biol **22** (12), 4073-4085 (2002).

99 J. Huang and B. D. Manning, "A complex interplay between Akt, TSC2 and the two mTOR complexes," Biochem Soc Trans **37** (Pt 1), 217-222 (2009).

100 D. G. Brooks, R. M. James, C. E. Patek, J. Williamson, and M. J. Arends, "Mutant K-ras enhances apoptosis in embryonic stem cells in combination with DNA damage and is associated with increased levels of p19(ARF)," Oncogene **20** (17), 2144-2152 (2001).

101 S. T. Dance-Barnes, N. D. Kock, H. S. Floyd, J. E. Moore, L. J. Mosley, R. B. D'Agostino, M. J. Pettenati, and M. S. Miller, "Effects of mutant human Ki-ras(G12C) gene dosage on murine lung tumorigenesis and signaling to its downstream effectors," Toxicol Appl Pharmacol **231** (1), 77-84 (2008).

102 Y. Yamazaki, Y. Kaziro, and H. Koide, "Ral promotes anchorage-independent growth of a human fibrosarcoma, HT1080," Biochem Biophys Res Commun **280** (3), 868-873 (2001).

103 K. E. O'Reilly, F. Rojo, Q. B. She, D. Solit, G. B. Mills, D. Smith, H. Lane, F. Hofmann, D. J. Hicklin, D. L. Ludwig, J. Baselga, and N. Rosen, "mTOR inhibition induces upstream receptor tyrosine kinase signaling and activates Akt," Cancer Res **66** (3), 1500-1508 (2006).

104 N. M. Hamad, J. H. Elconin, A. E. Karnoub, W. Bai, J. N. Rich, R. T. Abraham, C. J. Der, and C. M. Counter, "Distinct requirements for Ras oncogenesis in human versus mouse cells," Genes Dev **16** (16), 2045-2057 (2002).

105 E. A. Dunlop and A. R. Tee, "Mammalian target of rapamycin complex 1: signalling inputs, substrates and feedback mechanisms," Cell Signal **21** (6), 827-835 (2009).

106 M. C. Garassino, M. Marabese, P. Rusconi, E. Rulli, O. Martelli, G. Farina, A. Scanni, and M. Broggini, "Different types of K-Ras mutations could affect drug sensitivity and tumour behaviour in non-small-cell lung cancer," Ann Oncol **22** (1), 235-237 (2011).

107 P. I. Poulikakos, C. Zhang, G. Bollag, K. M. Shokat, and N. Rosen, "RAF inhibitors transactivate RAF dimers and ERK signalling in cells with wild-type BRAF," Nature **464** (7287), 427-430 (2010).

108 I. Hofmann, A. Weiss, G. Elain, M. Schwaederle, D. Sterker, V. Romanet, T. Schmelzle, A. Lai, S. M. Brachmann, M. Bentires-Alj, T. M. Roberts, W. R. Sellers, F. Hofmann, and S. M. Maira, "K-RAS Mutant Pancreatic Tumors Show Higher Sensitivity to MEK than to PI3K Inhibition In Vivo," PLoS One **7** (8), e44146 (2012).

109 S. Wee, Z. Jagani, K. X. Xiang, A. Loo, M. Dorsch, Y. M. Yao, W. R. Sellers, C. Lengauer, and F. Stegmeier, "PI3K pathway activation mediates resistance to MEK inhibitors in KRAS mutant cancers," Cancer Res **69** (10), 4286-4293 (2009).

110 K. H. Lim and C. M. Counter, "Reduction in the requirement of oncogenic Ras signaling to activation of PI3K/AKT pathway during tumor maintenance," Cancer Cell **8** (5), 381-392 (2005).

111 D. P. Modest, A. Reinacher-Schick, S. Stintzing, C. Giessen, A. Tannapfel, R. P. Laubender, T. Brodowicz, R. Knittelfelder, D. Vrbanec, W. Schmiegel, V. Heinemann, and C. C. Zielinski, "Cetuximab-based or bevacizumab-based first-line treatment in patients with KRAS p.G13D-mutated metastatic colorectal cancer: a pooled analysis," Anticancer Drugs **23** (6), 666-673 (2012).

112 D. A. Barbie, P. Tamayo, J. S. Boehm, S. Y. Kim, S. E. Moody, I. F. Dunn, A. C. Schinzel, P. Sandy, E. Meylan, C. Scholl, S. Fröhling, E. M. Chan, M. L. Sos, K. Michel, C. Mermel, S. J. Silver, B. A. Weir, J. H. Reiling, Q. Sheng, P. B. Gupta, R. C. Wadlow, H. Le, S. Hoersch, B. S. Wittner, S. Ramaswamy, D. M. Livingston, D. M.

Sabatini, M. Meyerson, R. K. Thomas, E. S. Lander, J. P. Mesirov, D. E. Root, D. G. Gilliland, T. Jacks, and W. C. Hahn, "Systematic RNA interference reveals that oncogenic KRAS-driven cancers require TBK1," Nature **462** (7269), 108-112 (2009).

113 C. Babij, Y. Zhang, R. J. Kurzeja, A. Munzli, A. Shehabeldin, M. Fernando, K. Quon, P. D. Kassner, A. A. Ruefli-Brasse, V. J. Watson, F. Fajardo, A. Jackson, J. Zondlo, Y. Sun, A. R. Ellison, C. A. Plewa, M. T. San, J. Robinson, J. McCarter, R. Schwandner, T. Judd, J. Carnahan, and I. Dussault, "STK33 kinase activity is nonessential in KRAS-dependent cancer cells," Cancer Res **71** (17), 5818-5826 (2011).

114 F. A. Karreth, G. M. DeNicola, S. P. Winter, and D. A. Tuveson, "C-Raf inhibits MAPK activation and transformation by B-Raf(V600E)," Mol Cell **36** (3), 477-486 (2009).

115 J. Huang and B. D. Manning, "The TSC1-TSC2 complex: a molecular switchboard controlling cell growth.," Biochem J **412** (2), 179-190 (2008).

116 L. Makowski and D. N. Hayes, "Role of LKB1 in lung cancer development," Br J Cancer **99** (5), 683-688 (2008).

117 F. S. Willard, M. D. Willard, A. J. Kimple, M. Soundararajan, E. A. Oestreich, X. Li, N. A. Sowa, R. J. Kimple, D. A. Doyle, C. J. Der, M. J. Zylka, W. D. Snider, and D. P. Siderovski, "Regulator of G-protein signaling 14 (RGS14) is a selective H-Ras effector.," PLoS One **4** (3), e4884 (2009).

118 L. Belanis, S. J. Plowman, B. Rotblat, J. F. Hancock, and Y. Kloog, "Galectin-1 is a novel structural component and a major regulator of h-ras nanoclusters.," Mol Biol Cell **19** (4), 1404-1414 (2008).

119 R. Shalom-Feuerstein, S. J. Plowman, B. Rotblat, N. Ariotti, T. Tian, J. F. Hancock, and Y. Kloog, "K-ras nanoclustering is subverted by overexpression of the scaffold protein galectin-3.," Cancer Res **68** (16), 6608-6616 (2008).

120 K. Farin, S. Schokoroy, R. Haklai, I. Cohen-Or, G. Elad-Sfadia, M. E. Reyes-Reyes, P. J. Bates, A. D. Cox, Y. Kloog, and R. Pinkas-Kramarski, "Oncogenic synergism between ErbB1, nucleolin, and mutant Ras.," Cancer Res **71** (6), 2140-2151 (2011).

121 M. Therrien, A. M. Wong, and G. M. Rubin, "CNK, a RAF-binding multidomain protein required for RAS signaling.," Cell **95** (3), 343-353 (1998).

122 M. Douziech, M. Sahmi, G. Laberge, and M. Therrien, "A KSR/CNK complex mediated by HYP, a novel SAM domain-containing protein, regulates RAS-dependent RAF activation in Drosophila," Genes Dev **20** (7), 807-819 (2006).

123 F. A. Karreth, K. K. Frese, G. M. DeNicola, M. Baccarini, and D. A. Tuveson, "C-Raf is required for the initiation of lung cancer by K-Ras(G12D)," Cancer Discov **1** (2), 128-136 (2011).

124 A. Loboda, M. Nebozhyn, R. Klinghoffer, J. Frazier, M. Chastain, W. Arthur, B. Roberts, T. Zhang, M. Chenard, B. Haines, J. Andersen, K. Nagashima, C. Paweletz, B. Lynch, I. Feldman, H. Dai, P. Huang, and J. Watters, "A gene expression signature of RAS pathway dependence predicts response to PI3K and RAS pathway inhibitors and expands the population of RAS pathway activated tumors," BMC Med Genomics **3**, 26 (2010).

125 A. Clapéron and M. Therrien, "KSR and CNK: two scaffolds regulating RAS-mediated RAF activation," Oncogene **26** (22), 3143-3158 (2007).

126 S. Shirasawa, M. Furuse, N. Yokoyama, and T. Sasazuki, "Altered growth of human colon cancer cell lines disrupted at activated Ki-ras," Science **260** (5104), 85-88 (1993).

127 A. McFall, A. Ulkü, Q. T. Lambert, A. Kusa, K. Rogers-Graham, and C. J. Der, "Oncogenic Ras blocks anoikis by activation of a novel effector pathway independent of phosphatidylinositol 3-kinase," Mol Cell Biol **21** (16), 5488-5499 (2001).

128 M. Drosten, A. Dhawahir, E. Y. Sum, J. Urosevic, C. G. Lechuga, L. M. Esteban, E. Castellano, C. Guerra, E. Santos, and M. Barbacid, "Genetic analysis of Ras signalling pathways in cell proliferation, migration and survival," EMBO J **29** (6), 1091-1104 (2010).

129 W. S. Park, W. D. Heo, J. H. Whalen, N. A. O'Rourke, H. M. Bryan, T. Meyer, and M. N. Teruel, "Comprehensive identification of PIP3-regulated PH domains from C.

elegans to H. sapiens by model prediction and live imaging.," Mol Cell **30** (3), 381-392 (2008); W. D. Heo, T. Inoue, W. S. Park, M. L. Kim, B. O. Park, T. J. Wandless, and T. Meyer, "PI(3,4,5)P3 and PI(4,5)P2 lipids target proteins with polybasic clusters to the plasma membrane.," Science **314** (5804), 1458-1461 (2006).

130 A. M. Ahad, S. Zuohe, L. Du-Cuny, S. A. Moses, L. L. Zhou, S. Zhang, G. Powis, E. J. Meuillet, and E. A. Mash, "Development of sulfonamide AKT PH domain inhibitors," Bioorg Med Chem **19** (6), 2046-2054 (2011); E. J. Meuillet, S. Zuohe, R. Lemos, N. Ihle, J. Kingston, R. Watkins, S. A. Moses, S. Zhang, L. Du-Cuny, R. Herbst, J. J. Jacoby, L. L. Zhou, A. M. Ahad, E. A. Mash, D. L. Kirkpatrick, and G. Powis, "Molecular pharmacology and antitumor activity of PHT-427, a novel Akt/phosphatidylinositide-dependent protein kinase 1 pleckstrin homology domain inhibitor," Mol Cancer Ther **9** (3), 706-717 (2010).

131 A. Mielgo, L. Seguin, M. Huang, M. F. Camargo, S. Anand, A. Franovic, S. M. Weis, S. J. Advani, E. A. Murphy, and D. A. Cheresh, "A MEK-independent role for CRAF in mitosis and tumor progression," Nat Med **17** (12), 1641-1645 (2011).

132 S. Wang, R. N. Ghosh, and S. P. Chellappan, "Raf-1 physically interacts with Rb and regulates its function: a link between mitogenic signaling and cell cycle regulation," Mol Cell Biol **18** (12), 7487-7498 (1998).

133 F. A. Karreth, K. K. Frese, G. M. Denicola, M. Baccarini, and D. A. Tuveson, "C-Raf is required for the initiation of lung cancer by K-Ras.," Cancer Discov **1** (2), 128-136 (2011).

134 T. Shimizu, A. W. Tolcher, K. P. Papadopoulos, M. Beeram, D. W. Rasco, L. S. Smith, S. Gunn, L. Smetzer, T. A. Mays, B. Kaiser, M. J. Wick, C. Alvarez, A. Cavazos, G. L. Mangold, and A. Patnaik, "The clinical effect of the dual-targeting strategy involving PI3K/AKT/mTOR and RAS/MEK/ERK pathways in patients with advanced cancer," Clin Cancer Res **18** (8), 2316-2325 (2012).

135 N. T. Ihle, G. Powis, and S. Kopetz, "PI-3-Kinase inhibitors in colorectal cancer.," Curr Cancer Drug Targets **11** (2), 190-198 (2011).

136 C. L. Mahoney, B. Choudhury, H. Davies, S. Edkins, C. Greenman, G. Haaften, T. Mironenko, T. Santarius, C. Stevens, M. R. Stratton, and P. A. Futreal, "LKB1/KRAS mutant lung cancers constitute a genetic subset of NSCLC with increased sensitivity to MAPK and mTOR signalling inhibition," Br J Cancer **100** (2), 370-375 (2009).

Vita

Nathan Ihle was born in Frederick, Maryland on May 19, 1978 and attended elementary school there until the age of 12. He then moved to Memphis and attended both White Station junior high school and Briarcrest high school. He then traveled to Tucson, Arizona to achieve his undergraduate degree in Environmental Science.

In Tucson he began working in his senior year, 2001, as a student worker in the Garth Powis lab cleaning dishes and stocking supplies. Upon graduation he worked as a technician in this lab for three years. In 2005, when this lab relocated to MD Anderson he traveled there to become a program coordinator, a position he held for five years

In 2010 he began attending the GSBS to obtain his degree in Experimental Therapeutics. Upon obtaining this degree he will relocate to San Diego, California to serve as a Principal Scientist in La Jolla, California at Pfizer Inc.